

For Reference

NOT TO BE TAKEN FROM THIS ROOM

Ex LIBRIS
UNIVERSITATIS
ALBERTAENSIS





Digitized by the Internet Archive
in 2020 with funding from
University of Alberta Libraries

<https://archive.org/details/Whitmore1981>

THE UNIVERSITY OF ALBERTA

RELEASE FORM

NAME OF AUTHOR Keith Daryl Whitmore
TITLE OF THESIS Microprocessor Controlled Gamma-Ray CT
 Scanner For Measurement Of Bone Density
DEGREE FOR WHICH THESIS WAS PRESENTED Master of Science
YEAR THIS DEGREE GRANTED Spring 1981

Permission is hereby granted to THE UNIVERSITY OF ALBERTA LIBRARY to reproduce single copies of this thesis and to lend or sell such copies for private, scholarly or scientific research purposes only.

The author reserves other publication rights, and neither the thesis nor extensive extracts from it may be printed or otherwise reproduced without the author's written permission.

THE UNIVERSITY OF ALBERTA

Microprocessor Controlled Gamma-Ray CT Scanner For
Measurement Of Bone Density

by



Keith Daryl Whitmore

A THESIS

SUBMITTED TO THE FACULTY OF GRADUATE STUDIES AND RESEARCH
IN PARTIAL FULFILMENT OF THE REQUIREMENTS FOR THE DEGREE
OF Master of Science

Electrical Engineering

EDMONTON, ALBERTA

Spring 1981

91-120

THE UNIVERSITY OF ALBERTA
FACULTY OF GRADUATE STUDIES AND RESEARCH

The undersigned certify that they have read, and recommend to the Faculty of Graduate Studies and Research, for acceptance, a thesis entitled Microprocessor Controlled Gamma-Ray CT Scanner For Measurement Of Bone Density submitted by Keith Daryl Whitmore in partial fulfilment of the requirements for the degree of Master of Science.

Abstract

The theory, design and construction of a microprocessor controlled gamma-ray CT bone scanner are described. This scanner, with its ability to determine the radiological density of trabecular bone at appendicular sites in the skeleton, provides an order of magnitude increase in sensitivity to changes in bone mineralization over existing techniques such as absorptiometry and radiographic analysis. This technological development could be invaluable to the clinician for diagnosis and in the evaluation of treatments of osteopenia. The design and implementation of both a single and multi-detector rotation-translation scanning system are detailed along with future plans for a fan-beam rotational system.

Acknowledgements

I would like to express my appreciation to my supervisor, Dr. T.R. Overton for his efforts (in terms of administrative assistance and moral encouragement) which have increased both the value and personal satisfaction of my education. This project has been a team effort and hence there are many people whose efforts I would like to recognize. These include: Mr. I. Yamamoto (for his aid in design and construction of the mechanical components), Mr. R. Heath (for the design, testing, and implementation of the HP programs), Mr. J.D. Ridley (for his aid in evaluation of the scanner), Dr. D. Menon (for his assistance in helping me to understand some of the theoretical aspects of CT and his review of this manuscript) and Dr. T.N. Hangartner (for his efforts in upgrading the CT system and his willingness to share his expertise). Lastly, I would like to express my thanks to my many friends in the Division of Biomedical Engineering who have made my educational experience truly enjoyable.

Table of Contents

Chapter	Page
I. Historical Aspects	1
A. Measurement of Bone at the University of Alberta	4
II. Bone Physiology and Pathology	7
A. Osteoporosis and Osteomalacia	9
B. Physical Evaluation of Bone	12
Bone Biopsy	12
Radiology (X-rays)	12
Absorptiometry	13
In Vivo Neutron Activation Analysis (IVNAA) ..	16
Compton Scattering	17
Radioisotope CT	17
III. Principles of CT Scanners	20
A. Back-Projections	25
B. Reconstruction Algorithms	31
Iterative Technique	31
Analytical Technique	32
Comparison of Analytical and Iterative Algorithms	41
C. Photon Attenuation	41
Statistical Considerations	42
Dead Time	43
Beam Hardening	45
D. Detector Types	46

Scintillation Detector	48
E. Performance Characteristics Of CT Scanners	52
Spatial Resolution	52
Contrast Resolution	56
F. Commercial CT Scanners	57
IV. System Design and Construction	60
A. Mechanical Operations	60
Stand	60
Source-Detector Alignment and Motion	62
Mechanical Drives	62
B. Radioactive Sources and Detectors	66
Signal Processing	67
C. Scanner Control	69
Timing Considerations	70
MPU Control	73
Reproducibility of Measurements	81
Single Stepping	83
HP/Microprocessor Interfacing	83
D. Multidetector System	86
Physical Limitations	87
Intervals and Subintervals	89
Centering	90
E. Data Processing	92
Open Count	95
Pixel Size and Grey Levels	95
Analysis Program	96
V. System Evaluation	100

A. Spatial Resolution	100
B. Precision	105
C. Accuracy	105
D. Radiation Dose	107
Thermo-Luminescent Detectors	115
E. Contrast Resolution	115
VI. System Limitations and Future Plans	117
A. X-Ray Tube	117
B. System Three	118
C. Control System	118
D. Processing Facilities	119
References	120
Appendix A. Iodine 125 Decay Mechanism	127
Appendix B. MPU Program Flow Chart	128
Appendix C. MPU Subroutines Used	129
Appendix D. Read Subroutine	150

List of Tables

Table	Page
1. Analysis Program Output	97
2. Precision Test - Repeat Measurements	106
3. Accuracy Measurements	109

List of Figures

Figure	Page
1. Conventional Tomography	2
2. Reconstruction Matrix	5
3. Absorptiometry	15
4. CT Generation 1	21
5. CT Generation 2	21
6. CT Generation 3	23
7. CT Generation 4	23
8. CT Generation 5	24
9. Parallel Beam Format	26
10. Rotational Beam Format	27
11. Back-Projection	29
12. Image Reconstruction Using Back-Projection	30
13. Beam Hardening Correction	47
14. Photomultiplier Tube and Related Circuitry	51
15. Effects of Aperture Size on Spatial Resolution	54
16. Effects of Aperture Size on Spatial Resolution	55
17. CT System	61
18. Plate #1	63
19. Plate #2	64
20. Plate #3	65
21. Preamp Circuit	68
22. Stepping Motor and Translator Circuit	71
23. Control and Data Processing Block Diagram	72
24. Image Obtained From Scout Scan	82

25. Single Stepping Circuitry	84
26. Current Sink For HP-Micro Signal Conversion	85
27. Voltage Divider Circuit	85
28. Multi-Detector Holder	88
29. The Cause of Centering Artifacts	91
30. Centering Artifacts in a Plexiglass Model	93
31. Image of a Normal Radius-Ulna	98
32. High Speed Spatial Resolution	102
33. Medium Speed Spatial Resolution	103
34. Low Speed Spatial Resolution	104
35. Test Cylinder of K_2HPO_4	108
36. Evaluation of System Accuracy	110

I. Historical Aspects

It has long been the goal of medical radiology to obtain clear cross-sectional views of the body. As early as 1921 (1) conventional or focal plane tomography was being used. Conventional tomography involves the movement of both the X-ray tube and film (or even the body itself) in a trajectory (Figure 1) so that only the desired layer remains in focus while all other layers are blurred. This type of tomography which is analogous to a narrow-depth-of-field in photography has the disadvantage of the blurred presence of unwanted fields.

Computed tomography (CT), which is the latest evolution in a series of techniques used in image reconstruction, eliminates these unwanted planes by limiting radiation to the desired plane. CT is based on the principle that if radiological attenuation is measured along a sufficient number of lines passing through a given plane, then the radiological densities throughout that plane can be determined.

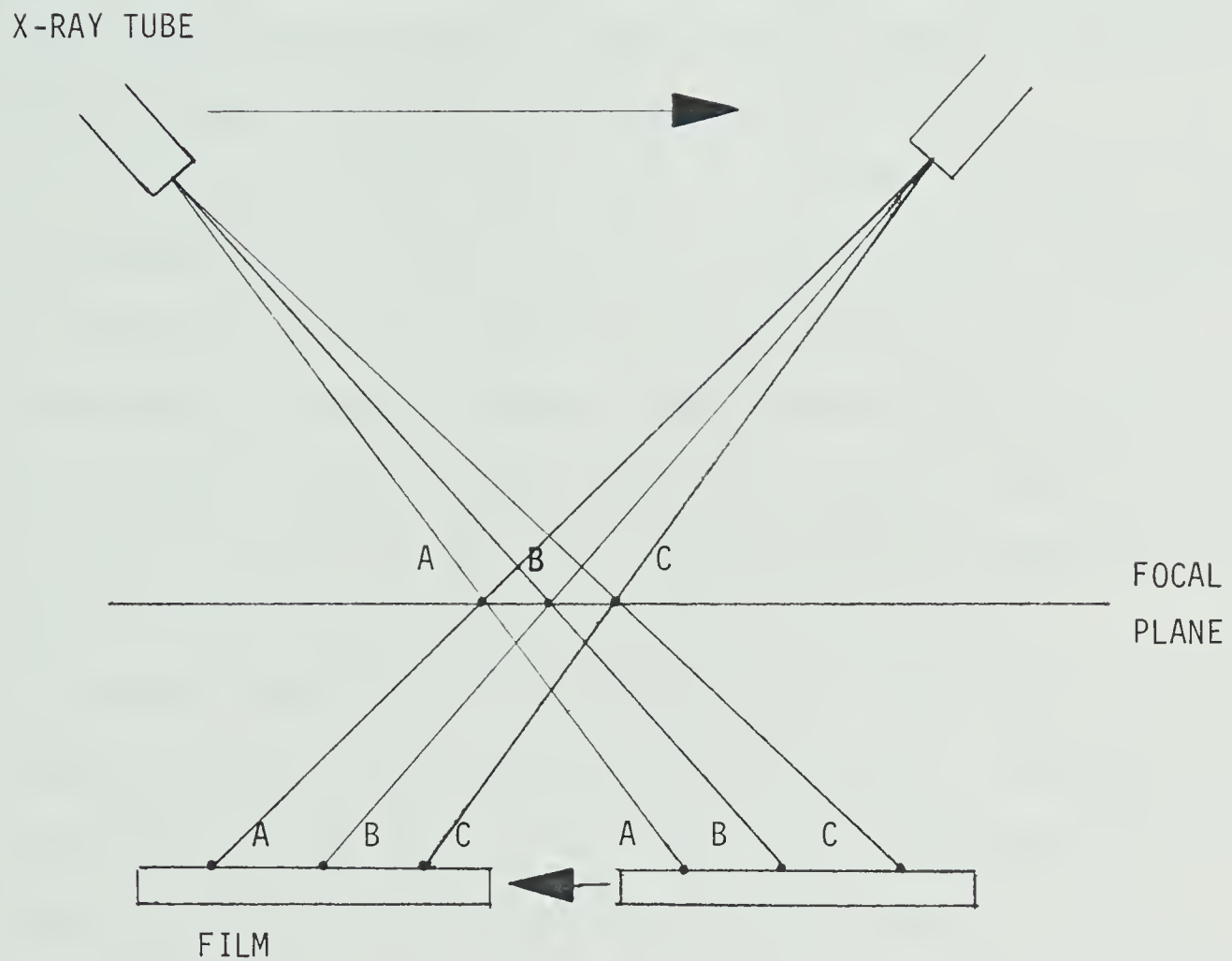
The mathematical basis for computed tomography was first described by Radon (2) in 1917. Given that

1. $f(x,y)$ denotes the attenuation coefficient at a point (x,y) in the plane, and

2. that L is any line in the plane:

then, the logarithm of attenuation is equal to the integral of f along L ; $P(L) = \int f(x,y) ds$

where s indicates a length along L . The problem then is to



ONLY POINTS ON THE FOCAL PLANE ARE CONTINUALLY REGISTERED ON THE SAME PART OF THE FILM. POINTS IN OTHER PLANES ARE IMAGED ONTO VARYING PARTS OF THE FILM AND HENCE ARE BLURRED.

FIGURE 1. CONVENTIONAL TOMOGRAPHY

invert the equation: that is, given $P(L)$, to determine $f(x,y)$. Assuming $P(L)$ is given for all lines L and that $f(x,y)$ is continuous with compact support, Radon showed that $f(x,y)$ could be calculated for all points in the plane. At the time of its development this mathematical basis for image reconstruction was purely theoretical in nature and in actual fact was derived by Radon while he was working with equations dealing with gravitational fields.

It was not until 1956 that this theory was made use of by Bracewell (3) in the field of radioastronomy. Bracewell was able to identify regions on the sun which emitted microwave radiation. However, the antennas being used could only focus on thin strips criss-crossing the solar surface. In order to map out the solar regions of microwave activity it was necessary to convert these strips into a representative plane of solar activity - the exact problem shown by Radon to be mathematically solvable. Bracewell developed both an analytical technique (equivalent to Radon's) and an iterative technique for image reconstruction.

The first medical application appeared 7 years later when Cormack (4) published his first experimental results. Cormack's work involved development of a mathematical technique for the accurate reconstruction of an image from x-ray projections and applications based on measurements of simple phantoms. This technique for reconstruction involved the expansion of P and f into Fourier series and the

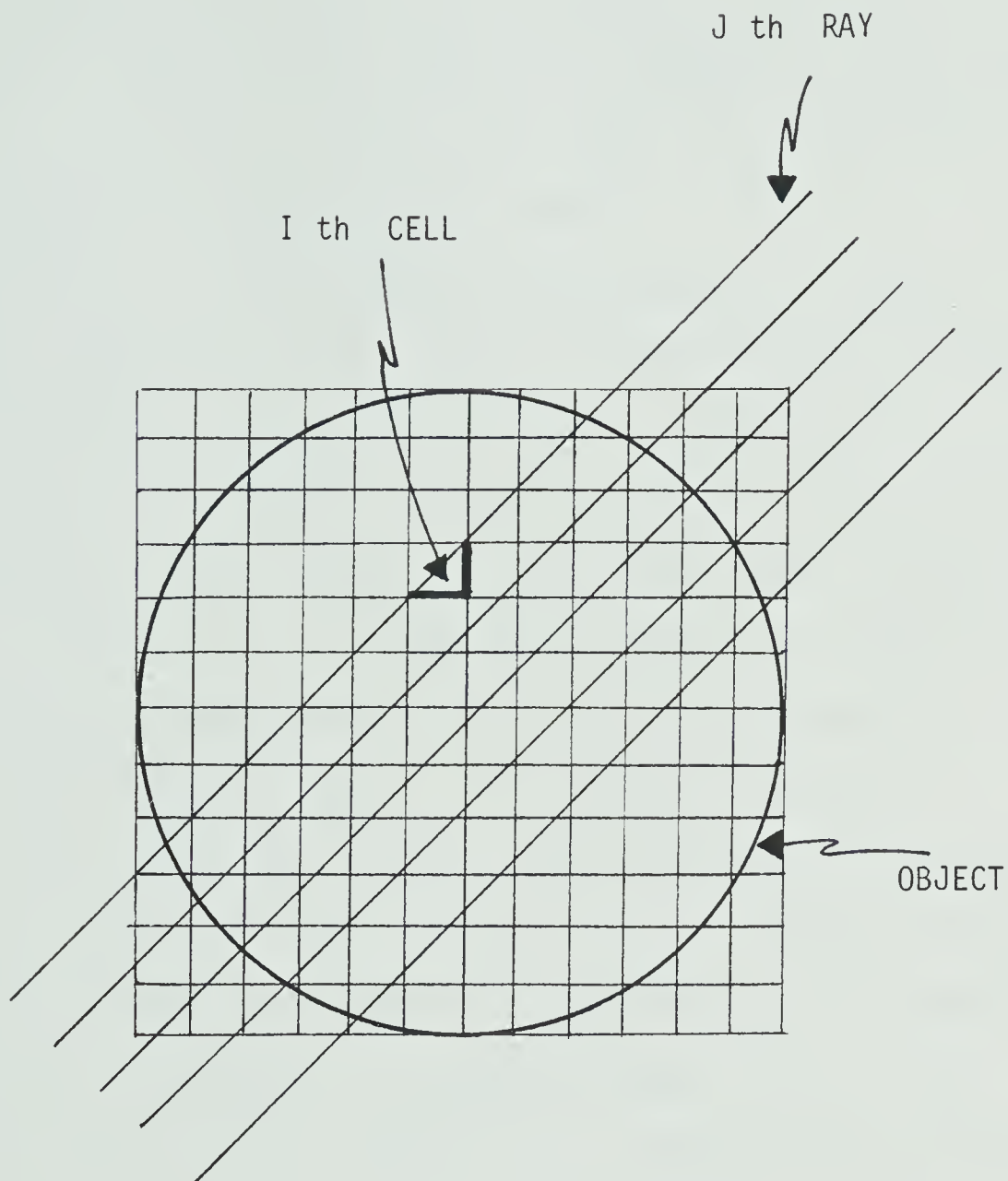
subsequent matching of Fourier coefficients.

The first commercial scanner was the E.M.I. Head Scanner described in 1973 by G. Hounsfield (5). Having realized that the ray-integrals essentially composed a discrete rather than a continuous number of equations, Hounsfield's approach to reconstruction involved an iterative solution to inversion of the equation defined by $P_j = \text{the summation over } i \text{ of } W_{ij} f_i$ (Figure 2) where W_{ij} is a weighting function of the radiological density, f_i . This weighting function represents the contribution of the i th cell to the j th ray.

From these early days CT has evolved from the point where only scans of the head could be performed to today where scans of the entire body can be made. A 1977 study of the U.S. Department of Commerce (6) predicted that by 1980 there would be some 2500 CT scanners in the U.S. and annual related expenditures of \$1.7 billion. Over a dozen different companies were involved in marketing CT machines in 1976: machines able to delineate differences in soft tissue density as low as 0.5 % (7).

A. Measurement of Bone at the University of Alberta

The use of CT for the measurement of bone density, as developed in Zurich by R  egsegger and Elsasser (8), is a relatively new phenomenon. Since changes in bone mineralization occur much more rapidly in trabecular bone than in cortical bone (9), detection of small changes in



THE RECONSTRUCTION MATRIX IS AN N BY N ARRAY OF CELLS.
 THE ACTUAL RAYS ARE STRIPS OF FINITE WIDTH. THE CONTRIBUTION
 OF THE I th CELL TO THE J th RAY IS DENOTED BY w_{ij} .

FIGURE 2. RECONSTRUCTION MATRIX

mineral content are only possible if trabecular bone density can be quantified. It is for this reason that CT scans which can be used to produce images of bone cross section are so valuable.

Although the principles involved in reconstruction of an image of bone are the same as in commercial whole body scanners, there are a sufficient number of differences to merit a specially designed CT scanner.

The Division of Biomedical Engineering at the U. of A. has been involved in the clinical determination of bone mineral content using absorptiometric techniques for the past 8 years (10). This clinical experience led to the development of a CT system for the measurement of bone mineral content at the University of Alberta. Based upon an original design by Elsasser (11) an eight detector, translation-rotation gamma-ray CT system has been constructed. With this scanner, measurements can be made of the distal forearm using Iodine 125 as a photon source.

This thesis is concerned primarily with the control system for the scanner. A microprocessor unit or MPU (Motorola 6800 D2 kit) serves as a system master clock, providing control of scanner movement and for data acquisition through the laboratory computer (HP 2100) and CAMAC systems. An MPU based controller was chosen as it was felt that the timing specifications on the scanner would be too tight to be controllable by the HP running under a multi-user operating system.

II. Bone Physiology and Pathology

In the diagnosis of various diseases of bone it is desirable to measure changes in mineral content of trabecular (spongy) bone. To understand this requirement it is necessary to examine the physiological and pathological characteristics of bone. Once the need for bone mineral density analysis has been described an examination of existing analysis techniques will be presented.

Bone consists of an organic matrix that is greatly strengthened by deposits of calcium salts (12-14). Five percent of this organic matrix is a homogeneous medium called ground substance while the other 95 % is made up of collagen fibers. It is these collagen fibers which give bone its tensile strength while the calcium salts provide its compressional strength. The calcium salts are composed principally of calcium and phosphate and are formed in a crystal called hydroxyapatite. The crystals are between 200 and 400 angstroms in length and between 10 and 30 angstroms in diameter. Under varying nutritional conditions the ratio by weight of calcium to phosphate in these crystals can vary from 1.3 to 2.0.

As well as having the obvious structural function the skeleton acts as a reservoir for many of the body's ions, notably calcium and phosphate. Bone contains 99% of the total body calcium and 90% of the total body phosphorus. From 0.4 to 1.0 % of this bone calcium is readily exchangeable and this exchange occurs at points in the bone

undergoing active calcium resorption (remodelling) (15). Thus there is a constant circulation of ions between the skeletal reservoir and body fluids and tissues. Ions not contained in the bone have a wide range of physiological activities. For example; calcium not in the bone affects enzyme activity, cell membrane permeability, cardiac rhythm and neuromuscular excitability. The concentration of calcium in the blood is maintained between 9 and 11 mg per 100 ml and it is the buffering action of bone that provides this control. Exchange of calcium with the bone is controlled mainly by parathyroid hormone from the parathyroids and calcitonin from the thyroid. Another means of control of calcium ion concentration is absorption from the gut. Vitamin D₂, for example, is required for calcium absorption from the gut.

Bone is made up of 3 types of cells. These cells are scattered throughout an interstitial matrix of fibrous protein and occupy 3% of the total volume of the bone. Osteocytes are the ordinary bone cells and comprise the bulk of the cells. They are incapable of mitosis and hence must be removed before new bone can be formed. Osteoblasts are the cells which secrete the ground substance and collagen onto the bone forming surface. This uncalcified organic matrix is known as osteoid. The osteoblasts produce an enzyme, alkaline phosphatase, which is thought to act by splitting organic phosphate compounds thus upsetting the local calcium-phosphate balance causing precipitation of

calcium salts in the ground substance. Osteoclasts or bone phagocytes are the cells involved in the removal of bone. This occurs by both a phagocytic action and the release of enzymes and acids which cause the simultaneous dissolution of mineral and matrix. Thus bone is continually being deposited by osteoblasts and being resorbed at sites where osteoclasts are active. Osteoblastic deposition is stimulated by physical stress while sex hormones and calcium supplements decrease both bone resorption and formation.

On a macroscopic level there are two main classes of bone: cortical or compact bone, which is the harder outer bone and trabecular or spongy bone which is the less dense inner bone. Average compact bone consists of 25 % by weight matrix and 75 % calcium salts while trabecular bone is made up of a much higher percentage of matrix. Due to a greater surface area it is in this less dense trabecular bone structure where physiological and pathological changes in matrix structure or calcium salt deposition occur more rapidly and hence it is desirable to measure the distribution of density in trabecular bone.

A. Osteoporosis and Osteomalacia

Two common diseases of bone are osteomalacia or "adult rickets" and osteoporosis. Osteomalacia is a lack of calcium salts and is due to a lack of calcium and phosphates in the extracellular fluid (16). This is often caused by a lack of calcium absorption from the gut possibly due to a vitamin D

deficiency. Kidney disorders are one common non-nutritional cause of osteomalacia.

Osteomalacia involves an increase in the proportion of uncalcified bone (osteoid) with a corresponding increase in both the number and thickness of osteoid seams. The mineralized bone mass is usually decreased due to a decrease in calcium and phosphate. The bones are soft and skeletal deformities may ensue. Symptoms of osteomalacia include weakness, bone pain and tenderness as well as radiologic evidence of decreased mineralization and pseudofractures of the long bones.

Osteoporosis is abnormal organic matrix formation (17,18) and may be caused by: (1) lack of use of the bones, (2) malnutrition to the extent that sufficient protein matrix cannot be formed, (3) lack of vitamin C, (4) postmenopausal lack of estrogen secretion, and (5) old age (due to dysfunction of various protein anabolic functions). Osteoporosis therefore involves a decrease in bone mass due to the absence of a normal quantity of bone caused by deficient production of bone matrix. The mineral content of the bone however, is grossly normal and there is no excess of osteoid. Thus there is an imbalance between osteoblastic bone deposition and osteoclastic bone resorption. Clinically there is a decrease in the number of and thickness of bony trabeculae. The cortical bone later becomes thinned; however, it is still relatively dense compared to the decreased density of the trabecular bone. There is an

increase in susceptibility to fractures from compression forces (eg. vertebral bone compression fractures).

The density of bone has been shown to decline in all people from the age of 20 onwards, the process accelerating after middle age (16,18). To this extent bone becomes osteoporotic after 50 years of age to a greater extent and somewhat earlier in women than in men.

Decreased bone mineralization, which may accompany osteopenia (general bone disorders), appears radiologically as areas of decreased density. As such, it is possible to use radiographic techniques to diagnose and to evaluate the effectiveness of treatment in diseases related to changes in bone mineralization.

"Since the disorders causing rickets and osteomalacia are generally of long standing and must have profound effects on matrix composition or mineral metabolism before they become apparent clinically, therapy may be necessary for months or years before healing is complete." ¹ The same may be said for osteoporosis. Some of the present treatments include mineral supplements, gonadal hormones and physical therapy. Some of these treatments may have other effects. For example, pharmacologic doses of vitamin D may cause hypercalcemia. Treatments then are very dose dependant and/or expensive and hence any technique which will provide an early and accurate means of diagnosis and measurement of changes in bone density has potential for both therapeutic

¹ Current Therapy 1977, Edited by Conn: pg 461.

and financial benefit. Since changes in bone density first appear in trabecular bone, a technique is required that is able to measure density of trabecular bone.

B. Physical Evaluation of Bone

This section will examine some of the techniques presently being used for physical evaluation of bone. These include both invasive and non-invasive techniques.

Bone Biopsy

Bone biopsies involve the physical removal of a sample of bone usually from the iliac crest (hip bone). This sample is then analyzed, usually by microscopic examination of the number of trabeculae and osteoid in a given area within the sample. Although this technique does provide valuable information the sample removal is an invasive technique and is traumatic for the patient. Results obtained vary greatly from site to site and once bone has been removed the same site cannot be re-examined. This then precludes the use of bone biopsies as an accurate means of monitoring both the course of any diseases such as osteoporosis and osteomalacia as well as the effectiveness of any treatments. Thus the use of bone biopsies is severely limited.

Radiology (X-rays)

Prior to 1963, diagnosis of osteoporosis and osteomalacia predominantly involved the radiological evaluation of vertebral skeleton. Radiographic techniques or X-rays show total density of a number of planes superimposed

together on one view and hence any one plane of high density will overshadow any of the other planes. Thus it is largely cortical bone that shows on X-rays and hence measurements of density of trabecular bone are not feasible. Accurate diagnosis of either osteoporosis or osteomalacia using X-rays requires the diseases to be significantly advanced involving decreases in bone mass of greater than 25% (16,18) and/or compression fractures. Due to the lack of precision of this technique, longitudinal studies (studies over time) are difficult to perform and it is virtually impossible to evaluate the progress of disease and the effectiveness of treatments. Radiographic distinction between osteoporosis and osteomalacia is also difficult and the two diseases may coexist.

Absorptiometry

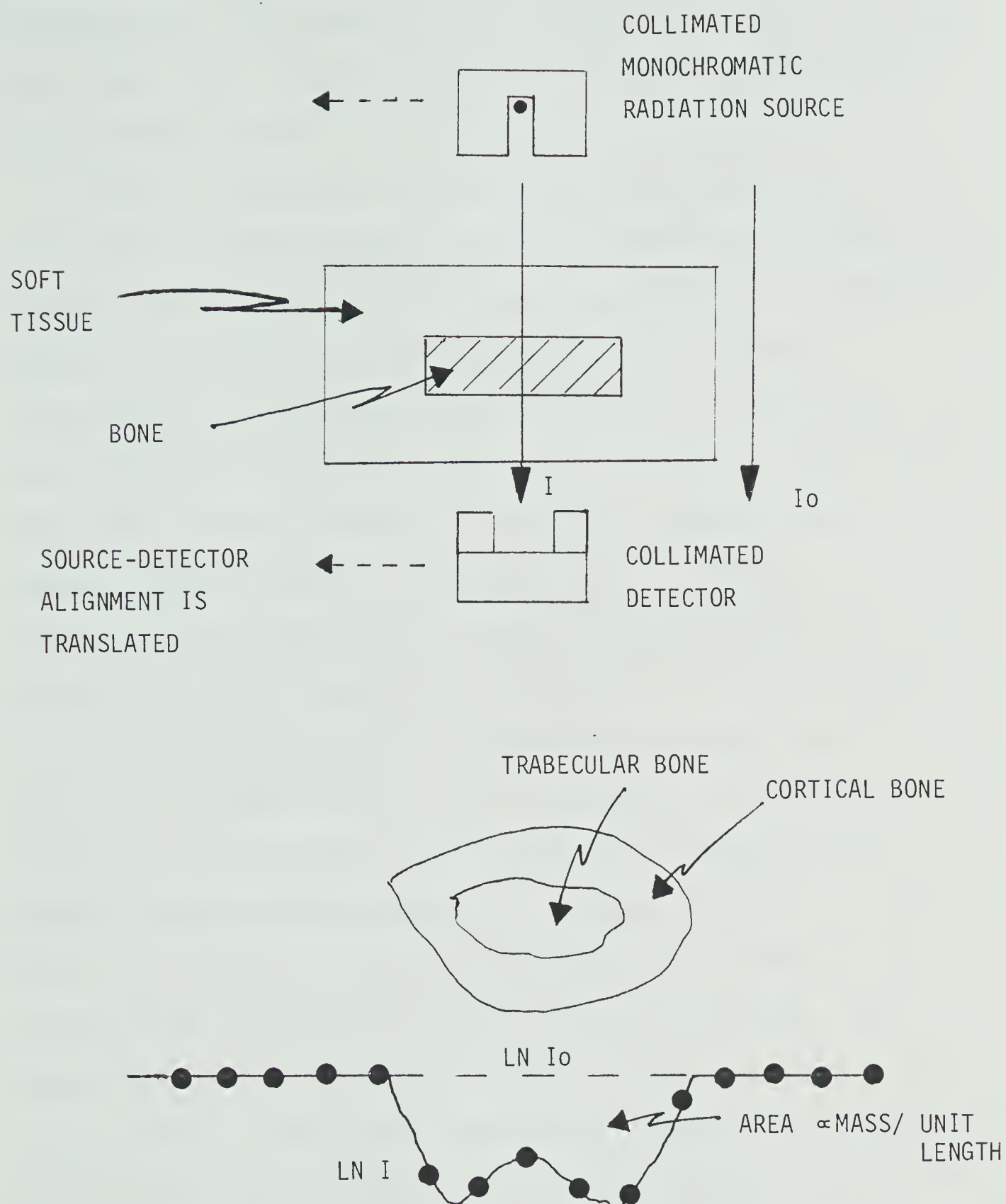
In 1963, Cameron and Sorenson (19) reported an improved technique, known as absorptiometry, for the in vivo measurement of bone mineral content. Their method involved the use of a nearly monoenergetic collimated source of photons mechanically coupled and collinear with a collimated scintillation detector. The scintillation detector, with appropriate electronics, is able to measure both the energy of, and the number of photons striking it in an interval of time. Therefore, one can measure both the number and energy of photons striking the detector with and without an object placed between them. These measurements allow the amount of energy absorbed by the object to be calculated. In the case

of bone the number of photons removed from the beam by the object is related to the mass of bone present. The measurement technique then involves movement of the source detector system along a linear path across the object with transmission measurements taken at discrete intervals throughout the translation (Figure 3). This results in an absorption profile of the object, the area of which is a function of the number of photons absorbed by the object.

Although this technique is similar to a conventional X-ray in that radiological attenuation is measured, the improved equipment results in marked improvements in both the accuracy and precision of the measurement.

Absorptiometry could be considered a digital form of radiology in that quantitative rather than qualitative transmission measurements are made. Measurement of bone mineral content on a cadaver forearm (20) using absorptiometry was found to have an accuracy to within 4-7 % of that obtained from measurements of bone weight.

Reproducibility of measurements on a single individual were found to have a coefficient of variation of 2.5 %. These improvements in accuracy and precision of absorptiometry versus conventional X-rays were due to elimination or reduction of such causes of error as film exposure, development and calibration; measurement errors due to scattered radiation and the broad beam polychromatic x-rays as well as errors from soft tissue effects. Variations in quantities of soft tissue are reduced by submersion of the



MEASUREMENTS ARE MADE AT REGULARLY SPACED INTERVALS

FIGURE 3. ABSORPTIOMETRY

limb in water, thus providing a constant pathlength of attenuation. The radiological attenuation of fat, collagen, water and other organic components of soft tissue are all approximately equal.

Loss of vertebral skeletal bone has been shown to be reflected in measurements of radial bone mass, in particular in the distal region. A study was done (21,22) of 169 white women, 113 of whom had no fractures while 56 had radiological evidence of spinal fractures. Those women with no evidence of fractures had higher values of radial bone mass with a significance of 98.8 % for cortical bone and better than 99.9 % for trabecular bone. Although total bone mineral content was found to be a reliable determinant for diagnosis of decreased mineralization it was also found that in cases of very slight or exceptionally heavy built patients, evaluation of mineral content divided by bone width provided a more useful parameter. Absorptiometry studies involve measurement of a single radiation absorption profile. This allows one to evaluate total bone mineral content and thickness of cortical bone but quantitative evaluation of bone mineral density is not possible. Thus, absorptiometry requires a measurable change in the thickness of cortical bone or total bone mineral content to evaluate disease processes and this typically requires a period of several months to years.

In Vivo Neutron Activation Analysis (IVNAA)

Neutron activation analysis involves irradiation of a

volume by neutron bombardment and the subsequent detection of emitted radiation to determine the quantity of a particular material present (23). Irradiation of calcium in bone results in the production of a number of different isotopes of calcium. By measuring the radiation given off by one of these isotopes the quantity of that isotope can be calculated. Using the ratio of the quantity of that isotope to total calcium, total bone calcium can be calculated. This technique although providing valuable information is a costly process (requiring 14 MeV neutron sources) with limited accuracy and precision (of the order of 5 %).

Compton Scattering

Another technique which has been used for the in vivo measurement of bone mineral density is the Compton scatter technique (24). This technique involves the irradiation of a collimator defined volume and the measurement of Compton scatter from a particular portion of this volume by a collimated detector. From these measurements it is possible to determine the average electron density of the measured volume. The major limitations of the technique relate to the fact that only a relatively small volume of material can be studied and as such repositioning problems (in order to measure the same volume at a future time) are a major concern.

Radioisotope CT

Although CT, with its ability to image cross sections, would appear to provide a technique for measurement of bone

density there are a number of problems with standard commercial X-ray scanners that preclude such measurements. These problems are mainly manifest in the areas of beam hardening (due to use of a multi-energy X-ray source), physical resolution (due to the degree of collimation of the source and detectors) and the sample spacing (which is required to cover an abdominal area, leaving too little matrix in an area of bone for sufficient analyses to be carried out). A technique able to measure density of both trabecular and cortical bone with a precision of better than 1 % using a radioisotope CT scanner was first reported by R  egsegger and Elsasser (8) in 1975. The principles behind this special purpose CT scanner are the same as for commercial whole body scanners; however, changes have been made in order to facilitate the measurement of bone rather than soft tissue density. The technique involves performing a scan of the radius and ulna at a distal site , usually 1/10 the distance from the ulna styloid to the proximal point of the ulna. At this site although some 50 % of the bone area is trabecular it contributes only 10 % to the total bone mineral content. Given this relatively large area of trabecular bone it is possible to separately determine the density of both trabecular and cortical bone at this site. The technique is non-invasive, not traumatic to the patient and allows repeat measurements of the same sample to be performed.

It is also hoped that CT may be used to examine the

bone-cement and metal-cement contact on artificial hips (25). Although this problem is somewhat distinct from the measurement of bone density (and will require an X-ray tube photon source) many of the problems encountered are similar (i.e. measurement of radiological attenuation in high density areas such as bone). Upon implantation it is difficult to determine the degree of bonding of artificial hips and subsequent loosening may result.

Use of a photon source with energies higher than the 27.5 KeV of Iodine 125, such as Gadolinium 153 (40 KeV, 100KeV), may allow the CT scanner to be used for examination of bone gaps and degradation in patients who are having knee joints implanted. A higher energy source is required because of the quantity of bone involved and hence the high radiological attenuation. At present it is often necessary to perform an exploratory operation to determine the sizes of bone gaps and the amount of degradation of the bones. It is possible that the CT Scanner may be used to eliminate this exploratory surgery.

In order to fully appreciate the potential uses of a CT Scanner it is first necessary to have a basic understanding of what computed tomography is and how it works. This area will be explored in the next chapter.

III. Principles of CT Scanners

"CT" or computed tomography (7,26-30) is now the preferred name for "CAT"(computerized (assisted) axial tomography). A tomogram is literally a picture of a slice or section at a given orientation. Radiation in the form of gamma or X-rays are passed through (transmission tomography) or originate (emission tomography) from the desired plane of view without entering other areas. The amount of radiation absorbed along a given pathlength is measured and is an indication of the sum of linear attenuation coefficients or radiological densities along the pathlength. A linear attenuation coefficient is a measure of the absorption of radiation as it traverses a distance in an object. It should be noted that the attenuation coefficient in any object is dependent on the material composition and the incident photon energy. This sum of attenuation coefficients is measured along a sufficient number of pathways so that an image depicting the radiological densities (or attenuation coefficients) throughout the object can be reconstructed. Since this work deals primarily with transmission tomography any further references to CT will be referring to transmission CT.

To this date there have been 5 generations of CT scanners. These generations are identified by the type of mechanical motion used and the number of detectors employed. The first two generations of scanners (Figures 4 & 5) are known as single detector and multiple detector translation-rotation systems. Scans are performed by

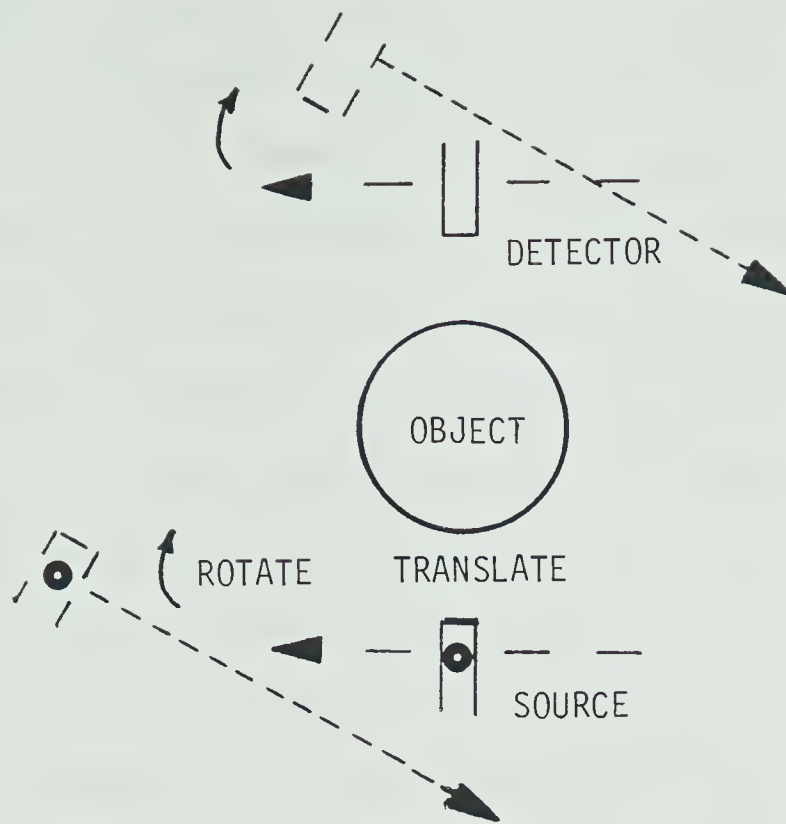


FIGURE 4. CT GENERATION 1

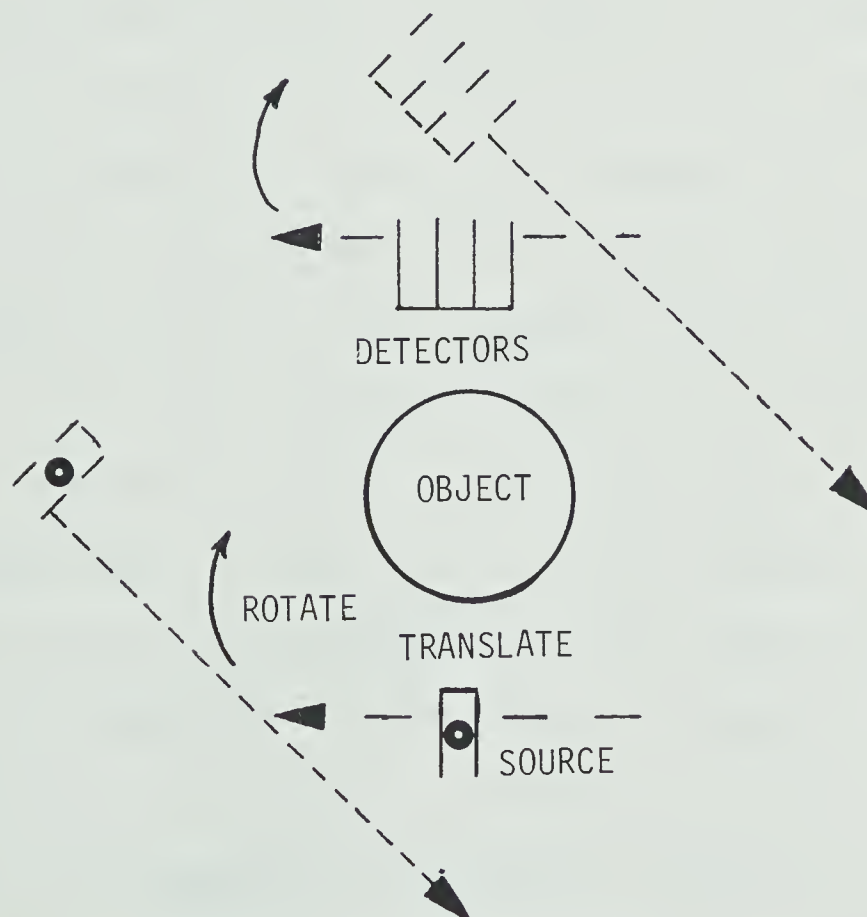


FIGURE 5. CT GENERATION 2

translating the source-detector configuration past the object at which point they are rotated about the object and the translation is repeated in the opposite direction. Measurements of ray-integrals or total radiological attenuation are continually measured during translation. This movement results in a "smoothing" or blurring of the object as the actual measured data is taken over a finite area of the object. Translations and rotations are repeated until the sum of the rotations meets or exceeds the 180 degrees required for complete reconstruction. Multiple detector systems are advantageous in that rotations between translations can be made through a larger angle and hence the number of translations and rotations can be decreased thus reducing scan time.

The third and fourth generation scanners (Figures 6 & 7) are multiple detector rotation-only systems. In the case of the third generation scanner the source and detectors each rotate about the same point through the required circle. In the fourth generation scanner the detectors form a stationary circle of 360 degrees and only the source is rotated. This eliminates the need to rotate the detectors and their associated high voltage and signal cables. The major advantage of the rotation only scanners versus the rotation-translation scanners is the reduction in scanning time. This reduction in scan time is important as it reduces image artifacts that can be caused by patient movement.

The fifth generation scanners (Figure 8) employ both

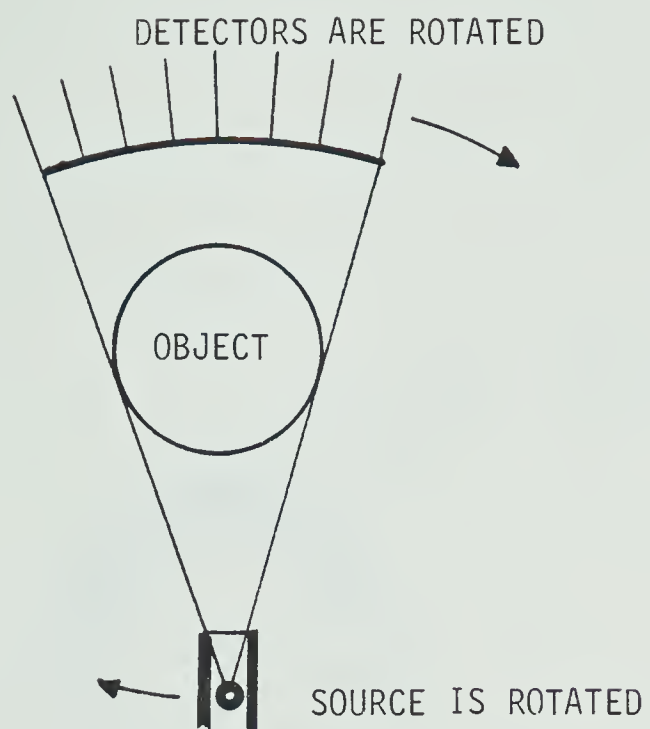


FIGURE 6. CT GENERATION 3

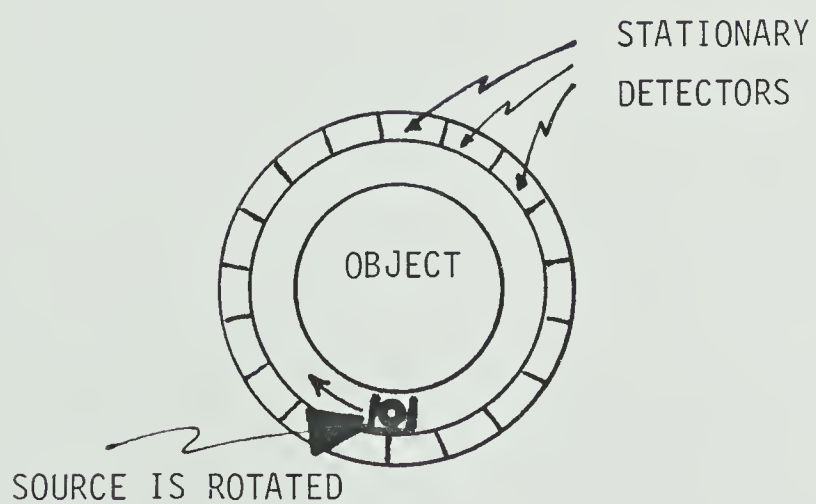


FIGURE 7. CT GENERATION 4

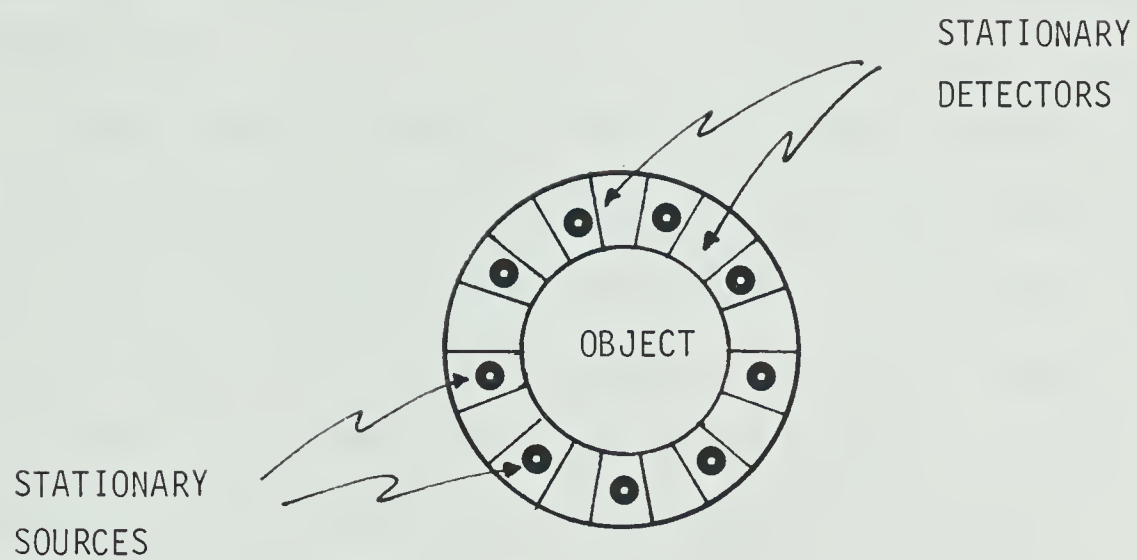


FIGURE 8. CT GENERATION 5

multiple sources and multiple detectors and may allow ultrafast scanning to produce dynamic representations of cardiac motion without special gating or synchronization techniques. Such scanners are a relatively new phenomenon and introduce additional problems in terms of expense and calibration.

Radiological attenuation along lines through the plane is often measured in a parallel beam format associated with the first two generations of scanners. This means that attenuations are measured along a series of regularly spaced parallel lines taken at a number of angular orientations (Figure 9). Each series of measurements taken at a given angular orientation is referred to collectively as a view or profile. In the cases of the third, fourth and fifth generation scanners data is collected in a rotational format(Figure 10). This data can be reordered and interpolated in order to create the parallel beam format thus permitting the same reconstruction algorithms to be used for all generations of scanners. However, special algorithms have been developed for the rotational format (31,32).

A. Back-Projections

The first technique (7) used for reconstruction involved a method now referred to as Back-Projection. ² For

² Capitalization is used to distinguish between Back-Projection as a method of image reconstruction, and back-projection as a process.

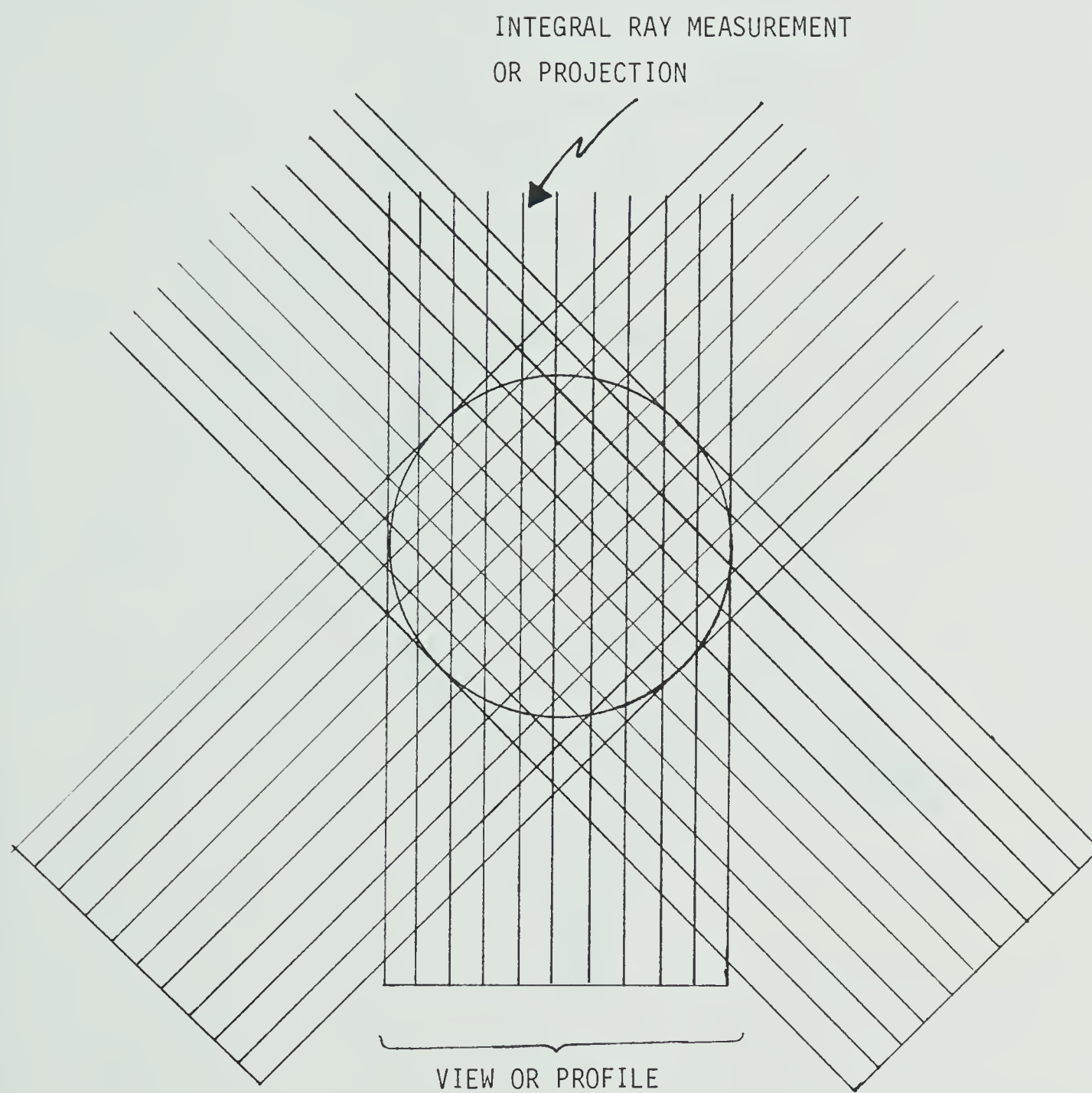


FIGURE 9. PARALLEL BEAM FORMAT

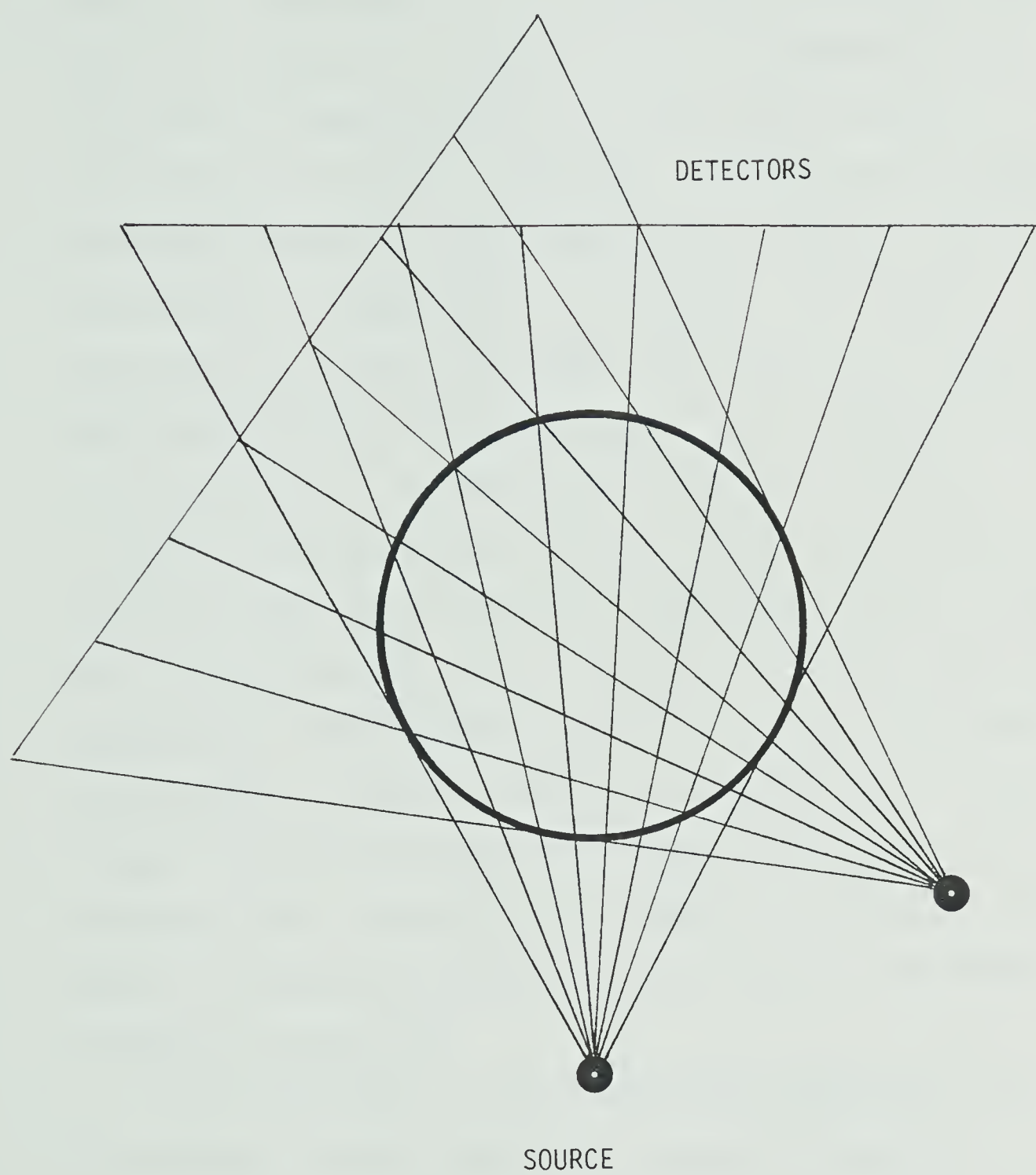
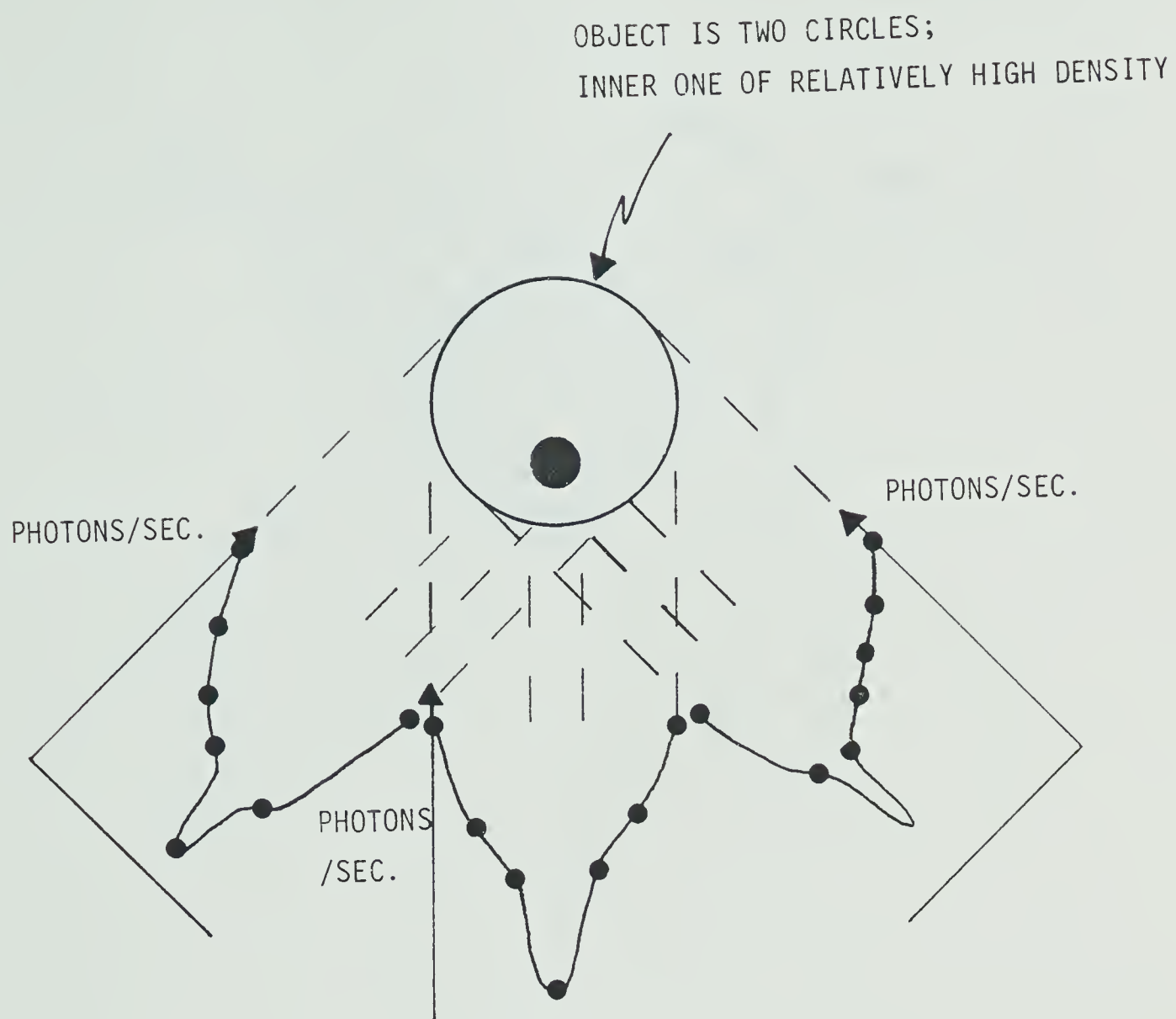


FIGURE 10. ROTATIONAL BEAM FORMAT

illustrative purposes three profiles or projections of an object have been taken (Figure 11) and are then back-projected to reconstruct the object in Figure 12. Each profile is made up of a discrete number of measurements taken at regularly spaced intervals. Reconstruction involves the back-projection of each profile onto a reconstruction matrix. This matrix reconstruction may be performed optically (for example on a screen), using analog electronics or digitally in a computer. The signal intensity according to a given ray sum is applied to all points that make up that ray and this is done for all projections giving an approximation to the original object. As seen in Figure 12 points outside of the original object may receive some of the back-projection intensity resulting in what is known as the "star" artifact. Points within the object also receive components from neighbouring points meaning that subtle differences in density cannot be determined. For these reasons Back-Projection is no longer being used as a technique for reconstruction. However, it does serve as a basis for understanding the reconstruction techniques presently being used.

The technique now used involves measurement of individual profiles and their respective angular orientations and the subsequent storage of this data in a computer. The data is then processed using mathematical algorithms and the reconstructed object is displayed on a plotter using different grey levels to represent the varying



PROFILES ARE MADE UP OF A DISCRETE NUMBER OF MEASUREMENTS

FIGURE 11. BACK-PROJECTION

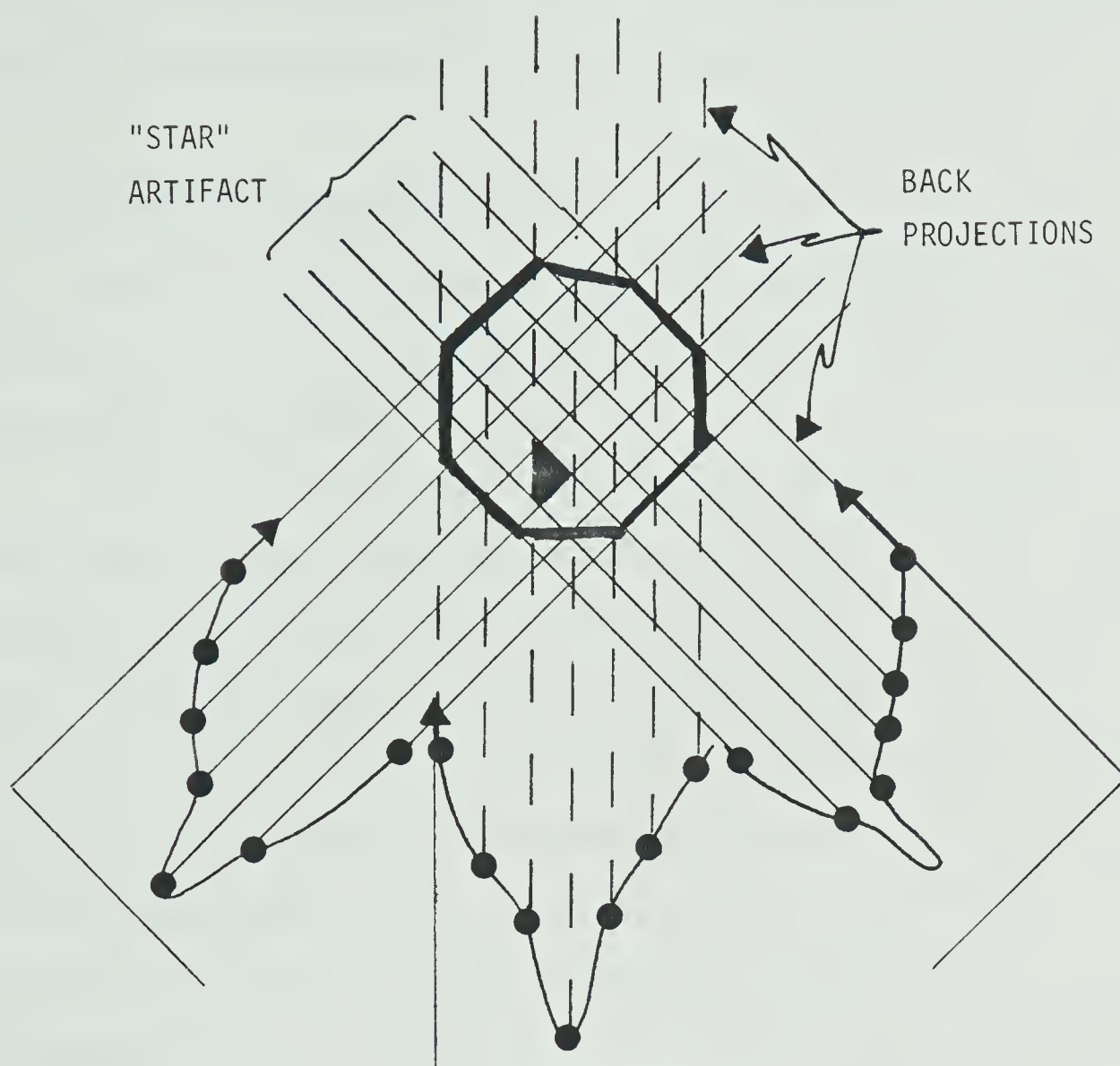


FIGURE 12. IMAGE RECONSTRUCTION USING BACK-PROJECTION

densities. Although the method depicted in Figures 11 and 12 merely sums the individual profiles, mathematical techniques allow for cancellation of back-projections and hence the object can be reconstructed more exactly.

B. Reconstruction Algorithms

The two main classes of algorithms used for reconstruction are the iterative and analytical techniques.

Iterative Technique

The iterative technique involves formulating an arbitrary image, calculating the profiles for that image and comparing these profiles to those obtained experimentally. The starting image is usually a blank screen (all ray profiles equal zero) or a circular grey object of uniform density (all ray profiles equal a constant). According to the differences in the measured profiles and those of the arbitrary image the image is modified and the profiles are compared again. This process is repeated until differences between the theoretical and experimental profiles are within acceptable limits. There are three general classes of the iterative technique (7). In the simultaneous correction technique each cell that contributes to a ray is altered and all projections are corrected simultaneously. This technique tends to overcorrect and hence iterations oscillate about the correct value. In the case of the ray-by-ray correction, corrections are made to all points of one ray at which point these corrections are taken into account prior to making

further corrections to a different ray. This technique is found to work best when large angles are taken between consecutive projections to be corrected. The third technique is a point-by-point correction in which each point is corrected for all rays that pass through it and all past changes are embodied into future changes.

In each of the three cases the corrective mechanism can be either additive or multiplicative. Additive, which is the method primarily used, refers to the fact that correction is divided among cells according to their weighting factor. In the multiplicative method, correction is applied to cells according to their present density. In this case a grey starting level is required. The iterative techniques can require a great number of iterations and computations and hence computing time may be a limiting factor.

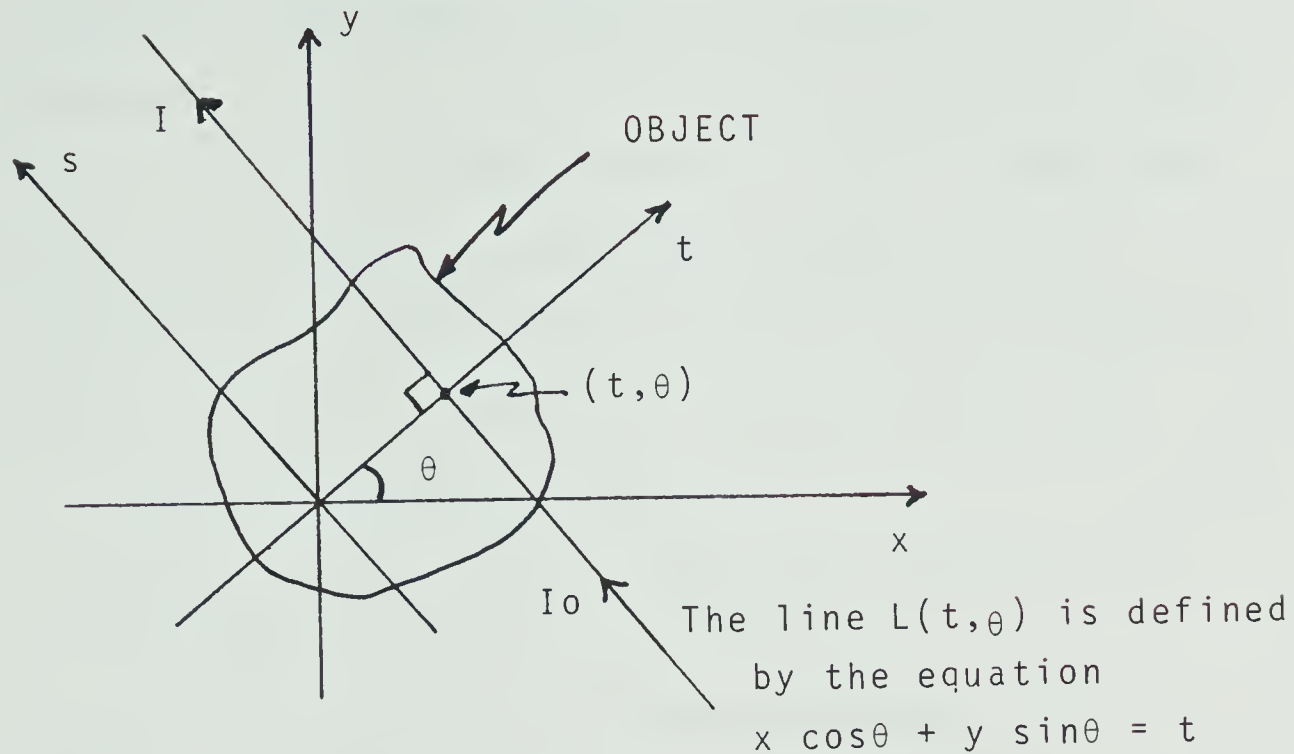
Analytical Technique

The Analytical Technique can be subdivided into two major categories: (1) two-dimensional Fourier reconstruction and (2) filtered Back-Projection. Two-dimensional Fourier reconstruction is based on the fact that the Fourier coefficients of the image are equal to the Fourier coefficients of the projections at the same angle. This means that if the Fourier coefficients of the projections are known then the Fourier coefficients of the image are also known and hence by taking their inverse transform the image of the object can be reconstructed. Until the introduction of the Fast Fourier Transform (FFT) and

improvements in high speed computers had taken place, this technique was not practical to use due to the number and complexity of the calculations involved. Mathematical development of this two-dimensional Fourier reconstruction technique is shown on the following pages.

Filtered Back-Projection or the convolution technique is based on this two-dimensional Fourier reconstruction. Papers by Shepp & Logan (33) and Ramachandran & Lakshminarayanan (34) have shown that this Fourier reconstruction may be viewed in the spatial domain as the sum of each ray-integral times a weighting function of the distance from the ray to the point of reconstruction. Thus reconstruction involves prefiltering each ray measurement by a weighting function and then back projecting these filtered ray measurements to reconstruct the object. This allows the image to be reconstructed as each ray measurement is taken rather than having to wait for all measurements to be completed. This method of reconstruction is accurate, simple and greatly reduces computation time over other available methods. The mathematical formulation of the convolution technique from Fourier reconstruction is also shown on the following pages.

ANALYTICAL RECONSTRUCTION TECHNIQUES



I_0 is the number of incident photons

I is the number of photons after passing through the object along line $L(t, \theta)$

In this diagram there are three different coordinate systems. The s - t coordinates are obtained by rotation of the x - y cartesian coordinate system while the ω - θ polar coordinate system uses ω as the radial component and the angle θ as the angular measure.

A line $L(t, \theta)$ (which is defined by the equation $x \cos \theta + y \sin \theta = t$) is chosen so as to pass through the object. This line depicts a ray integral measurement as would be made during a CT scan. In the parallel beam format a number of parallel ray-integral measurements (profile) would be made along a line $L(t, \theta)$ at which point

the angle θ would be altered and another profile measured. It is due to this pattern of measurement that the s-t coordinate system has been introduced. The use of the polar coordinate system permits convolution algorithms to be used for reconstruction. This aspect will be discussed later in the paper.

First, some definitions:

- (1) $f(x,y)$ is the linear attenuation coefficient at the point (x,y) ;
- (2) I_0 is the number of incident photons; and
- (3) I is the number of photons after passing through the object along line $L(t,\theta)$.

The total attenuation of the ray along line $L(t,\theta)$ is defined to be $P(t,\theta)$ which is equal to

$$-\ln(I/I_0) = \int_L f(x,y) ds$$

where ds is an incremental length along $L(t,\theta)$.

The one-dimensional Fourier transform of $P(t,\theta)$ is

$$\hat{P}(\omega, \theta) = \int_{-\infty}^{\infty} \exp(-i\omega t) P(t, \theta) dt = \int_{-\infty}^{\infty} \int f(x,y) \exp(-i\omega t) ds dt.$$

Now, consider the transform from the s-t coordinates to the x-y coordinates where

$$\begin{aligned} x &= t \cos\theta + s \sin\theta & , & \quad y = t \sin\theta - s \cos\theta & , \\ t &= x \cos\theta + y \sin\theta & \text{ and } & \quad s = x \sin\theta - y \cos\theta . \end{aligned}$$

The Jacobian which arises from the transformation is

$$\frac{\partial(s,t)}{\partial(x,y)} = \begin{vmatrix} \frac{\partial s}{\partial x} & \frac{\partial s}{\partial y} \\ \frac{\partial t}{\partial x} & \frac{\partial t}{\partial y} \end{vmatrix} = \begin{vmatrix} \sin\theta & -\cos\theta \\ \cos\theta & \sin\theta \end{vmatrix} = 1.$$

Hence $dsdt$ which is equal to the magnitude of the Jacobian times $dxdy$

$$= \left| \frac{\partial(s,t)}{\partial(x,y)} \right| (dxdy) = |1| dxdy = dx dy.$$

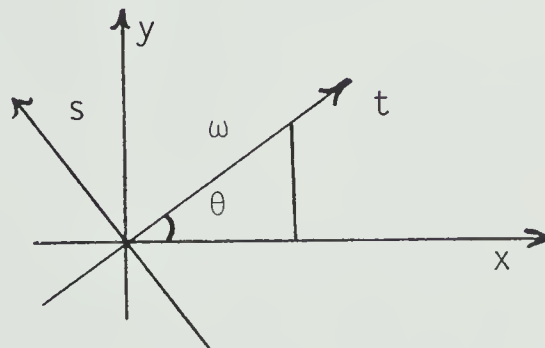
Therefore $\hat{P}(\omega, \theta)$ may be written as

$$\hat{P}(\omega, \theta) = \int_{-\infty}^{\infty} \int_{-\infty}^{\infty} f(x,y) \exp(-i\omega (x \cos\theta + y \sin\theta)) dx dy$$

which coincidentally is also the two-dimensional Fourier transform of x and y (define as $\hat{f}(\omega, \theta)$).

$$\text{i.e. } \hat{f}(\omega, \theta) = \int_{-\infty}^{\infty} \int_{-\infty}^{\infty} f(x,y) \exp(-i\omega (x \cos\theta + y \sin\theta)) dx dy$$

where ω is the spatial frequency in the direction of the t axis.



$$\text{Hence, } \cos\theta = x/\omega \quad \text{and } \sin\theta = y/\omega.$$

Now, if we consider the transformation from the x - y cartesian coordinate system to the ω - θ polar coordinate system the Jacobian arising from this transformation is

$$\frac{\partial(x,y)}{\partial(\omega,\theta)} = \begin{vmatrix} \frac{\partial x}{\partial \omega} & \frac{\partial x}{\partial \theta} \\ \frac{\partial y}{\partial \omega} & \frac{\partial y}{\partial \theta} \end{vmatrix} = \begin{vmatrix} \cos \theta & -\omega \sin \theta \\ \sin \theta & \omega \cos \theta \end{vmatrix} = \omega .$$

Hence, $dx dy$ which is equal to $\left| \frac{\partial(x,y)}{\partial(\omega,\theta)} \right| d\omega d\theta$
 $= |\omega| d\omega d\theta$.

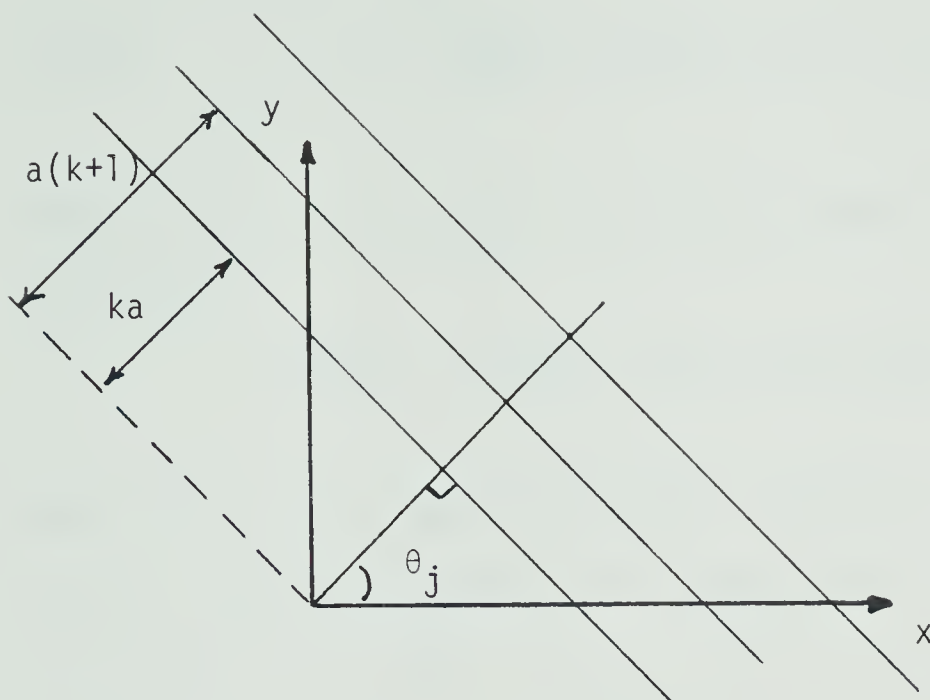
This means that $f(x,y)$ may be written as

$$f(x,y) = \frac{1}{4\pi^2} \int_0^\pi d\theta \int_{-\infty}^{\infty} P(\omega,\theta) \exp(+i\omega (x \cos \theta + y \sin \theta)) |\omega| d\omega .$$

Thus, $f(x,y)$ may be uniquely determined by a knowledge of $P(t,\theta)$ for all lines L . In reality $P(t,\theta)$ is known only along a finite number of lines which may be denoted by $t = t_k = ka$, $k = 0, \pm 1, \pm 2, \dots$;

$$j = \frac{j\pi}{n} , j = 0, 1, 2, \dots$$

where a is the parallel spacing between projections and n is the number of views.



Rewriting the integrals as finite sums we get

$$\int_0^\pi d\theta \approx \sum_{j=0}^{n-1} \frac{\pi}{n} \quad \text{and} \quad \int_{-\infty}^{\infty} d\omega \approx \sum_{k=-\infty}^{\infty} a.$$

By bounding the object to a circle of diameter a

$$\sum_{k=-\infty}^{\infty} \quad \text{can be rewritten as} \quad \sum_{k=-1/a}^{1/a}$$

where there are $2/a$ rays contained in each profile.

Hence, $f(x,y)$ may be written as

$$f(x,y) = \frac{a}{4\pi n} \sum_{j=0}^{n-1} \sum_{k=-1/a}^{1/a} P(\omega, \theta) \exp(-i\omega(x \cos\theta + y \sin\theta)) |\omega|.$$

Consider the Fourier inversion formula

$$f(x,y) = \frac{1}{4\pi^2} \int_0^\pi d\theta \int_{-\infty}^{\infty} \hat{P}(\omega, \theta) \exp(i\omega(x \cos\theta + y \sin\theta)) |\omega| d\omega$$

Substituting in $t = x \cos\theta + y \sin\theta$ the inner integral may be written as

$$Q(t, \theta) = \int_{-\infty}^{\infty} \hat{P}(\omega, \theta) |\omega| \exp(i\omega t) d\omega.$$

Now if $f(x,y)$ is a smooth function, then $P(t, \theta)$ will be a smooth function and hence $\hat{P}(\omega, \theta)$ will be bandlimited.

i.e. for $\omega > \Omega$ $\hat{P}(\omega, \theta) \rightarrow 0$.

If there also exists an even function

$$\hat{\Psi}(\omega) = \int_{-\infty}^{\infty} \Psi(t) \exp(-i\omega t) d\omega$$

which equals $|\omega|$ for $\omega < \Omega$

then $Q(t, \theta)$ can be approximated by

$$Q(t, \theta) \simeq \int_{-\infty}^{\infty} \hat{\Psi}(\omega) \hat{P}(\omega, \theta) \exp(i\omega t) d\omega$$

which according to the Convolution theorem is a convolution in the time domain.

$$Q(t, \theta) = 2\pi \int_{-\infty}^{\infty} \Psi(\tau) P(t-\tau) d\tau$$

$$\text{Therefore, } f(x,y) = \frac{1}{2\pi} \int_0^\pi \theta \int_{-\infty}^{\infty} P(\tau, \theta) \Psi(t-\tau) d\tau$$

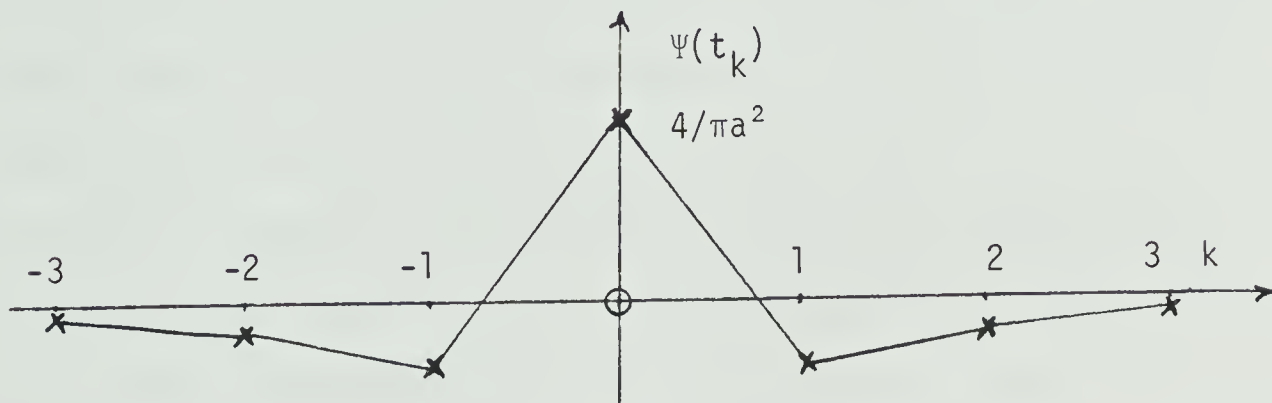
Once again writing the integrals as finite summations we get

$$f(x,y) = \frac{a}{2n} \sum_{j=0}^{n-1} \sum_{k=-1/a}^{1/a} P(t_k, \theta_j) \Psi(x \cos \theta_j + y \sin \theta_j - t_k)$$

Thus $f(x,y)$ can be written as a summation of the ray integrals times a weighting function Ψ which is a function of the distance between the line $L(t_k, \theta)$ and the point of reconstruction (x,y) . One commonly used weighting function (derived by Shepp and Logan) is

$$\Psi(t_0) = \frac{4}{\pi a^2} ; \Psi(t_k) = -4/(\pi a^2(4k^2-1)) , k = \pm 1, \pm 2, \dots$$

with linear interpolations in the intervals.



Allowing Ψ to be linear in the intervals is not incompatible with the requirement that for small w , $\hat{\Psi}(w) \approx |w|$ and greatly reduces computational time since the weighting function can be computed and stored and values at intermediate points can be obtained through interpolation.

The Shepp, Logan weighting function $\Psi(t)$ has the Fourier transform

$$\hat{\Psi}(w) = \left| \frac{2}{a} \sin \frac{wa}{2} \right| \left(\sin \left(\frac{wa}{2} \right) / \left(\frac{wa}{2} \right) \right)^2.$$

$$\text{When } w \rightarrow 0, \hat{\Psi}(w) \rightarrow \left| \frac{2}{a} \frac{wa}{2} \right| \left(\left(\frac{wa}{2} \right) / \left(\frac{wa}{2} \right) \right)^2 = |w| (1)^2 = |w|$$

and thus the necessary requirement is met.

Comparison of Analytical and Iterative Algorithms

Both the iterative and analytical techniques have characteristic advantages and disadvantages. It is generally accepted (7) that analytical methods are faster than are iterative. Use of the convolution technique also allows the image to be reconstructed as measurements are made. In both cases there are problems associated with reconstruction. Due to the digitization involved in analytical methods the projections must be bandlimited. This means that an overshoot phenomenon will occur at sharp edges such as bone-flesh interfaces. Although this effect can be partially corrected by prefiltering, any such gains will be offset by a loss in spatial resolution. Iterative techniques are able to avoid the problems associated with sharp interfaces.

With complete data the two types of algorithms are comparable with respect to the amount of noise in the image. However, in cases where some of the data is missing, the iterative technique will prove to be superior since it merely "smooths" the image while the analytical techniques assume the missing data is the same as the available data.

C. Photon Attenuation

The ability of CT to distinguish between narrowly differing densities is dependent on the characteristics of photon attenuation. As photon radiation passes through an absorbing medium it is absorbed exponentially according to the following relationship (35,36);

$$I(S) = I_0 \exp -(\mu(S-S_0))$$

where I_0 is the number of photons at a distance $S=S_0$ and μ is the linear attenuation coefficient. This absorption is due to four processes: the photoelectric process, the Compton process, coherent scattering and pair production. The linear attenuation coefficient (μ) has units of inverse distance and is a measure of the fraction of photons removed per unit length of absorber. μ may be converted to either the mass, electronic or atomic attenuation coefficients by dividing by either mass density ρ (gm/cm³), electron density ρ_e (electrons/cm) or atomic density ρ_a (atoms/cm³). At moderate energies (less than 1.02 Mev) photon attenuation predominantly consists of two contributions: (1) Compton scattering, which is proportional to electron density and (2) photoelectric absorption which is a function of the atomic number of the element (approximately Z^4). At the lower edge of the energy spectrum it is the photoelectric effect which is predominant and as such, measured attenuation is representative of the atomic numbers of the elements contained in the object. If either simultaneous or sequential scans at different energies (37) were used it would be possible to obtain measures of both the Compton and photoelectric effects allowing for evaluation of both electron density and atomic number. Hence an in vivo elemental identification is possible using CT (38).

Statistical Considerations

Radioactive decay is a statistical process that can be

modelled by a Poisson distribution (39-43). The characteristic of a Poisson process is that the mean and variance are equal. This means that the coefficient of variation (which is equal to the standard deviation divided by the mean) is equal to $1/\sqrt{\text{mean}}$. One implication of this is that the higher the associated count rate the lower the coefficient of variation will be. For example; a count rate of 10,000 has an associated coefficient of variation of $1/\sqrt{10,000} = 1\%$.

Thus the lower the radioactivity of the source the longer the required counting period in order to maintain the same coefficient of variation. In order that the statistics be maintained and further blurring of the image does not occur (due to measurement over a finite area) the scanner would have to translate more slowly and hence the overall time of the scan would be increased. If the scan takes too long, artifacts due to patient movement become a problem.

Dead Time

Radiation detectors and the associated electronics have finite resolving times. After a system records a pulse it is unable to respond to another pulse for a brief period, known as the dead time. As a result the number of pulses recorded by the counting system is less than the actual number of pulses that occurred. This means that the measured statistics of the process have been altered due to the measurement equipment.

In order to rectify this situation it is necessary to

measure the dead time of the system and to use this measurement to correct the measured pulse count. For most applications system dead time is independent of the count rate. Hence, once system dead time has been established, corrections can be made for any count rate.

System dead time (p) is determined by measuring (in order):

1. the background count rate (B),
2. the count rate resulting from one source (n_A),
3. the count rate resulting from two sources (sources A & B) (n_s), and
4. the count rate resulting from source B (n_B).

If this order of measurement is followed any errors due to accurate repositioning of sources will be eliminated. If the true count rate is N and $np < 0.05$ then the following expression is valid (44) ;

$$N = n(1 + np)$$

In the cases of the above measurements this results in the following three expressions;

$$N_A + B = n_A(1 + n_A p)$$

$$N_B + B = n_B(1 + n_B p)$$

$$N_A + N_B + B = n_s(1 + n_s p)$$

Adding the first two equations together and subtracting the third equation from the result leads to the following expression (solving for p);

$$p = (n_A + n_B - n_s - B) / (n_s^2 - n_A^2 - n_B^2).$$

Thus for a measured count rate (n) the fraction of lost

counts is $n(p)$ and hence $n(n)(p)$ counts must be added to n to give the true number of counts N . This correction is easily performed by a computer.

Beam Hardening

Absorption of radiation is dependent on the energy of the radiation. As a polyenergetic beam passes through an object the lower energy beams are more severely attenuated than are the higher energy beams. This results in the beam being "hardened" as it is composed of a greater proportion of high energy beams the farther along it is in the object (45-48). Thus in order to determine absolute densities of an object the beam must be either monoenergetic or else non-linear corrections must be applied. Correction for beam hardening may be either material selective or non-material selective. Material selective correction takes into account the type of absorption material and the resultant hardening. This requires knowledge of the types of absorption materials present and the quantities involved and hence an initial reconstruction must first be made. Then the raw data must be manipulated according to the first reconstruction to produce the corrected image. Non-material selective beam hardening merely recognizes that beam hardening has occurred and uses a beam hardening curve to correct the raw data before reconstruction.

If one measures the amount of beam hardening as a function of distance then these curves may be used to correct raw data. For example, if a measurement of $\ln(I_0/I)$

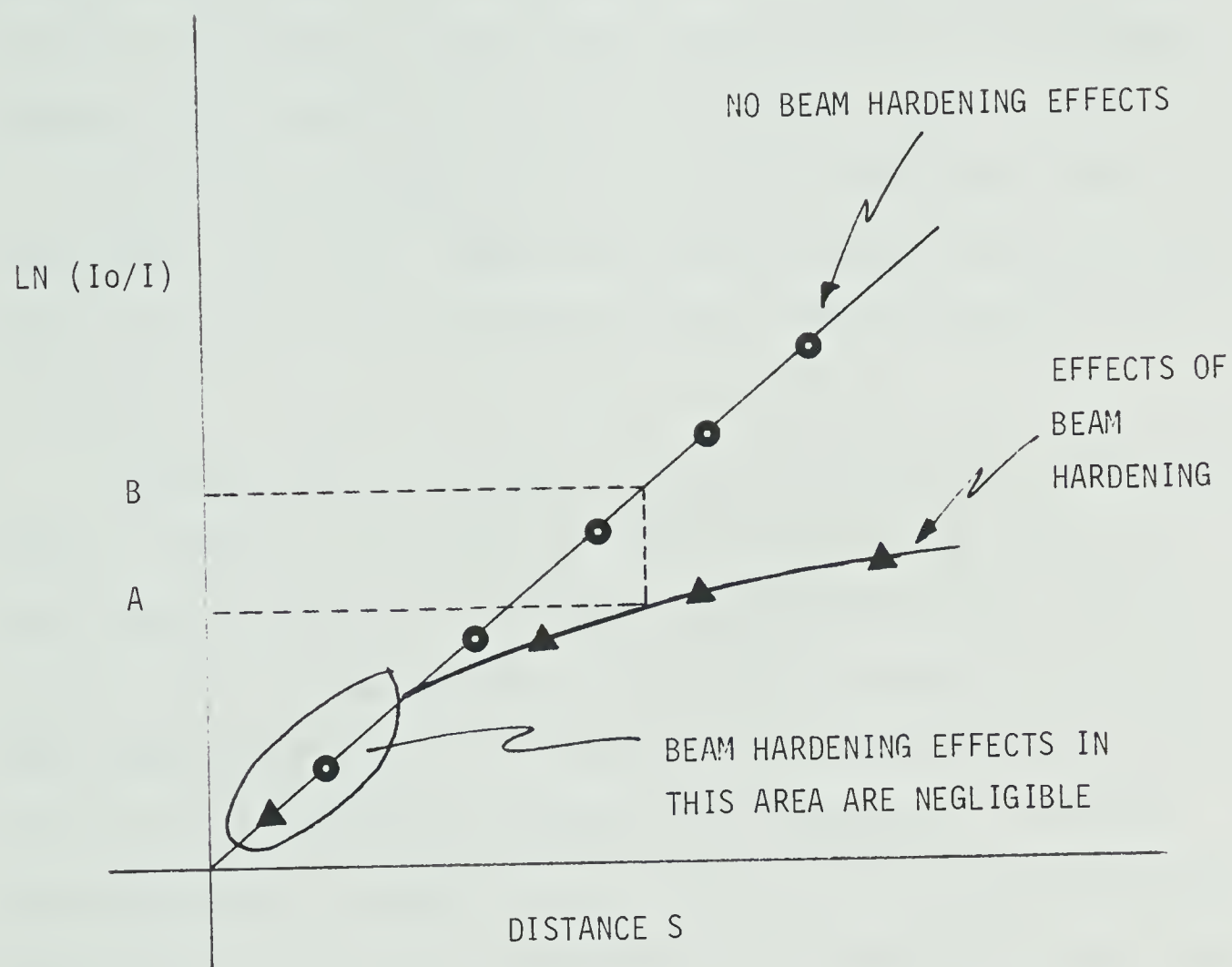
= A (Figure 13) is made, the corrected value B, which is the value that would be obtained if there was no beam hardening, is easily obtained from the curve. This procedure can easily be performed for all ray-integral measurements prior to reconstruction. It is interesting to note that the correction required for measurements of relatively low values of $\ln(I_0/I)$ is small and hence inaccurate corrections for measurements such as through skin (as contrasted to bone) introduces negligible error.

Non-material selective correction techniques for beam hardening are obviously not as accurate as are selective techniques however for objects consisting predominantly of one or two absorption materials it does provide a quick and simple correction technique.

D. Detector Types

Primary considerations in regards to selection of a detector include resolution, efficiency, energy of radiation, counting rates, and in some applications, size. Energy resolution of a detector is its ability to distinguish between different energy photons. This is often defined as a percentage or ratio of the full width half maximum divided by the primary energy level. Detector efficiency refers to the percentage of rays at a specified energy that will interact with the detector rather than being simply passed through the detector.

Three common detector types are gas, scintillation and



GIVEN A LINEAR ATTENUATION COEFFICIENT μ
 $\text{LN}(I_o/I) = \mu \times S$ OR $I = I_o \text{ EXP}(-\mu \times S)$

FIGURE 13. BEAM HARDENING CORRECTION

solid state, all of which work on the principle of photons exciting the detector material resulting in the production of ions, optical radiation and electrons respectively. These phenomena are then converted to electronic signals, the magnitude of which are proportional to the photon energy, and the frequency of which are proportional to the number of photons per second striking the detector.

Solid state detectors have better resolution than do the other two types. They are also much more expensive and hence are only used in applications where resolution is critical.

Gas detectors although usually having worse resolution and efficiency than scintillation detectors do have the advantage of generally being more economical and smaller in size. It is for this reason that most fan-beam machines use xenon gas detectors (7) instead of scintillation detectors. Scintillation detectors however are economical, readily available and are easy to use. These factors coupled with reasonable resolution, efficiency, and counting rates have led to the utilization of scintillation detectors for many spectroscopic applications.

Scintillation Detector

A scintillation detector is composed of two basic parts : (1) a scintillation crystal and (2) a photomultiplier tube.

Scintillation Crystal

The scintillation crystal is a transducer that

converts photons of energy to light pulses of proportional intensity to the energy of the photon. There are both in-organic and organic materials in use for this purpose. Sodium Iodide crystals NaI(Tl) are the most commonly employed crystals for gamma-ray spectroscopy. It is desirable to have a high ratio of counts under the full energy peak relative to the total number of counts and this ratio is approximately four times greater for Sodium Iodide than for example Cesium Iodide crystals CsI(Tl), with the same gamma-ray primary energy. This ratio is also increased by the use of collimators which restrict radiation to the central part of the crystal. Use of a Thallium impurity (0.1 %) acts as a wavelength shifter causing the crystal to emit 2 or more low energy photons (visible light) instead of a single Ultra Violet photon. UV photons are not suitable since they are absorbed by most materials even those transparent to visible light. At low energies, typical resolution for NaI crystals ranges from 6-8 % for crystals under 5 cm diameter to 8-10 % for crystals from 5-10 cm diameter. Thicker crystals provide more efficient light collection and increase crystal efficiency so that the same crystal may be used with higher energy sources. If the crystal is too thin high energy rays may not interact with crystal.

Photomultiplier Tube

A photoemissive cathode detects the light pulses

produced by the crystal and in response produces primary electrons. These electrons are electrostatically focused and accelerated by means of a voltage differential to the first dynode in the tube. Upon arrival at the dynode they possess enough energy so that for every primary electron more than one secondary electron is produced. This procedure is continued throughout an arrangement of dynodes (typically 10) until the final stage which is the anode. The voltage at the anode following the passage of a charged particle through the phosphor of the crystal is equal to the charge of the electrons at the anode divided by the capacitance of the anode and is proportional to the intensity of the light impulse over a wide range of photomultiplier gain. Head on type PMT's have a semitransparent photocathode which is in contact with the inside of the glass window. Head-on versus side-on photomultiplier tubes are generally used for scintillation counting due to improved uniformity and collection efficiency.

Anode Load

The signal on the anode has a rise time which corresponds to the fluorescence decay time of the crystal. This signal decays through the anode load R_L (Figure 14) which is the resistor between the anode and the high voltage supply and the parallel combination of the anode to ground capacitance (typically 10 pf) and the output line capacitance to ground (typically 10 pf).

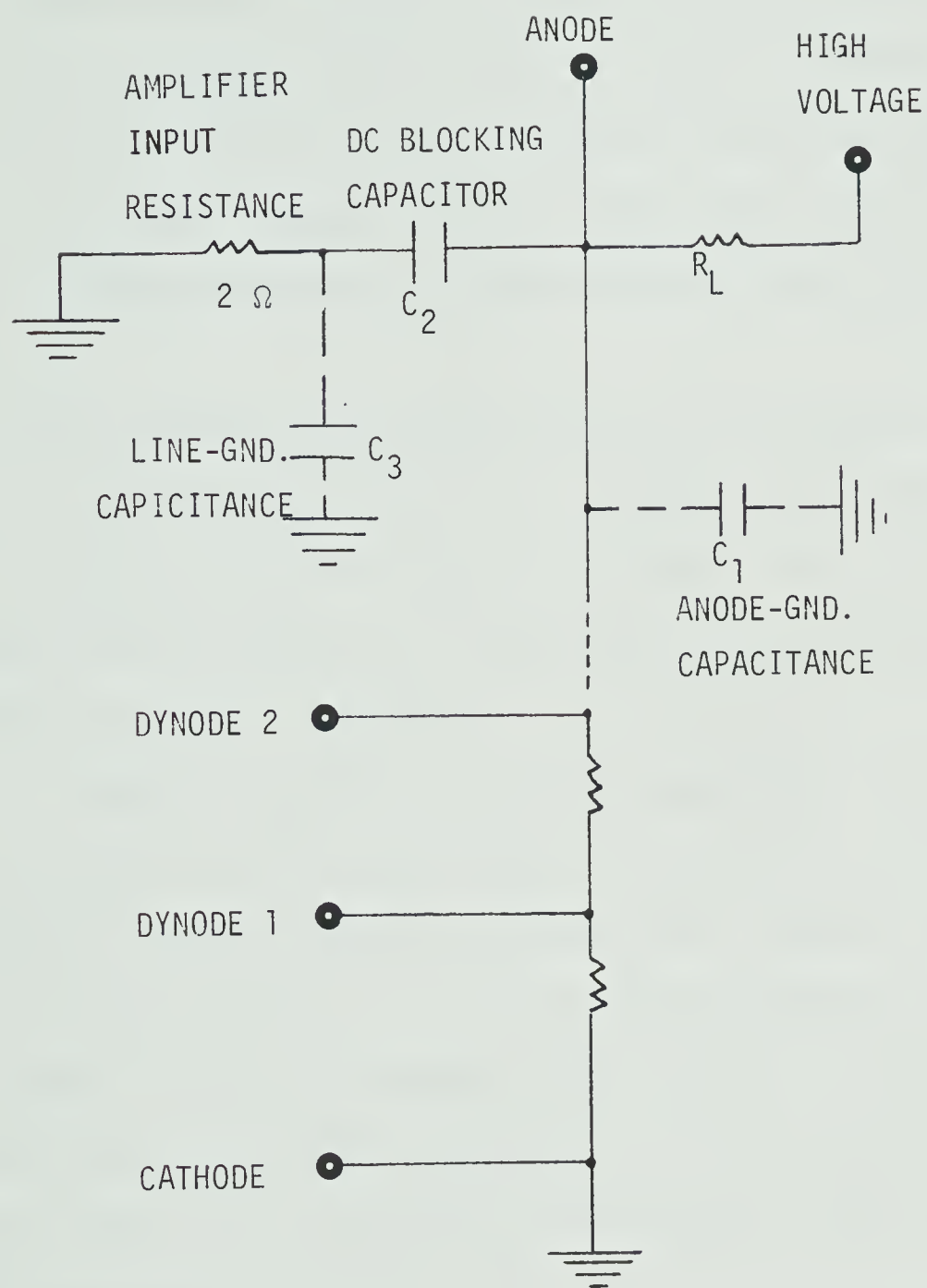


FIGURE 14. PHOTOMULTIPLIER TUBE & RELATED CIRCUITRY

The capacitances are virtually fixed values and are not easily changed and it is only the anode load that is easily altered. The signal on the anode must decay away fast enough so that pulse pileup is not a problem and slow enough so that pulse height is significantly larger than existing noise. Pulse pileup occurs when signals do not have enough time to decay away and the next signal is superimposed on the partially decayed signal.

E. Performance Characteristics Of CT Scanners

Prior to this point it has been the component parts of a CT system that have been reviewed. This section examines how some attributes of the overall system are related to these distinct segments.

Resolution of a CT system comprises two distinct, although interrelated types of resolution: spatial resolution and contrast resolution. Spatial resolution of a CT system refers to the minimum size object that can be imaged by the system when that object is part of a periodic structure. Contrast resolution is that percent change in contrast at an interface that can still be imaged given a minimum spatial resolution.

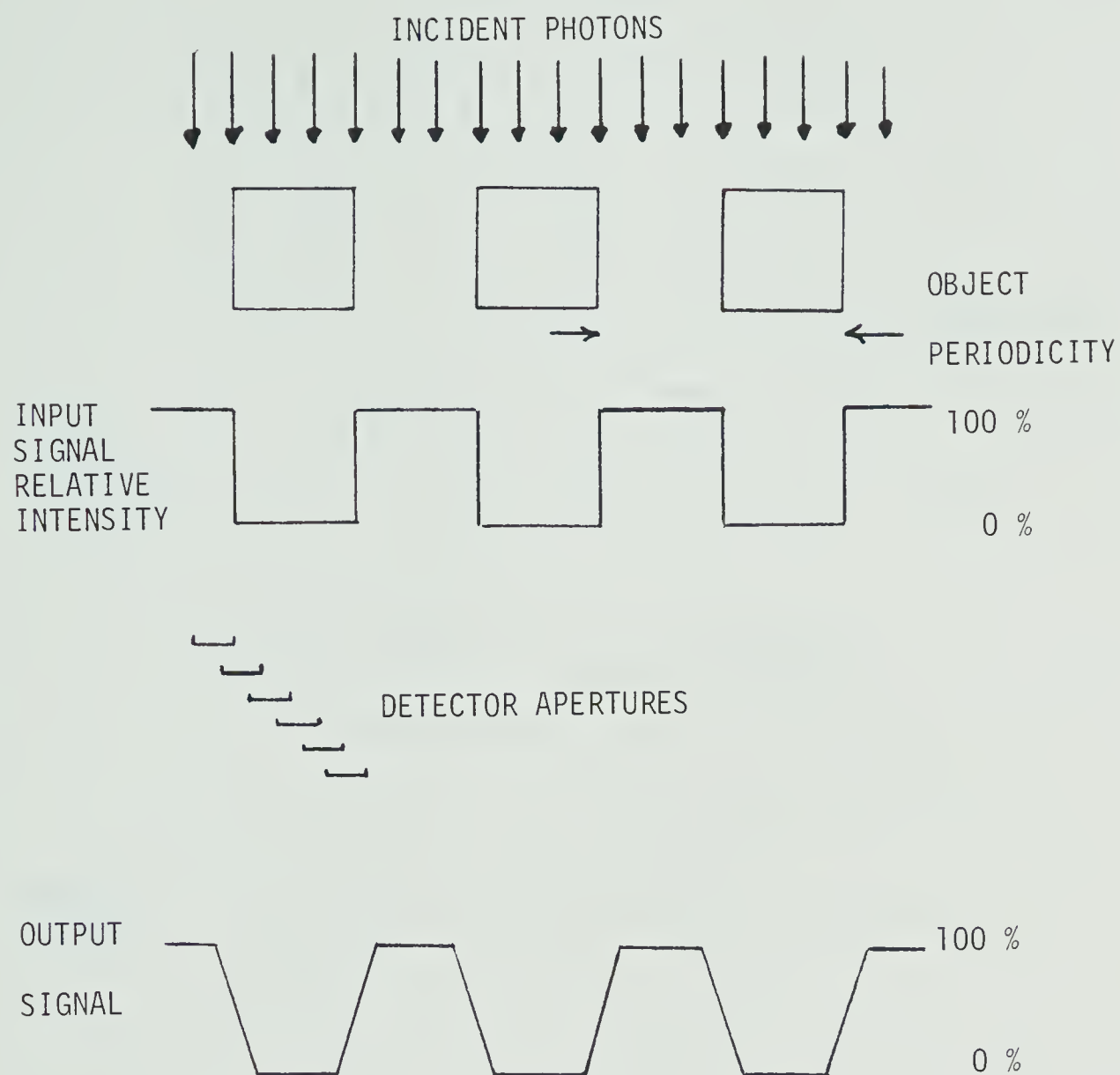
Spatial Resolution

Assuming a constant photon flux there are four major factors which affect the spatial resolution of a CT system (49). These are the width of the detector element aperture, the distance between reading or sampling points, the form of

the convolution filter used, and the element size of the display picture (pixel size). In order to examine the spatial resolution of a system it is useful to employ a concept known as the Modulation Transfer Function (MTF). Values of MTF vary from 0 to 1 and are an indication of how well the imaging system transfers the frequency components of the object into the final image. An MTF value of 1 (or 0) means that all (or none) of the frequencies present in the original object exist in the final image. Good spatial resolution then, would be indicated by large values of the MTF extending into the high frequency range.

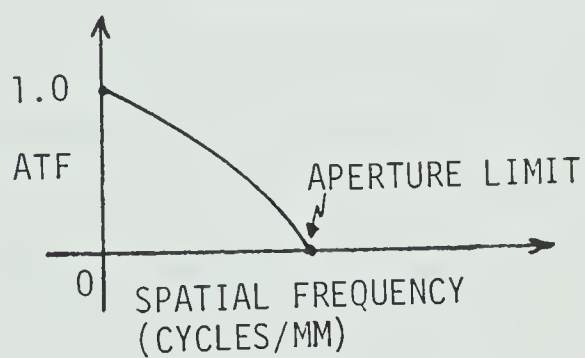
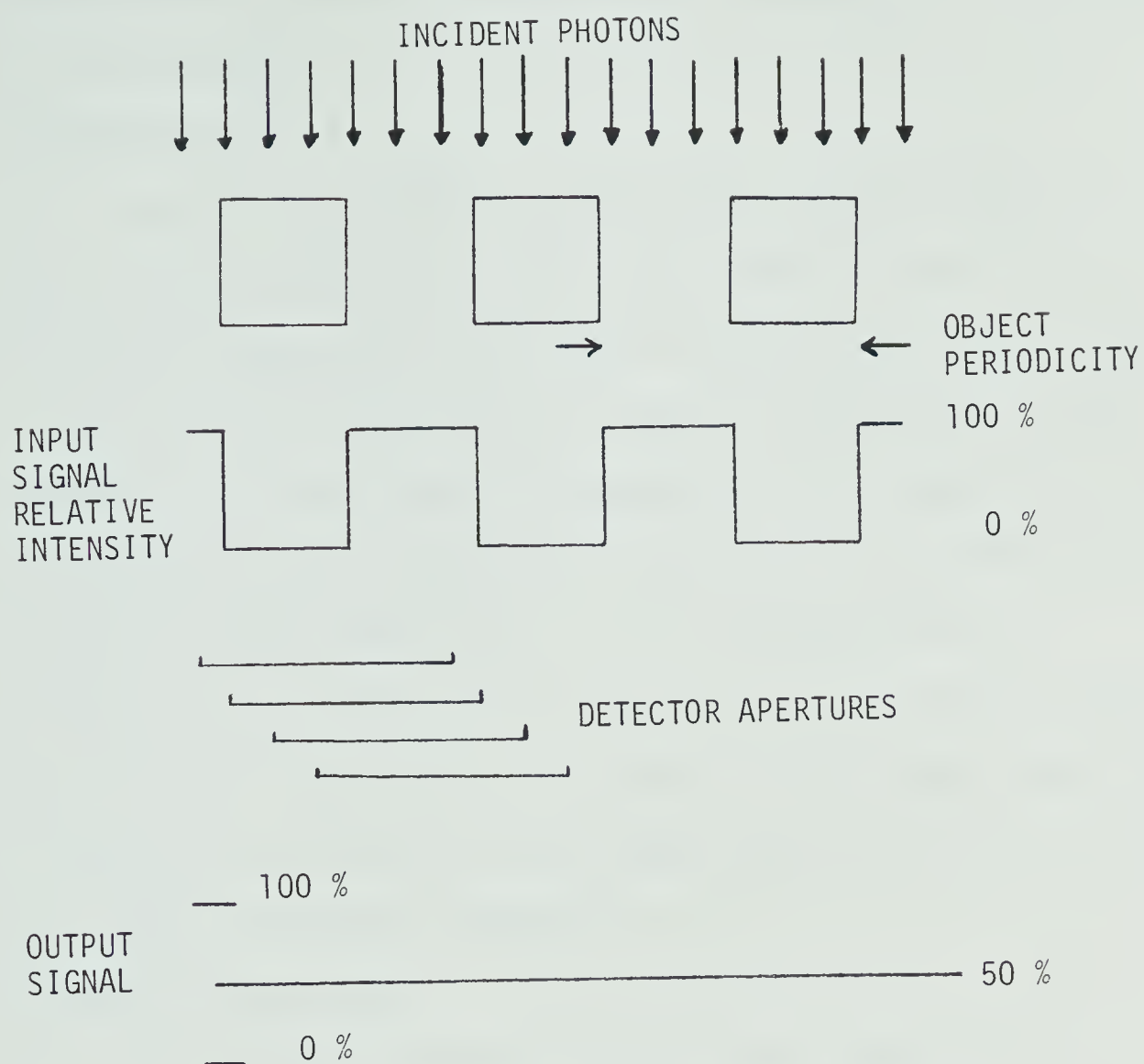
Aperture Size

The effect of aperture size can be seen by examining the results obtained by viewing a series of repeating objects through different size apertures while holding all other variables constant. From Figure 15 we see that when the size of the aperture is much smaller than that of the object spacing, the amplitude of the output signal approaches that of the input signal. Thus the aperture limited MTF or the ATF would approach unity. As can be seen from Figure 16, if the aperture size is increased, the amplitude of the output signal becomes smaller than that of the input signal and the value of the ATF is decreased. When the size of the apertures approach twice that of the object periodicity, all information is lost and the ATF approaches zero. The net effect is: the smaller the aperture, given other



WHEN THE OBJECT SPACING IS MUCH GREATER THAN THE DETECTOR APERTURE THE OUTPUT SIGNAL CLOSELY RESEMBLES THAT OF THE INPUT SIGNAL AND THE ATF APPROACHES 1.

FIGURE 15.



WHEN THE OBJECT SPACING IS EQUAL TO THE DETECTOR APERTURE
THE OUTPUT SIGNAL CONTAINS NO INFORMATION AND THE ATF IS 0.

FIGURE 16.

parameters constant, the greater the spatial resolution of the system.

Sampling Rate

According to the Nyquist theorem, in order to accurately reconstruct an object that is part of a periodic structure, the sampling rate must be at least twice that of the highest frequency component in the structure. The tradeoff associated with sampling at high frequencies is a resultant increase in the noise of the reconstructed image (33). If the image contains frequencies greater than the Nyquist frequency, aliasing will occur resulting in streaks in the image emanating from such sources as bone edges which contain a number of high frequency components.

Convolution Filter

It has been found (49) that the higher the frequency response of the convolution filter used in the reconstruction, the greater the resultant spatial resolution. The problem is that the higher the frequency response of the filter, the greater the resultant noise of the reconstructed image and hence a tradeoff is required.

Contrast Resolution

Another area of importance to CT scanners is their contrast resolution. This is measured by examining the system limiting spatial resolution with different contrast media. The limiting factor of CT systems in regards to

contrast resolution is the presence of noise. The signal to noise ratio can be improved by increasing the incident photon fluence rate (reflux). However, increasing radioactivity will result in a corresponding increase in patient dosage. One measure of contrast resolution used for commercial scanners (49) is obtained by multiplying the hole diameter (in mm) by the contrast (in percent) and the square root of the dose (in rads). Inclusion of the dose in this calculation results in a measure of contrast resolution independent of dose rate.

F. Commercial CT Scanners

As mentioned previously it is necessary to make alterations to commercial CT scanners before they can be effectively used for measurement of bone mineral density. Having examined some of the theoretical concepts of CT scanning an examination of the differences between a commercial CT scanner and one designed for measurement of bone mineral density will now be given.

Commercial whole body CT scanners are both large and expensive: typically \$600,000 - \$1,000,000 and the source of radiation is virtually always an X-ray tube. These scanners are oriented towards measurement of soft tissues such as the abdomen. In these areas the application of the scanner is generally to locate tumors which will be depicted as an area of density different from that of the surrounding region. Absolute densities are generally not of concern so much as

the ability to distinguish between areas of different densities. Commercial CT scanners are typically fourth generation scanners allowing scans to be performed in under five seconds. Increased speed reduces the problem of movement artifacts and means less inconvenience to the patient.

In transmission CT the source of radiation may be either an X-ray tube or a radioisotope. An X-ray tube is advantageous over a radioisotope due to a greater photon flux. They do however have the disadvantages of a high initial cost (\$30,000), large physical size and the requirement of a large amount of calibration and adjustment. There is also the possibility of a higher dose rate of radiation with an X-ray tube source.

There are also many problems that actually preclude the use of commercial CT scanners for measurement of bone density. The major problem is manifest in the area of system spatial resolution. Use of a multi-energy X-ray source means that beam hardening may be a major problem and the fact that such scanners are looking at relative rather than absolute density means that the data required for beam hardening correction is often not readily available. This is further complicated by the fact that the detectors used in commercial CT scanners are not operated in a pulse counting mode and hence they cannot provide energy discrimination of detected photons. Sources and detectors are usually not finely enough collimated to provide the initial physical

resolution and the size of the reconstruction matrix usually means that the area associated with an object the size of a bone is too small for an accurate determination of average density of the area. This is due to the fact that the reconstruction matrix of such a system is typically required to cover an area the size of an abdominal cross-section.

Commercial CT scanners could be used for the measurement of bone mineral density. However, they would first require recollimation of the source and detectors and software would have to be altered to correct for beam hardening and to increase the matrix size of the area of analysis. These changes would require a significant disruption of an expensive piece of equipment: a disruption not presently justified given the alternative use of a smaller, radioisotope CT scanner.

IV. System Design and Construction

This section will cover five areas of design and construction of the scanner. These include: (1) mechanical operation, (2) radioactive source and detectors, (3) scanner control, (4) adjustments required for a multi-detector system, and (5) data processing. The initial system design and construction were for a generation one CT system. Subsequent to the successful completion of the generation one system the necessary modifications to convert to a generation two system were undertaken.

A. Mechanical Operations

The major design requirement insofar as mechanical operation of this device is concerned, is the ability to properly position the source-detector configuration in both the longitudinal and rotational axes.

Stand

The stand (Figure 17) was designed to contain the controls such as the microprocessor unit, the power supplies, relays, source and detectors on one portable unit. The ability to position the scanner at different heights was required so as to facilitate measurement of both arms and legs. This was accomplished by mounting the scanner plates on a board with a 12 inch diameter hole cut in the center which slides vertically on ball bushings and is driven by a hand operated ball screw.

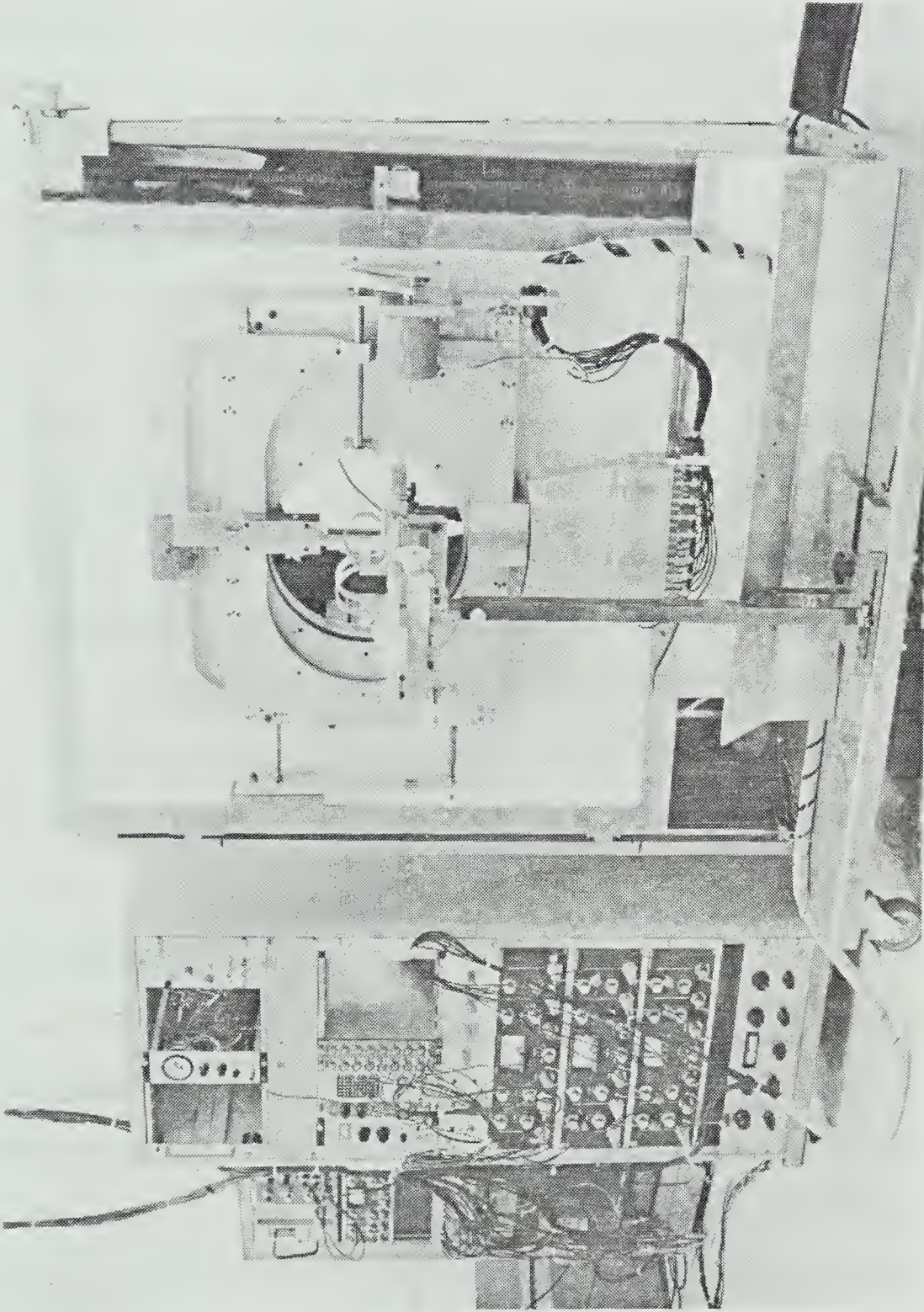


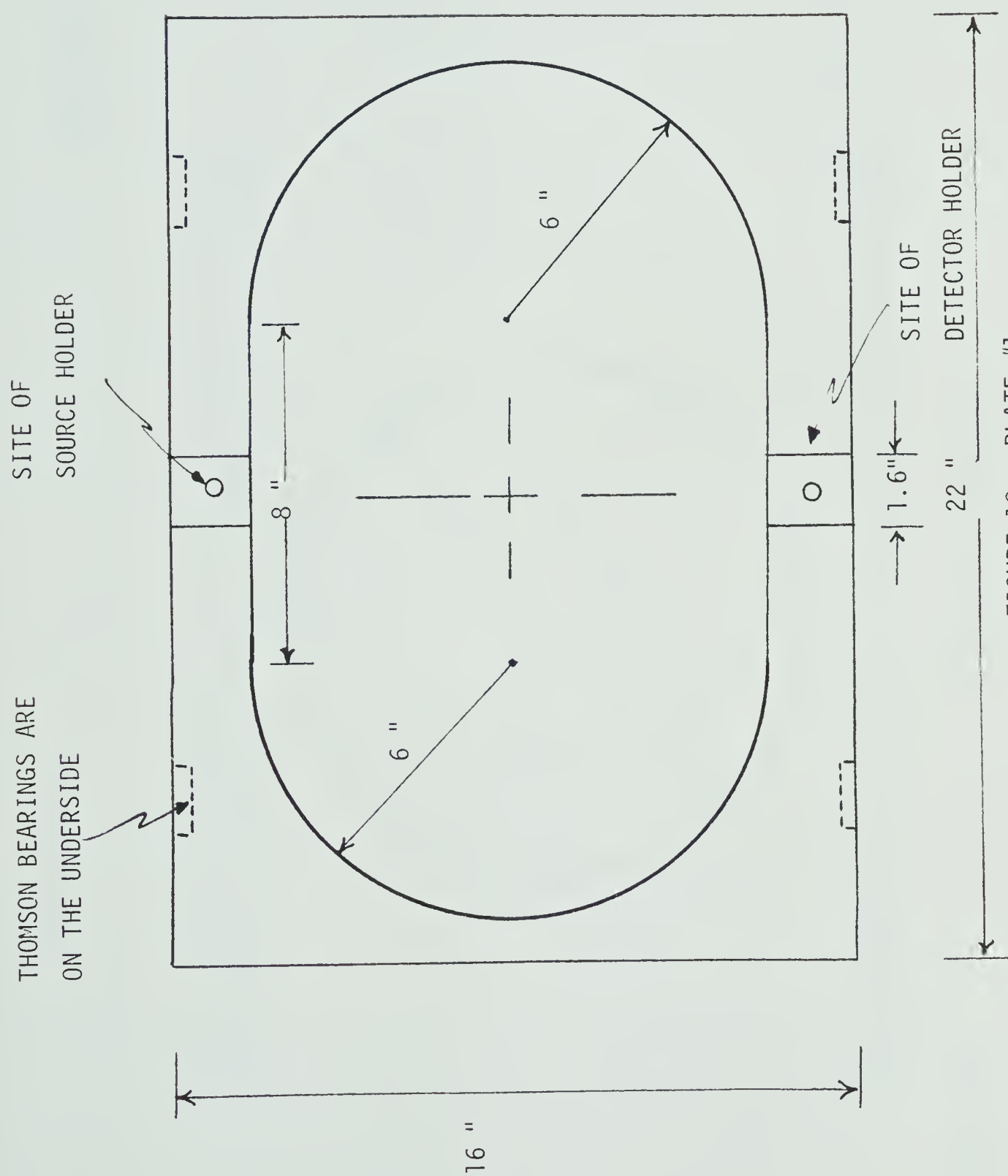
FIGURE 17. CT SYSTEM

Source-Detector Alignment and Motion

The source and detectors are mounted on the top and bottom edge of one side of a 1/2 inch thick aluminum plate with an elongated 12 inch circular hole cut in the center (Figure 18). The geometry of the source with respect to the detectors is fixed. This first plate is mounted upon a second plate (Figure 19) of 1/2 inch thick aluminum with a 12 inch diameter circular hole cut into it. The top plate is attached to the second plate by means of Thomson bearings mounted on the first plate being guided along case hardened steel rails fastened to the second plate. This arrangement allows the first plate (and hence the source-detector arrangement) to translate linearly with respect to the second plate. The second plate is mounted onto a third plate (Figure 20) which contains a circular bearing with an external gear drive which is used to rotate the source-detector arrangement about the object. These plates and the rotational bearing are mounted onto the stand's board.

Mechanical Drives

The drive for the translation is a stepping motor mounted on the second plate. This motor is used to drive a belt connected precision ball screw arrangement which is attached to the first plate. Each revolution of the ball screw results in a 2.5 mm motion of the plate. Since, in the half-step mode, the motor makes one revolution every 400 steps the resolution of one step is 2.5 mm/400 steps or



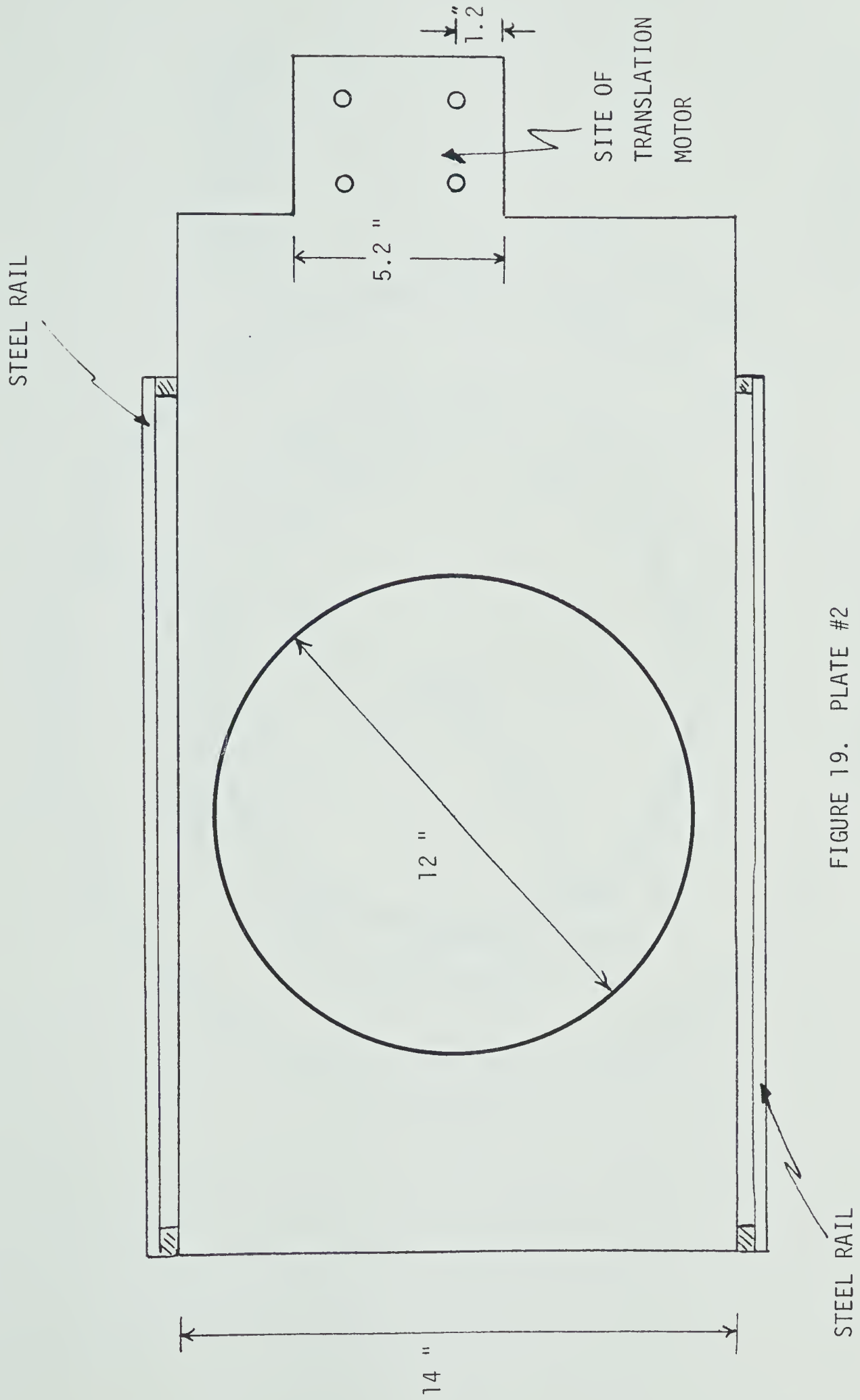


FIGURE 19. PLATE #2

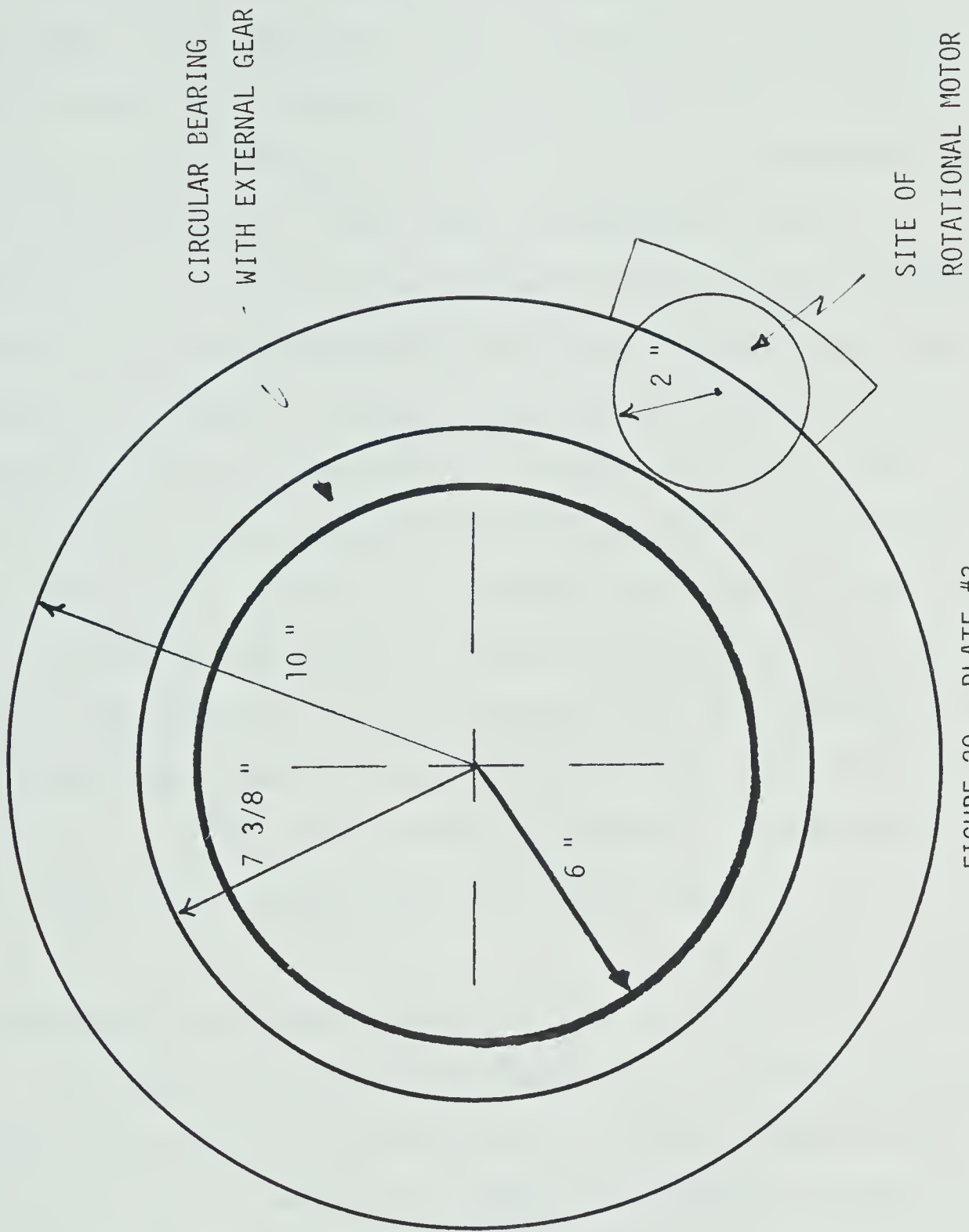


FIGURE 20. PLATE #3

6.25 $\mu\text{m}/\text{step}$. The ball screw is of such a high precision and hence expense that a number of microswitch controlled relays have been installed which shut off power to the stepping motors should the scanner be operated outside its normal scanning range. The plates are rotated by a second stepping motor which drives a worm gear arrangement that is mechanically linked to a spur gear which in turn drives the external gear on the circular bearing. The worm gear was necessary in order to reduce gear backlash caused by the stepping nature of the motors. The gearing ratios mean that approximately 200 steps of 0.9 degrees each are required at the motor shaft to induce a 1 degree rotation of the plates. All of the gearing ratios in the system were known exactly except the gearing ratio of the worm gear arrangement. This ratio was determined by counting the number of motor steps required to rotate the plates 360 degrees as measured by a dial gage with a resolution of 0.0005 inches.

B. Radioactive Sources and Detectors

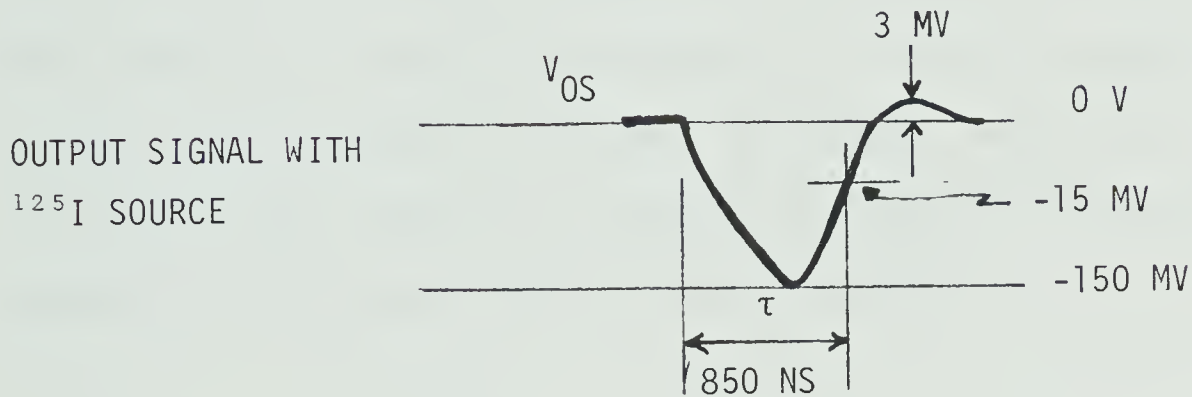
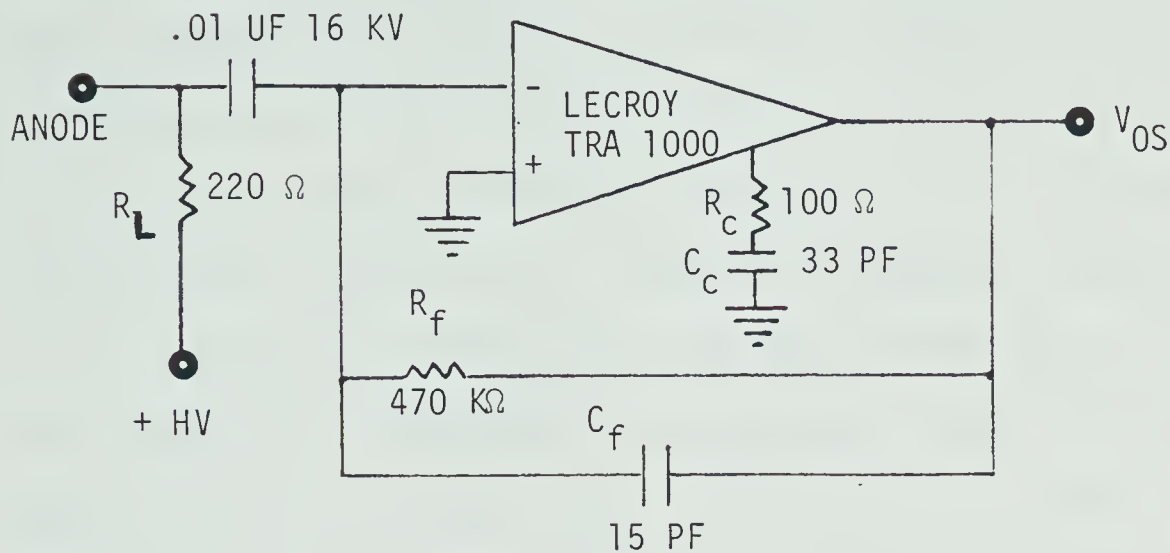
The underlying principle behind any tomographic scanner is the fact that if attenuation of a photon beam can be measured along a sufficient number of pathways through an object then the radiological density at any point within the object can be determined. The radioisotope photon source is 1.5 Curies of Iodine 125 adsorbed to a 2 mm diameter zeolite bead and encapsulated in aluminum. The detectors are $1/2$ inch diameter, $1/2$ inch thick NaI(Tl) crystals coupled to 13

mm diameter photomultiplier tubes with borosilicate windows and bialkali dynodes. The detectors were chosen predominantly on the basis of availability and ease of operation. A radioisotope was selected due to financial constraints and ease of operation. The half-life of Iodine 125 is 60.2 days and the source is replaced every 2-3 half-lives at a cost of approximately \$1400/source. The mechanism of radioactive decay of Iodine 125 is included in the appendix but basically a gamma-ray of approximately 27.5 Kev is produced during the decay process. This energy, being relatively low, has a comparatively large linear attenuation coefficient meaning that subtle differences in density are discernible. At this energy the total attenuation coefficient for NaI is approximately 23 per cm. Hence in a 1/2 inch thick NaI(Tl) crystal only 2.06×10^{-13} of the photons would be passed through the crystal. For Gadolinium 153 with an upper energy of 100 Kev the attenuation coefficient for NaI is 6 per cm. and the number of photons passing through a 1/2 inch crystal would be 4.91×10^{-4} of those incident upon the crystal.

Signal Processing

From the anode of the photomultiplier the signal is fed into a preamp (Figure 21). Since a NaI(Tl) crystal is used the rise time of the signal corresponds to the fluorescent decay time of Sodium Iodide (250 ns). Using a trial and error technique an anode load of 220 ohms was determined to be suitable in terms of pulse height and pulse pileup. The

PREAMP CIRCUIT USED WITH 8 DETECTORS AND NARROW HV CABLES



NOTE: -15 MV IS THE UPDATING POINT OF THE LECROY 623 DISCRIMINATOR.

DECREASING R_1 SHORTENS PULSE WIDTH AND SLIGHTLY DECREASES PULSE HEIGHT.

I.E. IF R_1 IS CHANGED FROM 3.3 K Ω TO 220 Ω : V -300 MV TO -150 MV

τ 2.2 μS TO 0.85 μS

V_{OS} +18 MV TO + 3 MV

DECREASING C_C AND C_f WILL DECREASE τ BUT ALSO WILL CAUSE OSCILLATION.

THEREFORE, C_C AND C_f WERE CHOSEN AS SMALL AS POSSIBLE WITHOUT OSCILLATION.

FIGURE 21. PREAMP CIRCUIT

preamplifier then shapes the signal, increases its amplitude and transforms the impedance. The preamp used is a Le Croy TRA 1000 preamp and is able to provide a signal of sufficient amplitude so that a linear amplifier is not required. This particular preamp was chosen because of its low input noise (30 pA/ $\sqrt{\text{Hz}}$ r.m.s.) and its frequency response (20 MHz at 1 mV/uA gain). The output of the preamp goes into a Le Croy Model 623 8-channel discriminator which provides an output pulse for every input pulse over a preset energy. Thus lower energy pulses are discriminated against and only pulses above a certain energy are counted. From the discriminators the output pulses are sent to a CAMAC 50 M Hz Scaler which counts the number of pulses received in a given interval. This counting interval can be set by the HP 2100 computer which is interfaced to the CAMAC.

C. Scanner Control

The drive motors are two Slo-Syn model M092 FC09 stepping motors with nominal torque ratings of 200 oz inches. A stepping motor translates an electrical pulse into a precise mechanical motion of the shaft. This motion is in fixed, repeatable increments permitting accurate positioning of the motor shaft. The motors can move in either 0.9 degree or 1.8 degree increments per input pulse. The position of the shaft is to within 3 % accuracy and this error is noncumulative from step to step. These motors require a DC power supply and associated electronic drives which contain

the required circuitry to convert pulses into the proper switching sequences for the motor. The power supplies are 2 Slo-Syn MPS3000 24 V DC while the electronic drives are 2 Slo-Syn STM103 3000 step per second motor controllers (Figure 22). These controllers have internal oscillators that can be used to drive the motors in either direction and either in the half-step (0.9 degrees per step) or the full-step (1.8 degrees per step) modes. They are also able to receive pulses from external logic devices such as microprocessors and minicomputers. In the scanner external logic sources include a Motorola microprocessor unit (MPU) and a monostable multivibrator which is used to provide single stepping capability.

The control system for this scanner was designed keeping in mind available equipment and computing facilities (Figure 23). A Motorola MEK 6800 D2 microporocessor unit (MPU) provides the central clock for the system. It is used to control the two stepping motors which provide the rotational and translational motions, as well as to signal the computer when to collect data from the scalers. All MPU software programs have been assembled and are contained in the appendix.

Timing Considerations

Since the microprocessor unit is used to control the stepping motors and hence scanner position it is also necessary that the MPU clock be used to determine when data from the detectors should be collected. Upon receipt of a

STEPPING MOTOR AND TRANSLATOR CIRCUIT DIAGRAM

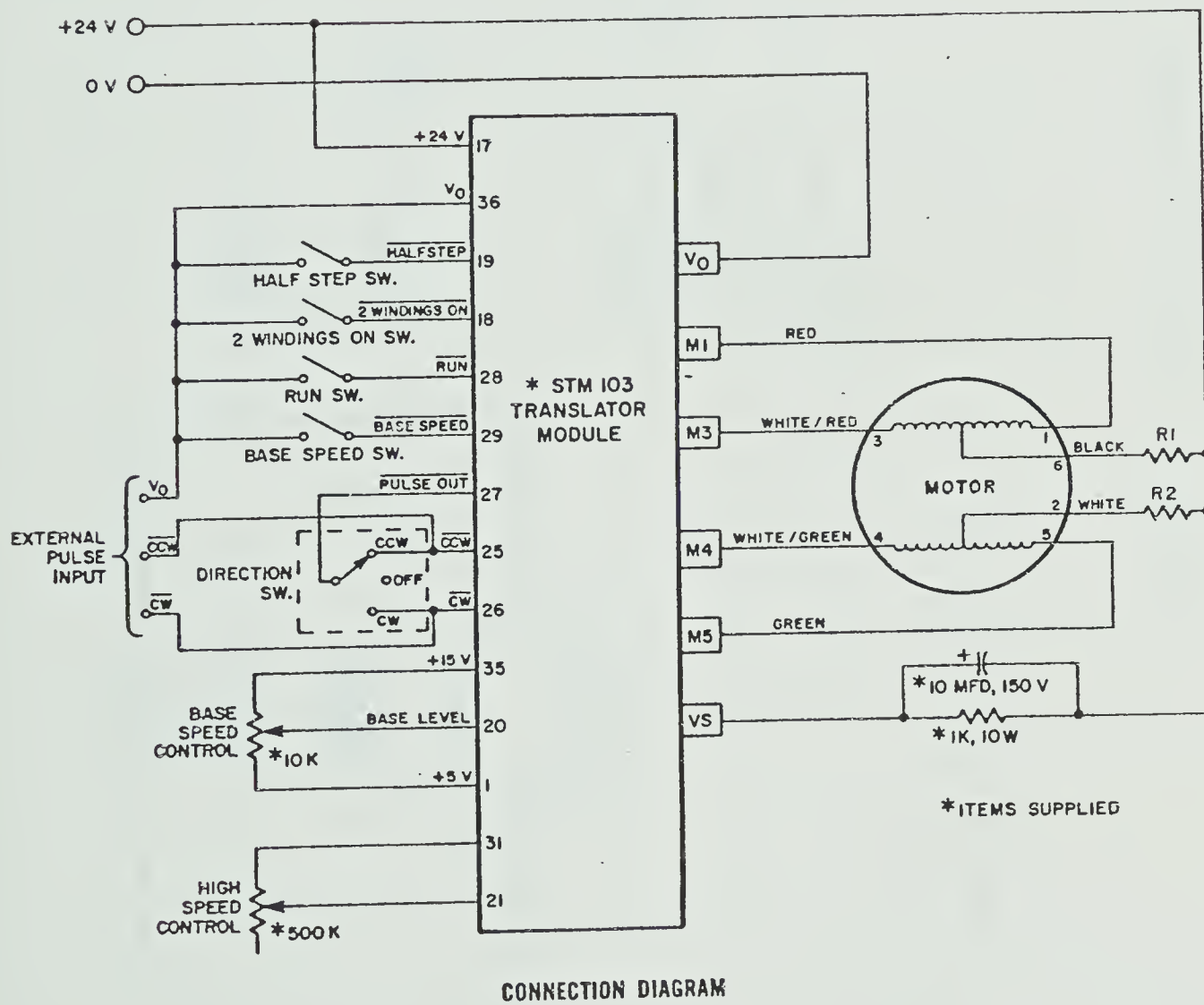
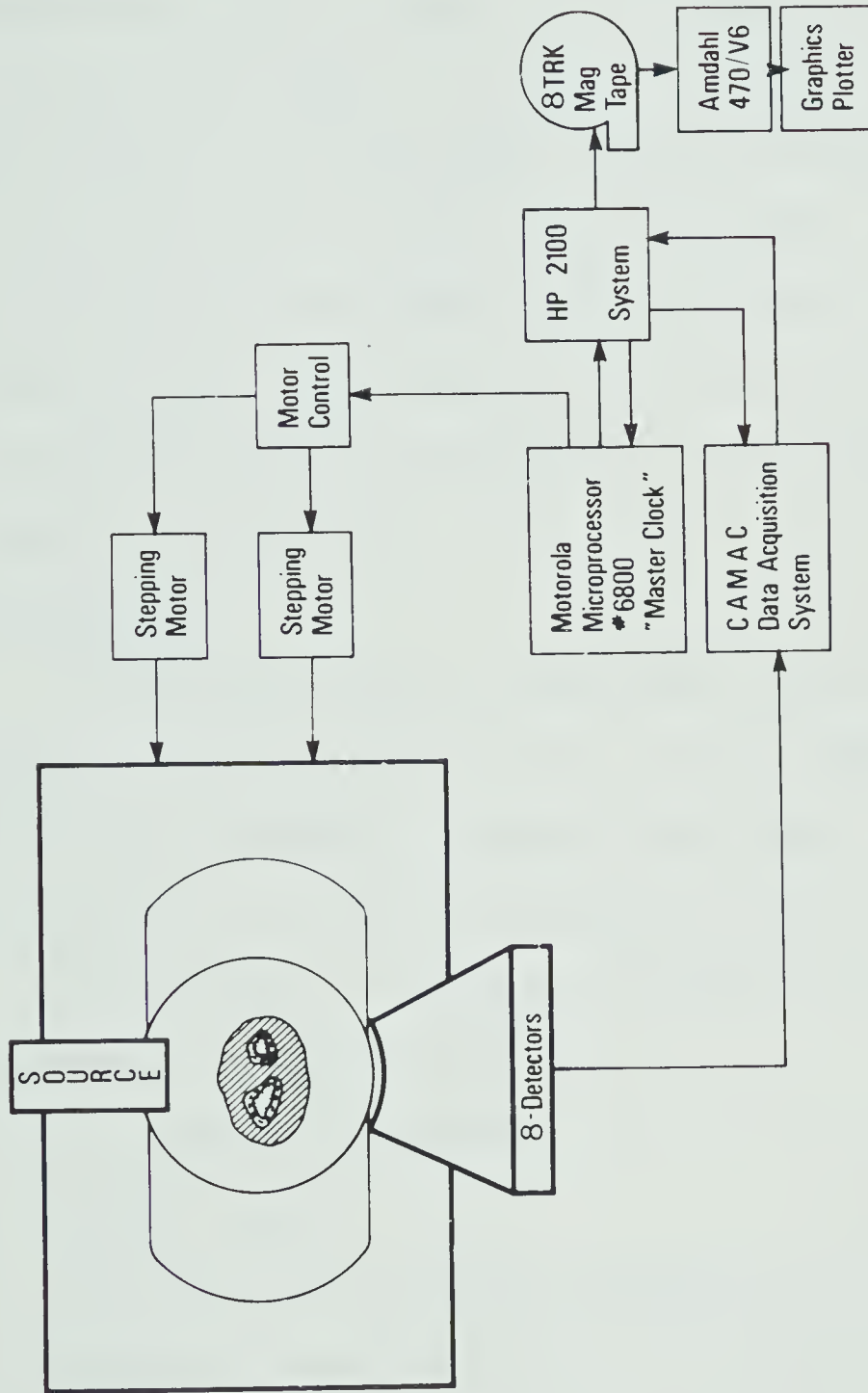


FIGURE 22.



General System Philosophy : Data Acquisition

FIGURE 23. SYSTEM BLOCK DIAGRAM

signal from the MPU the HP must respond quickly to the signal and collect data since the scanner is continually moving. Although it was hoped that this could be accomplished with the HP running under its normal multi-user operating system it was found necessary to operate the HP in a stand alone mode while operating the CT system. This was due to the fact that under the multi-user system the time from a data-ready signal (from the MPU) until data was actually collected from the scalers was variable over too great a range. The stand-alone mode allows data to be collected within 4 microseconds (2 HP clock pulses) of a signal from the MPU.

MPU Control

The Motorola MPU is the basic D2 kit with the only additions being that of 1/2 K of Ram (M6810) and 2 K of EPROM (Intel P2708). Program development and EPROM loading were done on an AMI microcomputer development center.

The choice of the 8 bit Motorola as the control processor was based upon:

1. availability of parts,
2. price, and
3. facilities for EPROM programming.

Although the trend is toward 16 bit and 32 bit microprocessors it was felt that the 8 bit microprocessor was sufficient for this particular application and this combined with the aforementioned constraints led to the selection of the M 6800.

To facilitate insertion and removal of the object to be scanned the scanner must begin and end operation in a "park" position which may not coincide with the actual scanning path. The sequence of events which occur during a scan are as follows:

1. the MPU determines the park to start distance and direction and sends the appropriate pulses to the motor controllers;
2. a signal is sent to the HP signifying that a scan is to begin;
3. a signal is returned from the HP to the microcomputer unit signifying that the HP is ready and that a scan may begin;
4. a signal is sent from the MPU to the HP signifying that a scan has been started and that acceleration of the translational motor has begun;
5. a second signal sent to the HP from the MPU signifies that acceleration has ceased and that translation velocity has been reached;
6. all translation pulses are sent to the motor controllers from the MPU;
7. pulses are sent from the MPU throughout the scan to the HP signifying when to collect data from the detectors;
8. after translation is complete the MPU decelerates the translational motor, determines the required rotation and sends the appropriate pulses to the motor;
9. the pattern (2-8) is repeated until the appropriate

number of rotations and translations have been performed;

10. at which point the appropriate pulses are sent to the motors so that the scanner is returned to the park position.

Acceleration and deceleration of the stepping motors is required since motor torque decreases with increasing speed. Thus in order to ensure that all pulses sent to the motor result in a step while at the same time operating at the maximum allowable speed, acceleration and deceleration of the motors is needed. This is accomplished by the microprocessor which uses a subroutine ASD (see appendix) to provide a series of pulse trains at varying frequencies.

MPU Based PIA

The microprocessor unit (MPU) is interfaced to the motor controllers and the HP by an on-board integrated circuit (M 6820 PIA - peripheral interface adapter). The PIA contains an 8-bit bidirectional data bus for communication with the MPU, two bidirectional 8-bit buses (output registers) for interface to peripherals, two programmable control registers, two programmable data direction registers and four individually-controlled interrupt input lines; two of which are usable as peripheral control outputs. The MEK 6800 D2 kit contains two PIAs, one of which is used to interface the keyboard. The second PIA appears to the MPU as four memory locations located at \$8004 - \$8007

(where "\$" denotes a hexadecimal number). The output register (OR) and data direction register (DDR) of port A (one 8-bit bus used for interfacing) are located at \$8004 and the control register (CR) is located at \$8005 while the corresponding registers for port B are located at \$8006 and \$8007. The contents of the control registers determine the operation mode of the interrupt lines and whether an output register or data direction register is to be addressed. This latter feature is required since the OR and DDR share the same address location. The data direction register determines whether the corresponding interface lines to the output register are inputs (DDR=0) or outputs (DDR=1).

To control the scanner 6 lines of the PIA port A are used. Two lines are needed for each of the two stepping motors (bidirectional) and two lines are used in a handshake mode between the HP and the MPU. The MPU is initialized by a subroutine (PIA) which first sets control register A (CRA) permitting DDRA to be addressed. DDRA is then set to \$1F (bit 7 is the most significant bit) so that lines 0-4 of ORA are outputs while lines 5-7 of ORA are inputs. Control register A is then reset so that ORA can be addressed. The normal state of the output register is set equal to \$1F (only bits 0-4 may be set by the MPU). Signals to the translation motor are sent along lines 3 and 4 (\$0F and \$17) while signals to the rotational motor are sent

along lines 0 and 1 (\$1D and \$1E). A signal to the HP is sent on line 2 (\$1B) and a signal from the HP is received on line 5. Bits 0-4 are active on the positive transition meaning that subsequent to the normal state of the output register the desired signal must be stored in ORA and then the normal state must again be stored in ORA at which point the message is transmitted. This pattern was used since it was found necessary to initialize the output register at the start of any scan in order to be certain of the contents of the register. The signal from the HP is level sensitive and responds to a positive signal in bit 5.

Acceleration - Deceleration Ramp

When operating the stepping motor from the internal oscillator, the translator module automatically accelerates and decelerates the motor to prevent the motor from missing steps or overshooting when stopping. This ramping of the pulse rate is also necessary when operating the translator module from pulses supplied by an external source (in this case the MPU). When using the internal oscillator, acceleration and deceleration times to a high speed are independantly adjustable from 50 milliseconds to 1 second. The acceleration and deceleration ramps are used during the transition from a preset although adjustable base speed to a preset although adjustable high speed.

In order that the number of steps and time for

acceleration and deceleration be kept to a minimum known quantity a suitable MPU controlled ramp had to be found. The base speed of the control module was set to zero and using the internal oscillator a suitable ramp for a high speed of 1500 Hz was obtained through trial and error. It was found that the same ramp was suitable for use with both stepping motors. The upper speed of 1500 Hz was selected since it had been decided that the maximum speed of the motors during a rotation or a translation would be at approximately that frequency. Once a suitable ramp had been obtained these pulses were then measured with an Ortec ratemeter (which converted the pulse frequency to a proportional voltage): the output from which was displayed on a storage oscilloscope. Thus acceleration via the internal oscillator produced a ramp on the oscilloscope representative of the accelerating ramp used. The next step was to mimic this ramp using the MPU as the pulse source. A subroutine (ASD - acceleration, speed, deceleration) was developed that produces twelve ramps of varying lengths and frequencies. As a test of the MPU generated ramp the MPU output was also measured with the Ortec ratemeter and displayed on the oscilloscope and the resultant waveform was compared with that obtained from the internal oscillator of the control module. Once a close approximation had been found the MPU based ramp was tested on the scanner.

The frequencies, corresponding ramp lengths, and type and direction of motion are loaded by ASD from RAM and must be set in RAM prior to calling ASD. These parameters may be set so that ASD can be used for only acceleration or deceleration or to preset the scanner location. A count of all pulses sent during subroutine ASD is made. A number of smaller subroutines are used in conjunction with ASD. These include various acceleration and deceleration subroutines which set the parameters in RAM so that ASD may be used to accelerate to or from a certain speed. There are three deceleration subroutines (DECEL, DECEL32, DECEL5) which are used to decelerate the scanner from speeds of less than 1500 Hz, less than 400 Hz and less than 100 Hz respectively. The respective lengths of these three ramps are 200 steps, 32 steps and 5 steps. The upper speed limit of acceleration is variable up to 1500 Hz merely by setting the ramp length parameter contained in two RAM locations. For a normal scan (with a top speed of 1318 Hz) the frequencies and ramps are loaded from two subroutines (F and INIT) contained in EPROM into the RAM locations. The frequencies vary from 20.2 Hz to 1115 Hz and the corresponding ramp lengths vary from 1 to 42 pulses. The same ramp is used for acceleration and deceleration with two hundred steps being required in both cases. The number of pulses at a maximum frequency of 1422 Hz can be varied from 0 to over 4 million and hence ASD is

suitable for presetting the scanner position.

Another minor subroutine R8D initializes parameters in RAM and then calls ASD resulting in a 25.7 degree rotation of the scanner. This is the rotation required between translations in a normal scan using the 8-detector holder.

Translation

Once the motor has been accelerated up to the desired speed a subroutine (TRANSL) is called. This subroutine makes use of a number of parameters previously loaded into RAM which determine the delay between motor pulses and the number of motor pulses per signal to the HP. A signal to the HP signifies that data is to be collected from the scalers.

Start

At the start of every translation of a scan an MPU based subroutine (START) is called. This routine (which uses the handshake arrangement between the MPU and the HP) sends a signal to the HP (signifying that a translation is desired) and in return waits for a signal from the HP (prior to allowing the MPU program to continue). An additional signal is sent to the HP prior to the start of the ramp.

Program Location

The MPU contains two EPROMs (1024 x 8 bit) located at \$6000-\$63FF and \$C000-\$C3FF. The EPROM located at \$C000 contains all subroutines such as ASD and TRANSL

(see flowchart in appendix) while the main body of the control programs are located in the EPROM at \$6000.

Since the subroutines are rarely altered this means that most changes to the system control programs can be made by altering just one of the EPROMs. The RAM contained in the MPU is static RAM (128 x 8 bit) and is located at addresses \$0000 through \$03FF. The reason that many of the control parameters are loaded by the subroutines from RAM is that this theoretically makes it possible to alter the control parameters from the keyboard. At present however, most of the RAM parameters are loaded into RAM from the main control programs (which are stored in EPROM) at the same time as the main control program is run. This is due to the fact that the control parameters are at present seldomly changed.

Reproducibility of Measurements

Bone mineral changes are significant along the longitudinal aspect of the extremities. Consequently, for a valid quantification of changes in time in a given individual, it is important to be able to reproduce the site of the scan (50). To achieve this required positioning accuracy a MPU controlled scout scan system was developed which locates the desired measurement site.

The scout scan involves measurement of 26 single profiles at different points axially about the measurement site. Reconstruction of these profiles (see Figure 24) yields an X-ray like image which depicts the relative sizes

RADIUS

WRIST REGION

ULNA

FIGURE 24. SCOUT SCAN

and orientations of the bone(s) (femur vs. radius, ulna). This information when compared to the same information obtained from previous scans of the same patient permits accurate location of the desired measurement site.

The anatomical criteria used to define the scan site are the distances from the distal tips of the radius and ulna axially along the bones. At present, sites two millimeters to either side of the measurement site are also being evaluated. These three sets of data are then interpolated in order to provide a reconstructed area identical to those previously measured.

Single Stepping

In order to provide the desired accuracy for initial positioning of the scanner it was necessary to provide some means for single stepping both the rotational and translational drive motors. This was accomplished by use of a 74123 retriggerable monostable multivibrator (51) as shown in Figure 25.

HP/Microprocessor Interfacing

The microprocessor unit both sends and receives positive signals of + 5 volts while positive signals sent from the HP are +12 volts. In order to sink the required current (12 mA) to provide a low signal to the HP the output from the PIA is tied into two inverters before being connected to the HP (Figure 26). Positive signals from the HP are converted to +5 volts by use of a resistor-zener diode divider circuit (Figure 27).

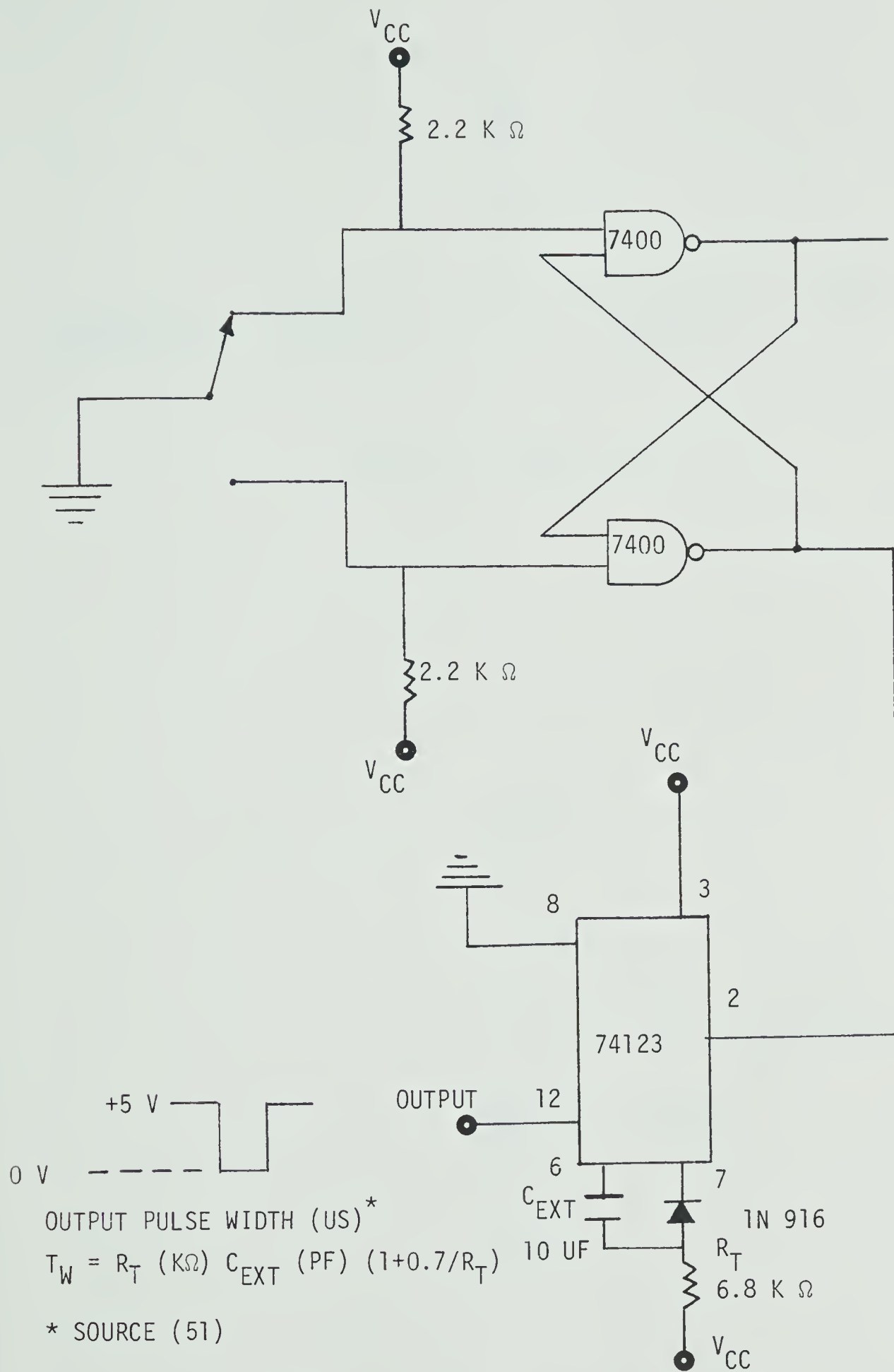


FIGURE 25. SINGLE STEPPING CIRCUITRY

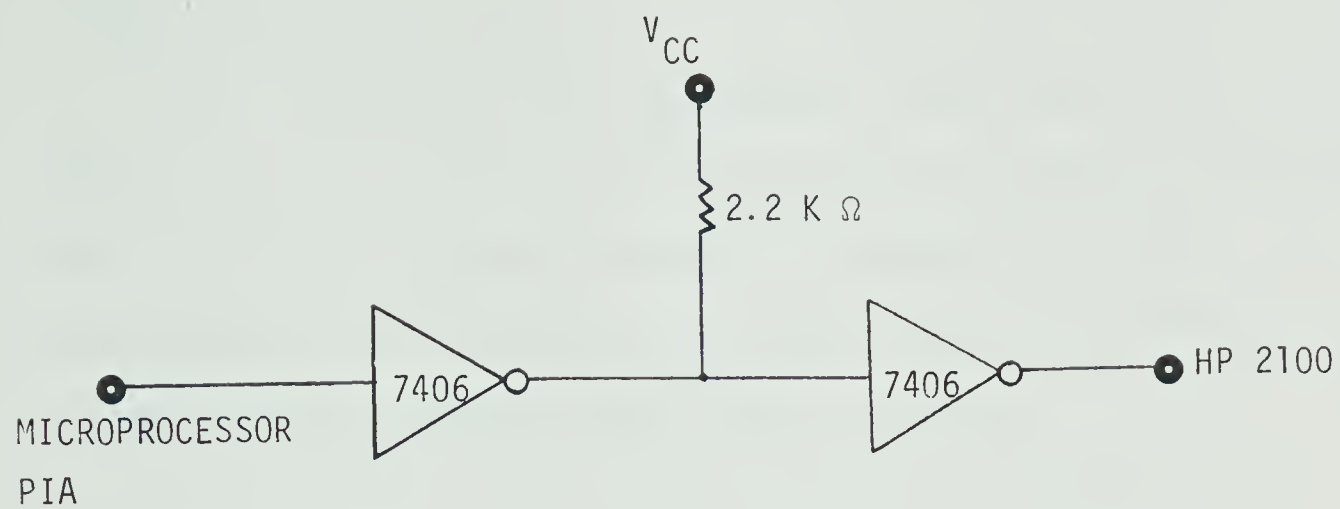


FIGURE 26. CURRENT SINK

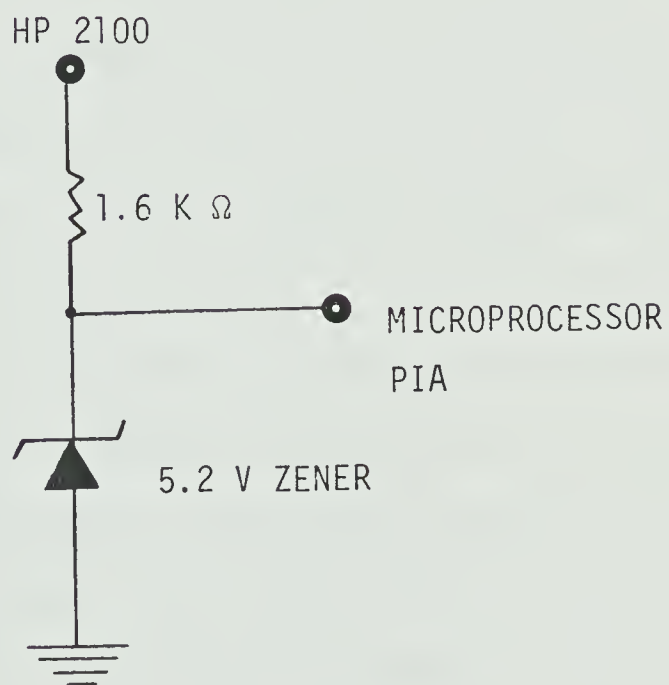


FIGURE 27. VOLTAGE DIVIDER

D. Multidetector System

Upon completion and subsequent testing of the generation one system the modifications necessary to change the system to a generation two configuration were undertaken. This chapter will describe the problems encountered in making these modifications.

The principle of the multidetector system is to collimate a single radioactive source so that an array of photons is produced which subtend a solid angle emanating from the source. The detectors are also collimated so that scattering of rays between detectors is reduced. Linear scans are made in exactly the same fashion as for the single-detector systems however the angle of each rotation is n times greater where n is the number of detectors (this assumes the detectors are spaced at the desired angular increments). Thus the number of linear translations and the number of rotations can be greatly reduced decreasing the time required for a scan. This reduction in scan time is significant in that errors caused by patient movement can be reduced. In this particular scanner moving from a generation one system to an eight-detector generation two system reduced the normal scan time from approximately 5 minutes to approximately 1.5 minutes. Although the order of data collection in a multi-detector system is different from that of a single detector system the reconstruction algorithm used is exactly the same.

Physical Limitations

In order for radiological attenuation of the object to be determined the detectors must be allowed to measure what is known as an "open" or unattenuated count rate during a scan. This means that in the multi-detector system, for each translation, all source-detector alignments must be totally clear of the object at some point in the translation. Given a finite translational pathlength this means that either one or both of the object size and the angle of the detector arc must be restricted. In this arrangement it is always possible to scan larger objects by not using the outer detectors in an array and effectively reducing the angle of the detector array. This would mean that the rotational angle between translations would have to be reduced.

Another limitation is the size of the detectors. The fact that these detectors can only be packed together within limits means that in order to have a desired angle between detectors the source-detector distance cannot be less than a certain minimum. This distance is of utmost importance since the photon flux impinging on the detectors follows the inverse square law meaning that the further the source-detector distance the worse the available statistics given the same radioactive source and counting interval. Other considerations in regards to the detector geometry include scan time, count rates and available channels for signal processing. The final result, an 8 detector unit similar to the one depicted in Figure 28, is a compromise

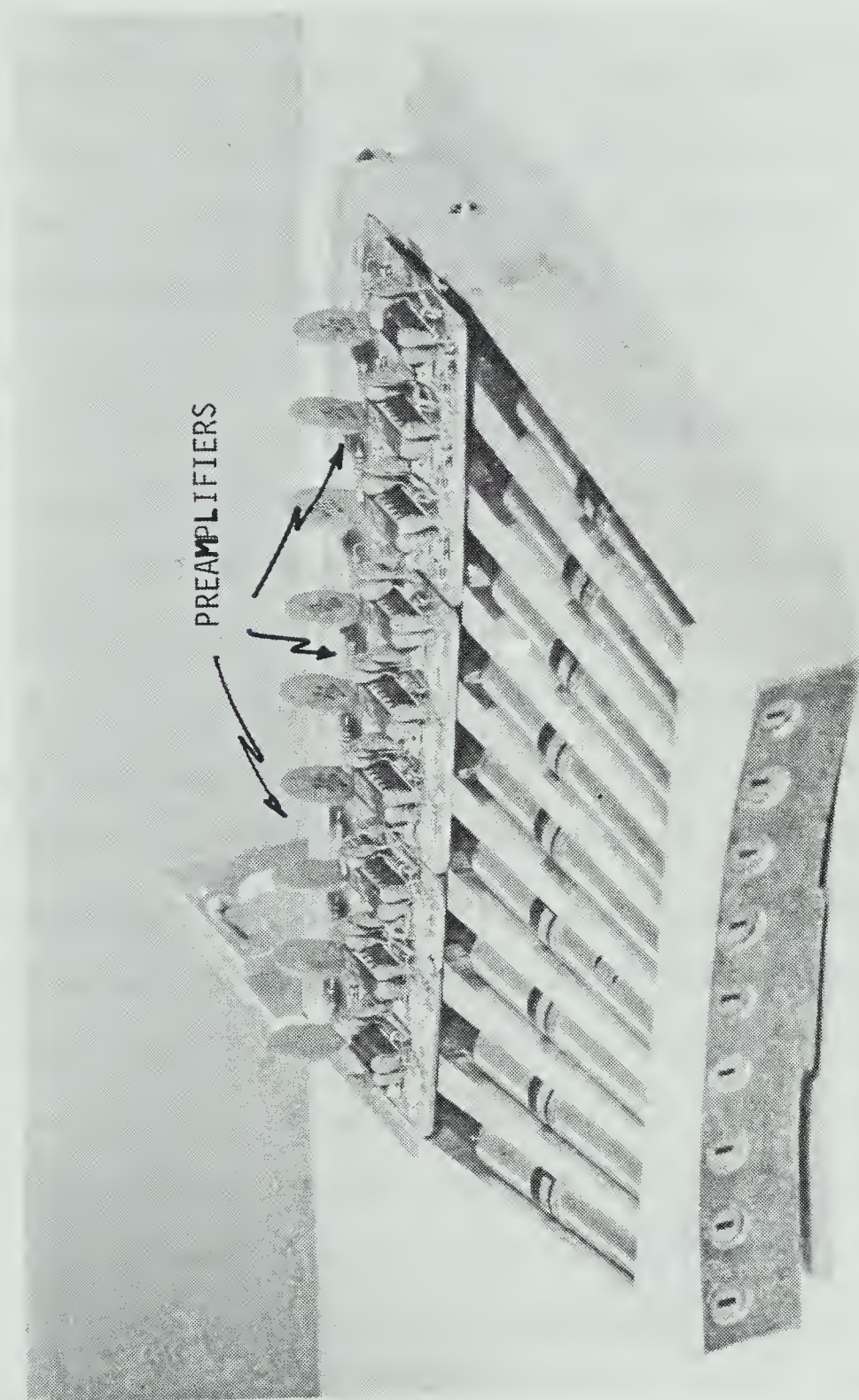


FIGURE 28. DETECTOR HOLDER

between the aforementioned factors.

Intervals and Subintervals

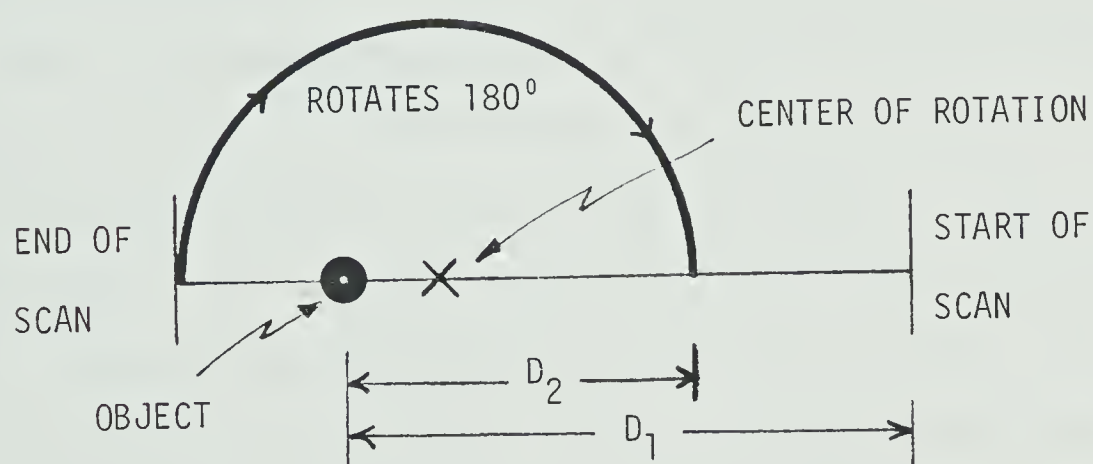
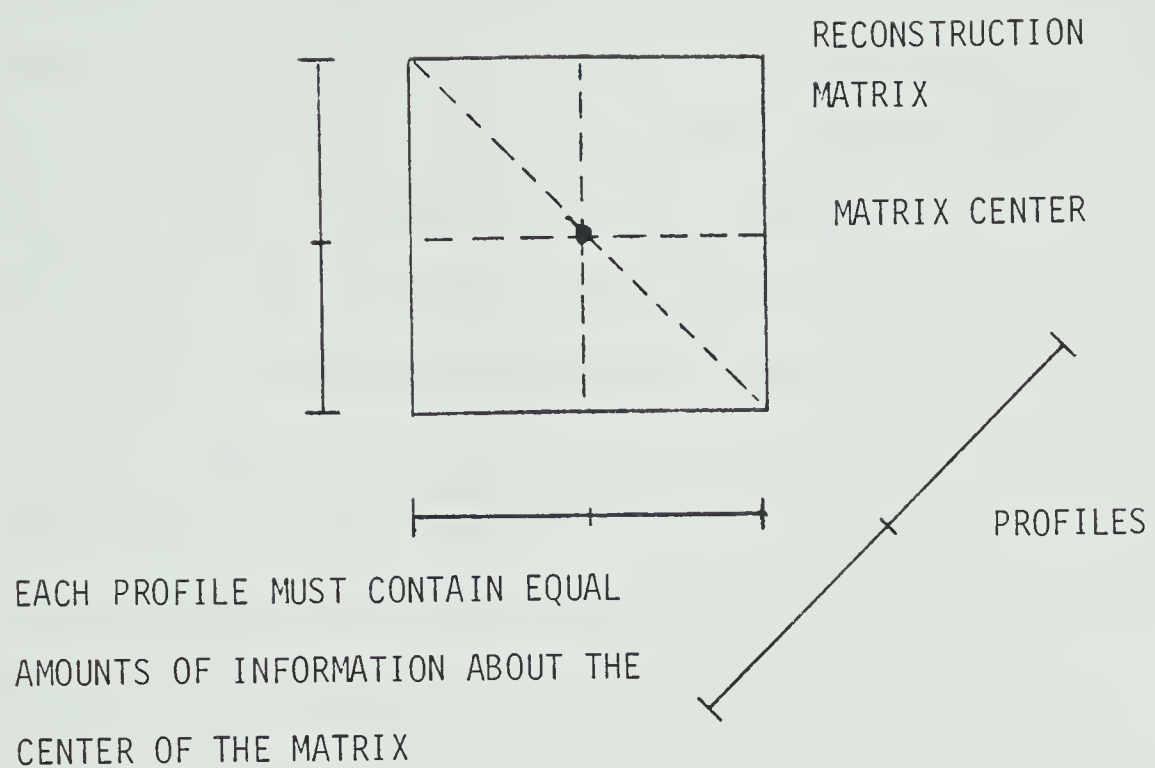
In the case of the multidetector system the translation of the scanner is perpendicular in direction to at most one of the source-detector orientations. Thus, while during a translation one detector may move a distance of "A" perpendicular to its orientation, the other detectors will move distances somewhat different than "A" perpendicular to their own orientations. The reconstruction algorithm requires that all the detector spacings have to be the same distance apart and therefore some means of correction has to be applied. This is done by measuring subintervals; each interval or ray-integral measurement consisting of a number of subintervals. Thus while the detector that is aligned perpendicular to the direction of motion will have intervals consisting of a specified number of subintervals the other detectors' intervals will be made up of more subintervals. The number of subintervals per interval varies from detector to detector according to their respective angular deviation from the line perpendicular to the direction of translation. Interpolation between subintervals is typically required in order to accurately define an interval. In this particular system 8 subintervals are measured for every interval of the detector aligned perpendicularly to the direction of motion. Thus while in a normal scan some 1024 subintervals are measured per detector per translation they are later compressed on the HP to 128 intervals prior to

reconstruction.

Centering

The reconstruction matrix requires that each profile consist of equal amounts of data collected about the center of the reconstruction matrix. This is due to the fact that the convolution algorithm weights all ray measurements according to their distance from the point of reconstruction. In the case of the multidetector scanner each detector has a different starting point so it is impossible for all of them to collect equal amounts of data about the center of the scanner. In order to compensate for this, offsets must be calculated and applied to the collected data from each detector.

This problem is most easily seen by examining the case of a single detector scanner. Assume that the scanner moves a distance D_1 from the start of a scan to an object O before completing the scan (Figure 29). Then, if the scanner is rotated through 180 degrees and started once again the distance from the start of the scan to the object O is now D_2 . In order that equal amounts of data be collected about both sides of the object the data will have to be offset by an amount equal to $(D_1 - D_2)/2$. Thus if equal amounts of data have been collected about both sides of the object D_1 is equal to D_2 and no offsets are required. These calculations are aided by a special microcomputer program (Cent) which is a high resolution measurement. An object of high density and small physical size (i.e. a wire) is placed approximately in



IF THE PROFILE IS TO CONTAIN EQUAL AMOUNTS OF DATA ABOUT BOTH SIDES OF THE OBJECT THE POSITION OF THE DATA WILL HAVE TO BE OFFSET BY $(D_1 - D_2)/2$.

FIGURE 29. CENTERING CONSIDERATIONS

the middle of the scan path. The scanner is then translated at low speed and data is collected every two motor steps. The scanner is then rotated through 180 degrees and the scan is repeated. Looking at Figure 29 we see that information so obtained will allow one to calculate the offsets for each detector. This procedure must be repeated every time the mechanics of the scanner (such as the source) are altered.

With an aluminum-plexiglass model, centering errors of 100 motor steps or 0.625 mm. per detector are noticeable (Figure 30). In the case of a circular object the centering artifact appears on the image as two circles of slightly different radii being joined.

E. Data Processing

Data for one translation is stored in the HP 2100 and during a rotation is transferred to magnetic tape. This is then processed and analyzed on the University Computer (Amdahl 470/ V7) and hard copies of the image are obtained on the associated electrostatic plotter printer. The reconstruction program uses the convolution technique with the filter function proposed by Shepp and Logan to produce a 256 x 256 reconstruction matrix. Prior to reconstruction both dead time and a non-material selective beam hardening correction are made on the Amdahl as is an interpolation between ray measurements and angles. The interpolation takes the 128 data points per projection and interpolates between them in order to produce 256 data

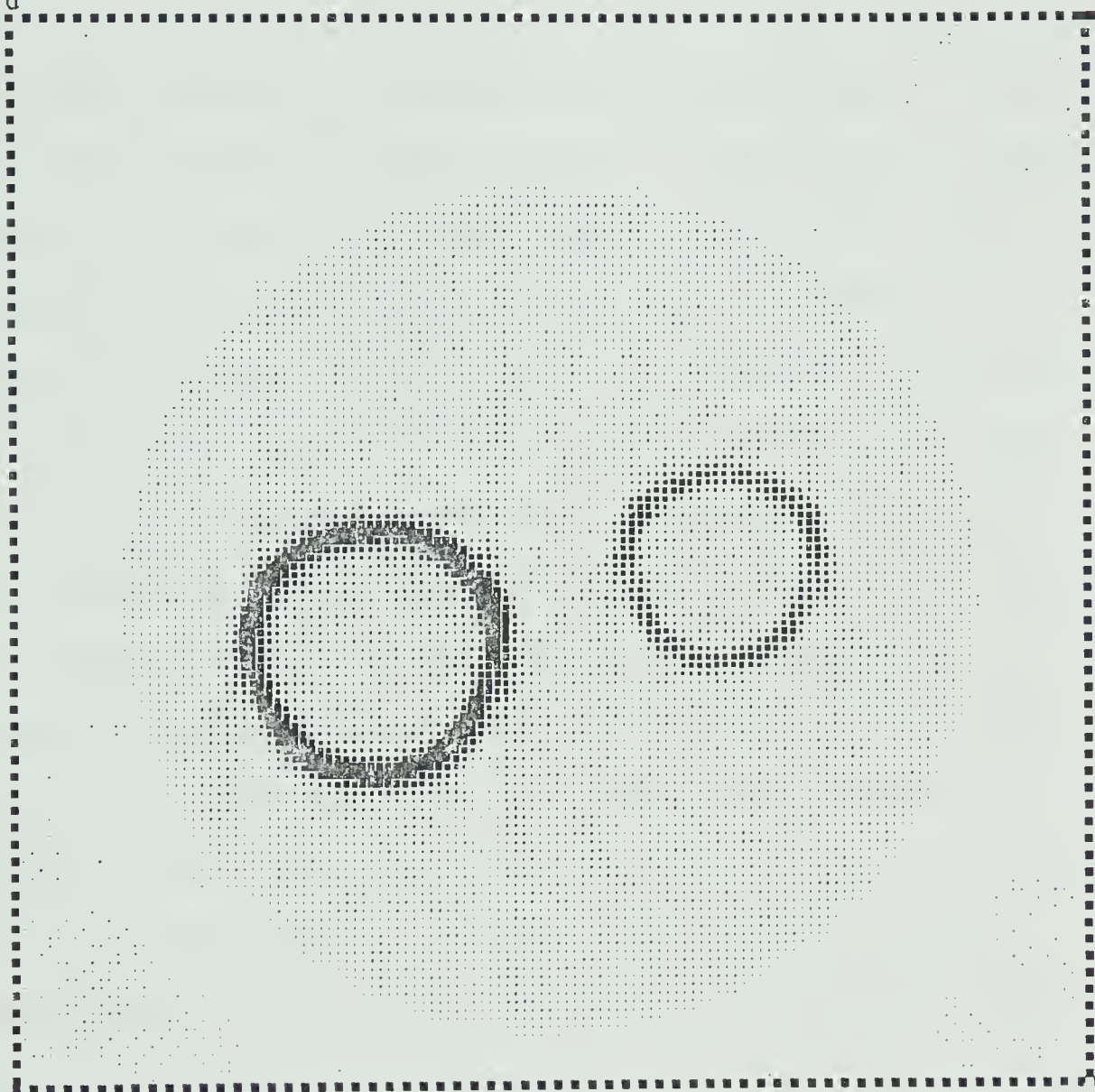
d
d
d
d
d

MEASUREMENT

1890

11-NOV-80

d



PLEXIGLASS PHANTOM WITH TWO CIRCULAR ALUMINUM TUBES

FIGURE 30. CENTERING ARTIFACTS

points per projection and also interpolates between projections to produce 112 instead of the normal 56 projections. Although these interpolations do increase computation time and have a smoothing effect on the image the increased matrix size is needed in order that the analysis program has enough pixels with which to work. Interpolation between the angles is necessary to remove angular artifacts from the image. It has been shown (7) that if there are N ray-integral measurements made per projection, then for the data to be complete there should be M projections, where $M = (\pi/4)N$. Thus if there are 128 ray-integral measurements made there should be $128(\pi/4)$ or approximately 100 projections made in order for the data to be complete. Hence if the number of angles were not interpolated to produce 112 projections instead of 56 projections, angular artifacts would be present in the reconstructed image. The interpolation between measurements is to produce 256 ray-integral measurements so that reconstruction on a 256×256 matrix can be performed easily. It should be noted that it is not necessary to reconstruct on a matrix the same size as there are number of ray-integrals per profile; however, reconstruction is facilitated if this is the case.

In order to use a Grinnell CRT display, which is tied into the HP system it is necessary to either reconstruct the matrix on the HP 2100, which takes about 30 minutes (for a 128×128 matrix), or else to load the Amdahl reconstructed

matrix onto magnetic tape and to subsequently load the matrix into the HP.

Open Count

Although the open count rate is measured for all detectors during each translation the statistics associated with such counts are of limited accuracy due to a short counting period. For this reason an open count rate is made at the start of the day. This count is made over a period of several minutes (using the Scout Scan program) so that the coefficient of variation associated with the measurement is low. This open count (I_o) is then used throughout the day to calculate the ray-integral measurements ($\ln(I_o/I)$).

Pixel Size and Grey Levels

The pixel size of the system is determined by dividing the scan length by the number of pixels in one side of the reconstruction matrix. The maximum size object that can be scanned is 76.8 mm and the size of the reconstruction matrix is 256 x 256. Hence the pixel size of the system is 76.8 mm/256 or 0.3 mm. Each pixel level in the reconstructed matrix is defined by a two's complement 16 bit number and hence there are 32,768 possible positive pixel levels. Although the system pixel size is 0.3 mm corresponding to a 256 x 256 matrix the hard copy imaging system is not able to resolve points of that size. As a result a 128 x 128 matrix with 32 grey levels is used with a corresponding pixel size of 0.6 mm. Since there are four times as many pixels in the actual reconstruction matrix as in the image matrix, four of

the actual pixels are averaged together to produce one of the image pixels. The Grinnell display system is able to reproduce matrices of size 512 x 512 with 256 grey levels and hence the system limiting pixel size for this display mode (CRT) is 0.3 mm.

Analysis Program

While the image depicting the bones may be aesthetically pleasing it is really the parameters contained in subsequent analysis programs that are of clinical value. The image's main function is to ensure that the scan was done properly and that no artifacts due to such factors as patient movement have been introduced. Once an image of the bone has been reconstructed an analysis program is used to identify such parameters as area, total mineral content and average density. These parameters are defined for total bone, trabecular bone and the cortical or compact bone (Table 1).

The analysis program first defines where the cortical bone begins and strips away the surrounding fleshy material (Figure 31). This is done by defining a cortical bone density level (8000 is normally used) and defining all levels of material outside of those pixels with levels greater than or equal to 8000 as being zero. The radius and ulna are then separated and each bone is analyzed separately. Each bone is then separated into a number of shells by essentially moving the cortical bone contour in, one pixel at a time. Trabecular bone was initially defined

MEASUREMENT : 596 13-MAR-80
RADIUS EVALUATION LEVEL 8000

	SHELL				REST BONE				REST AREA	
	DENSITY		SM		DENSITY	SM	S	S	A	A
	[G/CCM]	[G/CCM]	[G/CCM]	[%]	[G/CCM]	[G/CCM]	[%]	[G/CCM]	[PIX]	[%]
0	0.0	0.0	0.0	0.0	0.8266	0.0093	1.12	0.5374	3374	100.00
1	0.9161	0.0078	0.85	12.18	0.8208	0.0098	1.20	0.5534	3168	93.89
2	1.2343	0.0148	0.85	16.97	0.7931	0.0102	1.29	0.5582	2969	88.00
3	1.4802	0.0206	1.39	19.37	0.7453	0.0103	1.38	0.5408	2776	82.28
4	1.5982	0.0256	1.60	21.92	0.6837	0.0098	1.43	0.4984	2589	76.73
5	1.5921	0.0281	1.76	23.72	0.6155	0.0089	1.44	0.4356	2408	71.37
6	1.4603	0.0267	1.83	24.11	0.5497	0.0078	1.41	0.3674	2234	66.21
7	1.2573	0.0253	2.01	26.24	0.4914	0.0067	1.36	0.3042	2064	61.17
8	1.0512	0.0247	2.35	30.21	0.4427	0.0057	1.29	0.2495	1899	56.28
9	0.8709	0.0207	2.37	30.12	0.4031	0.0050	1.24	0.2076	1738	51.51
10	0.7063	0.0183	2.59	32.32	0.3732	0.0045	1.21	0.1797	1582	46.89
11	0.5664	0.0147	2.60	31.96	0.3528	0.0044	1.25	0.1670	1431	42.41
12	0.4715	0.0135	2.87	34.44	0.3395	0.0045	1.33	0.1622	1287	38.14
13	0.4059	0.0152	3.75	43.71	0.3316	0.0047	1.41	0.1586	1151	34.11
14	0.3710	0.0163	4.38	50.15	0.3266	0.0048	1.48	0.1541	1020	30.23
15	0.3742	0.0145	3.87	43.42	0.3199	0.0051	1.59	0.1518	894	26.50
16	0.3983	0.0133	3.34	36.71	0.3076	0.0054	1.74	0.1490	773	22.91
17	0.3875	0.0139	3.58	38.44	0.2936	0.0056	1.92	0.1447	658	19.50
18	0.3479	0.0136	3.90	40.49	0.2830	0.0061	2.16	0.1432	550	16.30
19	0.3233	0.0152	4.69	47.34	0.2738	0.0066	2.40	0.1394	448	13.28
20	0.3108	0.0157	5.06	48.54	0.2642	0.0071	2.70	0.1348	356	10.55
21	0.2817	0.0156	5.53	50.97	0.2587	0.0080	3.09	0.1317	271	8.03
22	0.2499	0.0169	6.74	58.39	0.2621	0.0090	3.44	0.1261	196	5.81
23	0.2554	0.0179	7.02	57.48	0.2656	0.0101	3.79	0.1144	129	3.82
24	0.2970	0.0159	5.34	38.90	0.2437	0.0125	5.13	0.1090	76	2.25
25	0.2514	0.0200	7.95	47.70	0.2367	0.0157	6.62	0.0992	40	1.19
26	0.2250	0.0215	9.56	45.86	0.2525	0.0228	9.05	0.0942	17	0.50

TOTAL BONE :				TRABECULAR BONE :				COMPACT BONE :			
AREA :	3.0366	[CM**2]	REL. AREA :	61.1737	[%]	ABS.THICKNESS :	0.2142	[CM]			
TOT.MIN.CONTENT :	2.5102	[G/CM]	TOT.MIN.CONTENT :	0.9128	[G/CM]	REL.THICKNESS :	21.7863	[%]			
AV.DENSITY (BD) :	0.8266	[G/CCM]	AV.DENSITY (TBD) :	0.4914	[G/CCM]	AV.DENSITY (CBD) :	1.3549	[G/CCM]			

TABLE 1.

MEASUREMENT

596

13-MAR-80

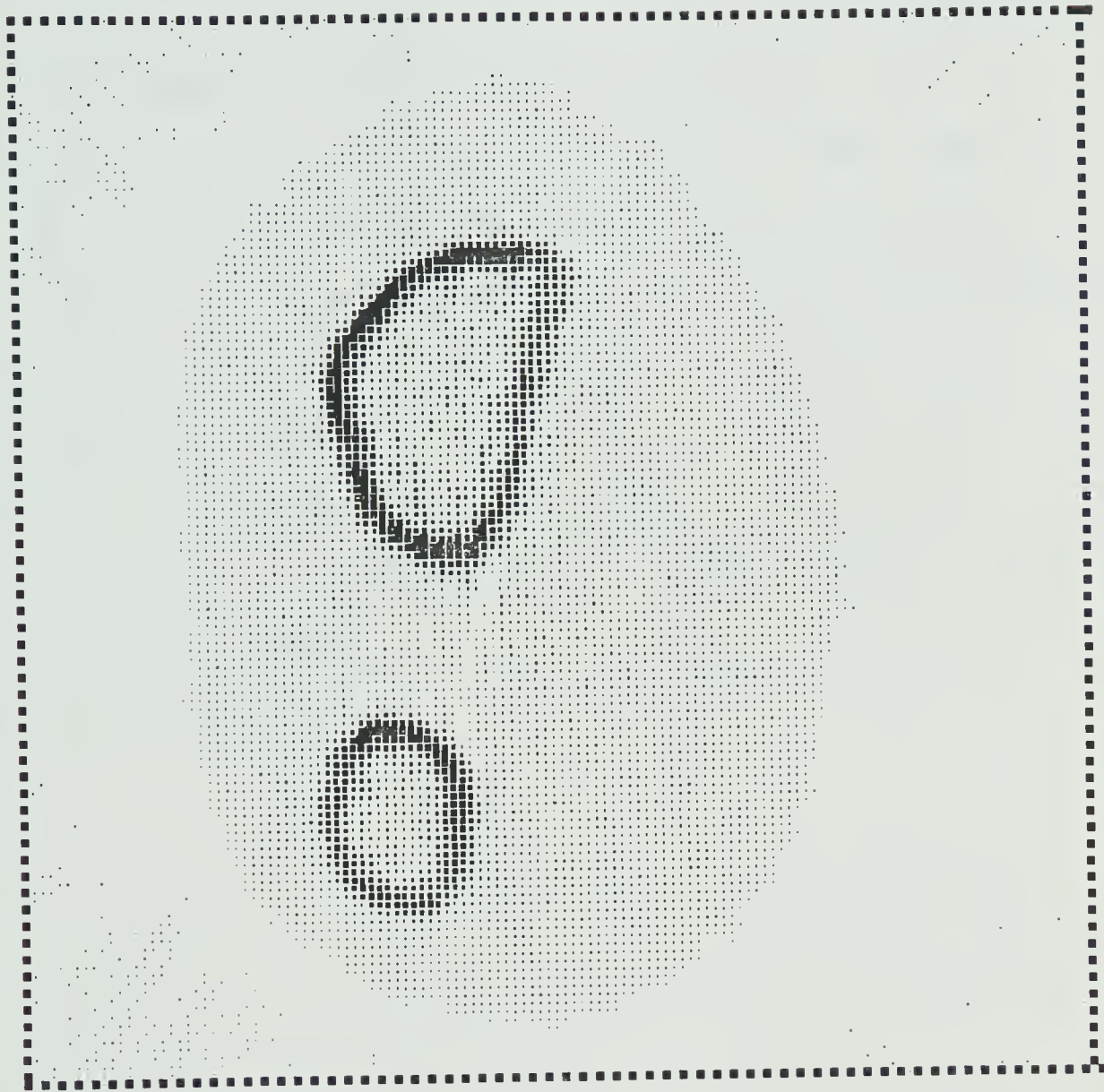


FIGURE 31. NORMAL RADIUS-ULNA

as that area of bone which comprised the inner 50 percent of the total bone area. It was felt that this arbitrary definition of trabecular bone may not be applicable to all patients. The criteria now used involves first calculating the average densities for all shells. Trabecular bone is then defined as the inner area of bone bordered by the maximum change in adjacent shell densities. The CT attenuation coefficients are converted to bone density (g/ccm) by dividing μ by the average mass attenuation coefficient for bone. Due to the fact that a non-material selective beam hardening correction is applied (as contrasted to a material selective correction (48)) these measures of density are only valid for longitudinal studies. Cross-sectional (i.e. population) studies require absolute values for bone density and this necessitates material selective corrections.

V. System Evaluation

The scanner was evaluated in terms of: (1) spatial resolution, (2) precision, (3) accuracy and (4) radiological dosage. The results of these evaluations are discussed in this section and a technique for measuring contrast resolution is suggested.

A. Spatial Resolution

Physical resolution of the system was evaluated using a 2 1/2 inch diameter circular plexiglass model with periodic structures of various size holes drilled into it. These holes are drilled so that the space between holes is equal to the hole diameter. The model was subsequently scanned at three different speeds and the holes were left open to the air. Motor pulses during the three speeds of translations were sent at 1318 Hz, 330 Hz and 82.4 Hz and data from the CAMAC scalars was collected every 12 motor pulses in all three instances. Since these speeds are ratios of 16:4:1 respectively the resultant subinterval counts obtained during the scan were in the ratios of 1:4:16 respectively. Since coefficient of variation (C.V.) is inversely proportional to the square root of the number of counts this means that the C.V.s associated with each of the ray-integral measurements were improved by a factor of two with each decreasing speed of scan. The open count rates of the source for detectors 1 through 8 were; on a subinterval basis: (1) 374.42, (2) 349.92, (3) 334.08, (4) 345.49, (5)

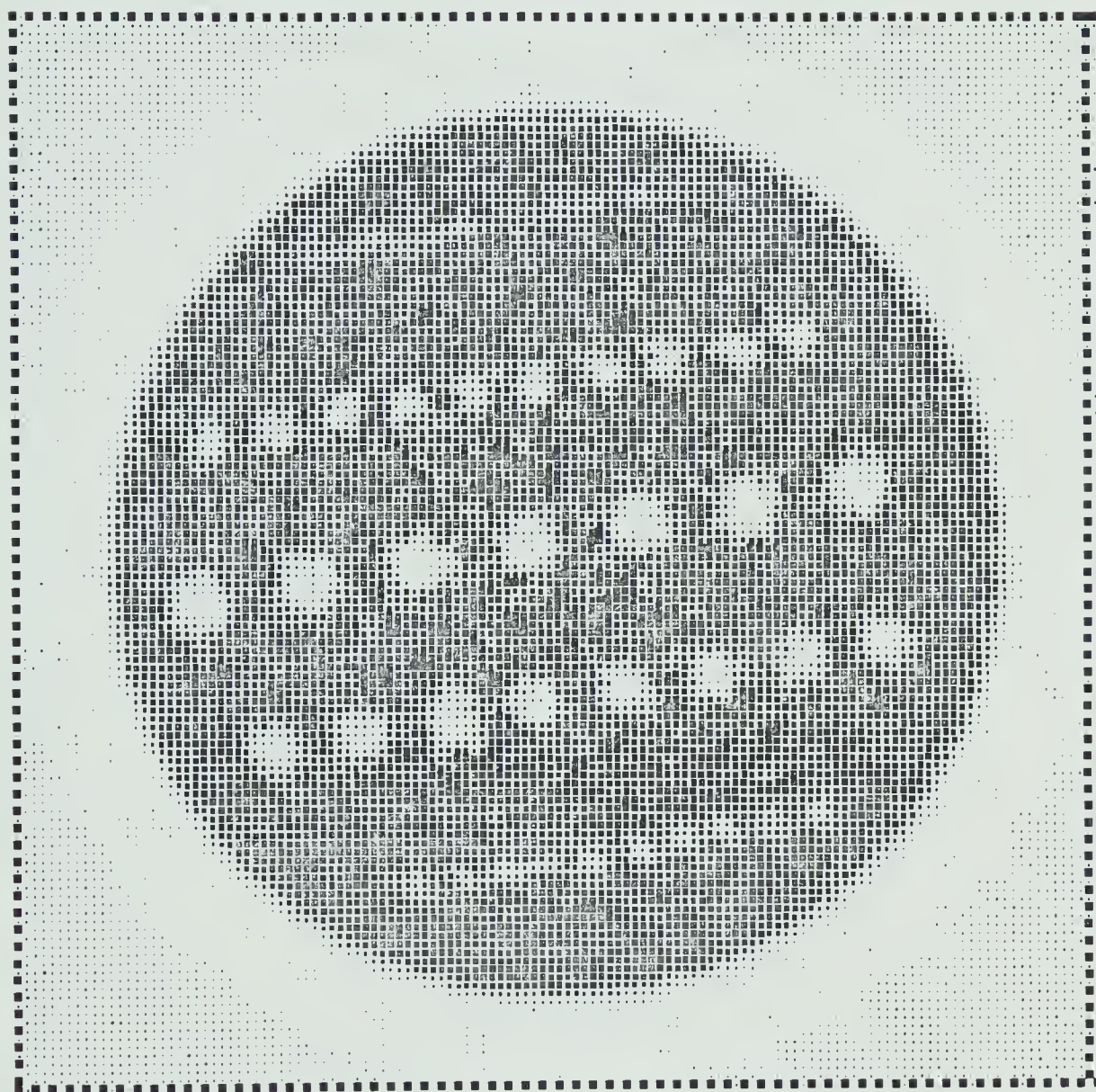
389.56, (6) 369.65, (7) 405.93, and (8) 379.45. Thus the C.V. associated with an average 8 subinterval per interval open count measurement is $1/\sqrt{(2948.49)} = 1.84\%$. At the medium speed (interval C.V. = 0.92 %) the spatial resolution has been improved whereas a further decrease in the interval C.V. to 0.46 % (low speed) had no apparent impact on the spatial resolution of the system.

It should be noted that one limit of the system in regards to spatial resolution is the spatial resolution of the imaging system. In this case although the reconstructed matrix is of size 256 x 256 with a 0.3 mm pixel size, the hard copy image matrix is only of size 128 x 128 with a corresponding pixel size of 0.6 mm. To further complicate matters the image display has a magnification effect of 1.6 times that of the object. Using the Grinnell display system one can display a matrix size of 512 x 512 and hence it is possible to view the system limited resolution on the video screen and yet essentially the same results were obtained as with the hard copy display. At high speed (Figure 32) the system spatial resolution was limited to 1/8 of an inch while at medium speed (Figure 33) the spatial resolution is improved to one sixteenth of an inch (approximately 1.5 mm). However, a further decrease in speed to low speed (Figure 34) had little or no effect on the spatial resolution. This is evidence that beyond a certain level statistics are no longer the limiting factor in regards to spatial resolution.

MEASUREMENT

319

17-JAN-80



HOLE DIAMETERS (INCHES) ARE (TOP TO BOTTOM) $1/32$, $3/32$, $5/32$,
 $1/8$ AND $1/16$.

FIGURE 32. HIGH SPEED RESOLUTION

MEASUREMENT

318

17-JAN-80

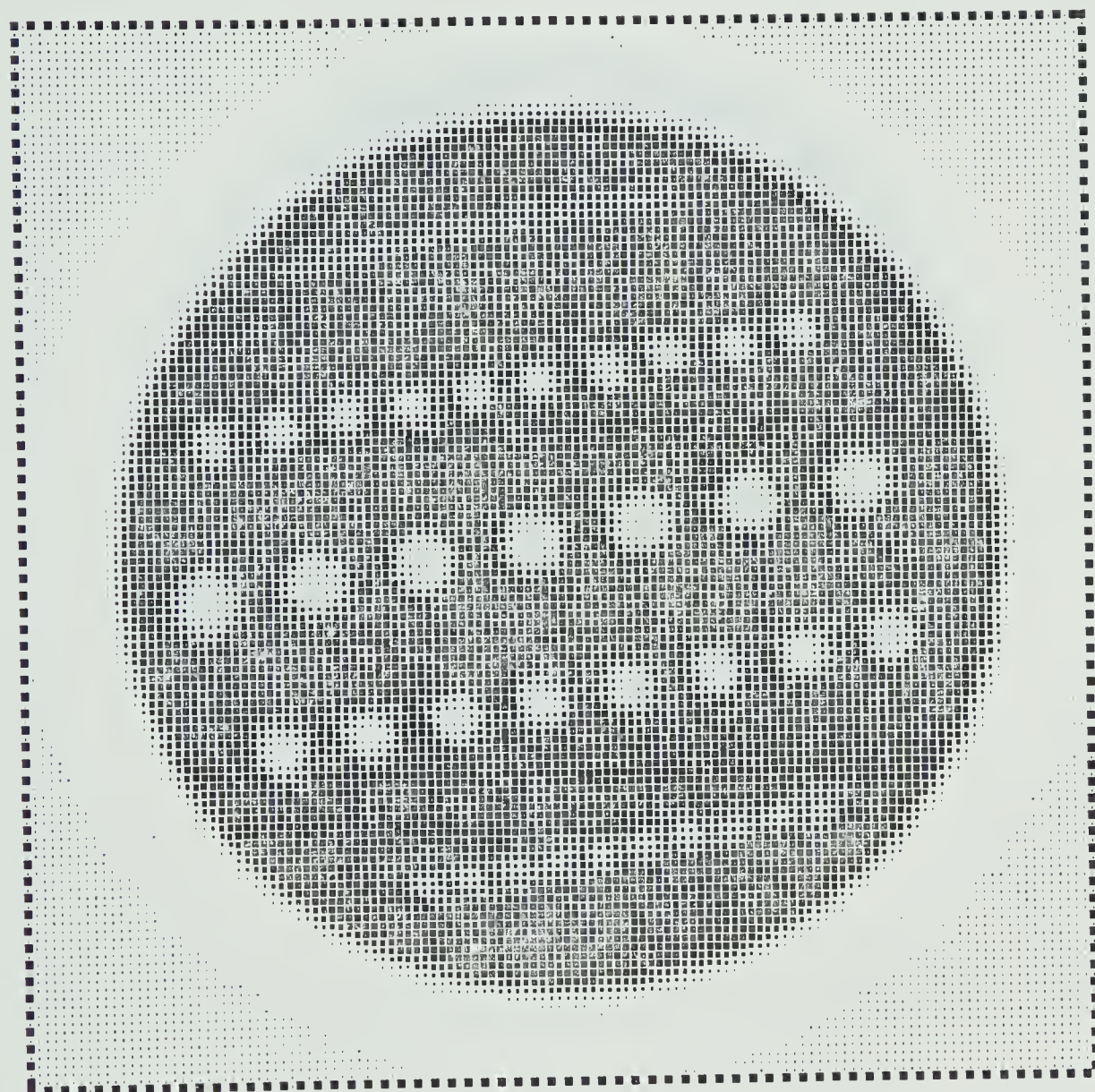


FIGURE 33. MEDIUM SPEED RESOLUTION

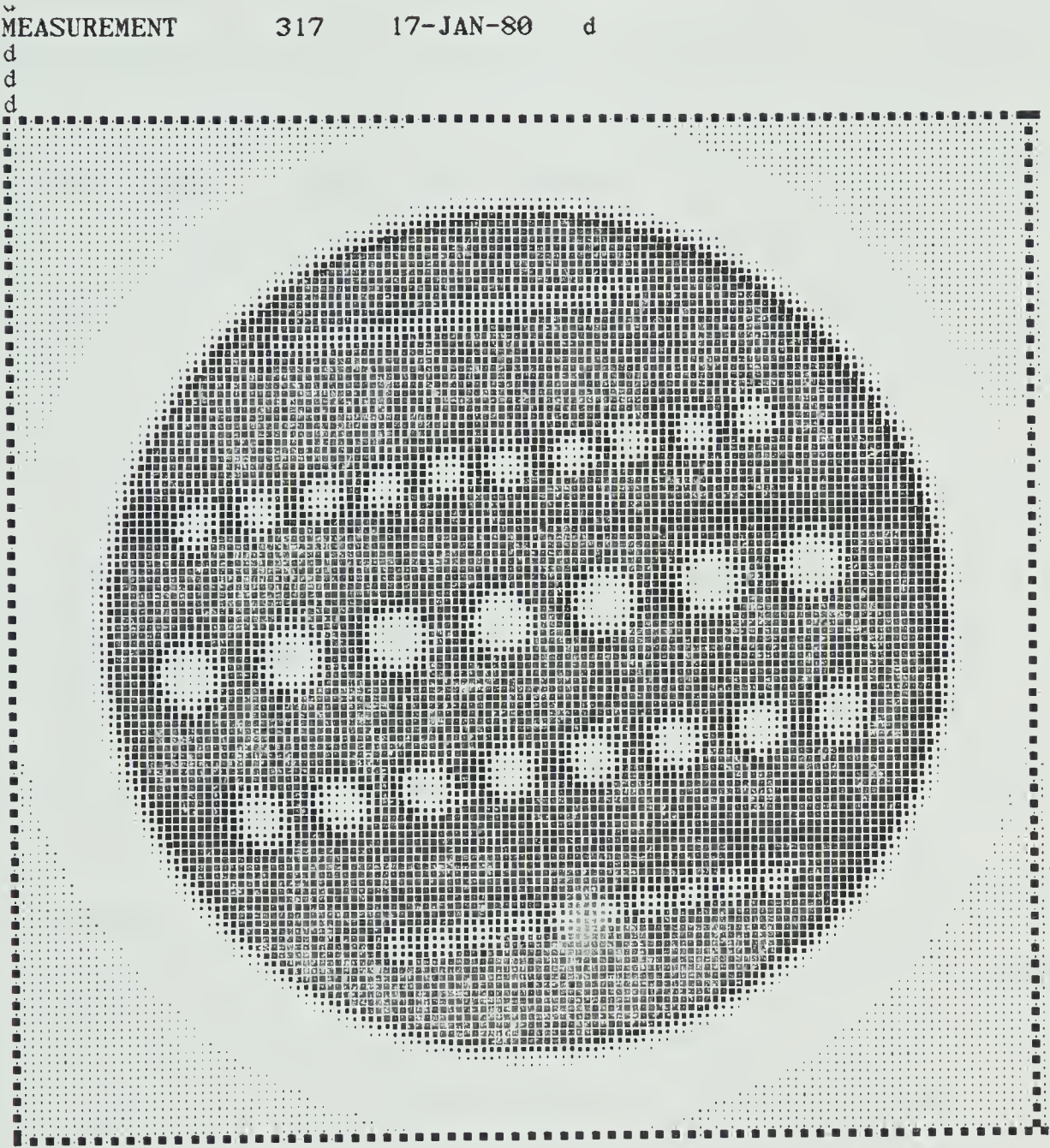


FIGURE 34. LOW SPEED RESOLUTION

B. Precision

The critical factor for the overall precision of the system is not so much the precision associated with the machine as with the ability to remeasure the patient at exactly the same site since both the amount of trabecular bone and its density vary significantly at sites axially along the arms or legs. This means that precision of the system is predominantly a function of the ability to determine the site of measurement. To reduce these errors in precision due to repositioning use of the scout scan was instituted.

A number of repeat scans were made on a 40 year old male normal (52). Each scan involved repositioning the arm using the scout scan and making three measurements on the arm. The first measurement was made at the site selected by the scout scan while the other two measurements were made at sites two millimeters of either side. These three measurements were then interpolated to produce the same area of bone for analysis purposes as was used in prior analyses. The data obtained from these measurements (Table 2) shows that a precision of better than $\pm 1\%$ is achievable for both cortical and trabecular bone density.

C. Accuracy

Accuracy of the scanner is a difficult quantity to define since it relates to a "correct" value being obtained. For measurements of bone this means that the bone would have

PRECISION EVALUATION

Measurement Number	Scan * Number	Bone Area (Pixels)	Trabecular Bone Density	Cortical Bone Density
1	1	3362	0.503	1.301
	-	-	-	-
2	1	3577	0.491	1.250
	2	3293	0.519	1.333
3	1	3552	0.501	1.250
	2	3248	0.522	1.328
4	1	3389	0.509	1.275
	2	3155	0.535	1.370
5	1	3586	0.497	1.237
	2	3308	0.510	1.330

With the above scans interpolated so as to produce a bone area of 3362 the results are as follows

1	3362	0.503	1.301
2	3362	0.512	1.313
3	3362	0.514	1.299
4	3362	0.512	1.286
5	3362	0.507	1.292

These interpolated results, when considering a normal distribution, result in standard deviations of 0.884 % for trabecular bone density and 0.847 % for cortical bone density.

*Note: Although three scans were made during each measurement only those two scans that were used in the interpolation are included.

TABLE 2.

to be removed and "ashed" to determine the true mineral content. Obviously, this is only possible to perform with cadavers and consequently the sources of data are limited.

To circumvent these problems a solution of di-Potassium Hydrogen Phosphate (K_2HPO_4) was used (53). The solution was mixed to a known concentration and placed inside a plexiglass cylinder (Figure 35). CT measurements were made on a number of different concentrations and the resultant linear attenuation coefficients of the image were compared to the known values of the dilute solution. Results of these tests are shown in Table 3 and Figure 36. These results show that although the absolute values may not be entirely accurate, the percentage change in value is quite accurate. Since the mineral content present in bone does vary tremendously from person to person it is measures of percentage changes that are of clinical importance rather than absolute values of mineral density. One reason that the absolute values are of limited accuracy is that the linear attenuation coefficients for the solution are calculated on the basis of a single energy which does not coincide exactly with the energy spectrum of Iodine 125.

D. Radiation Dose

Calculations of a theoretical radiological dose (as performed on the following pages) show that the total radiation dose received during the course of a scout scan and three adjacent scans is 0.9 rads.

MEASUREMENT

861

3-JUN-80

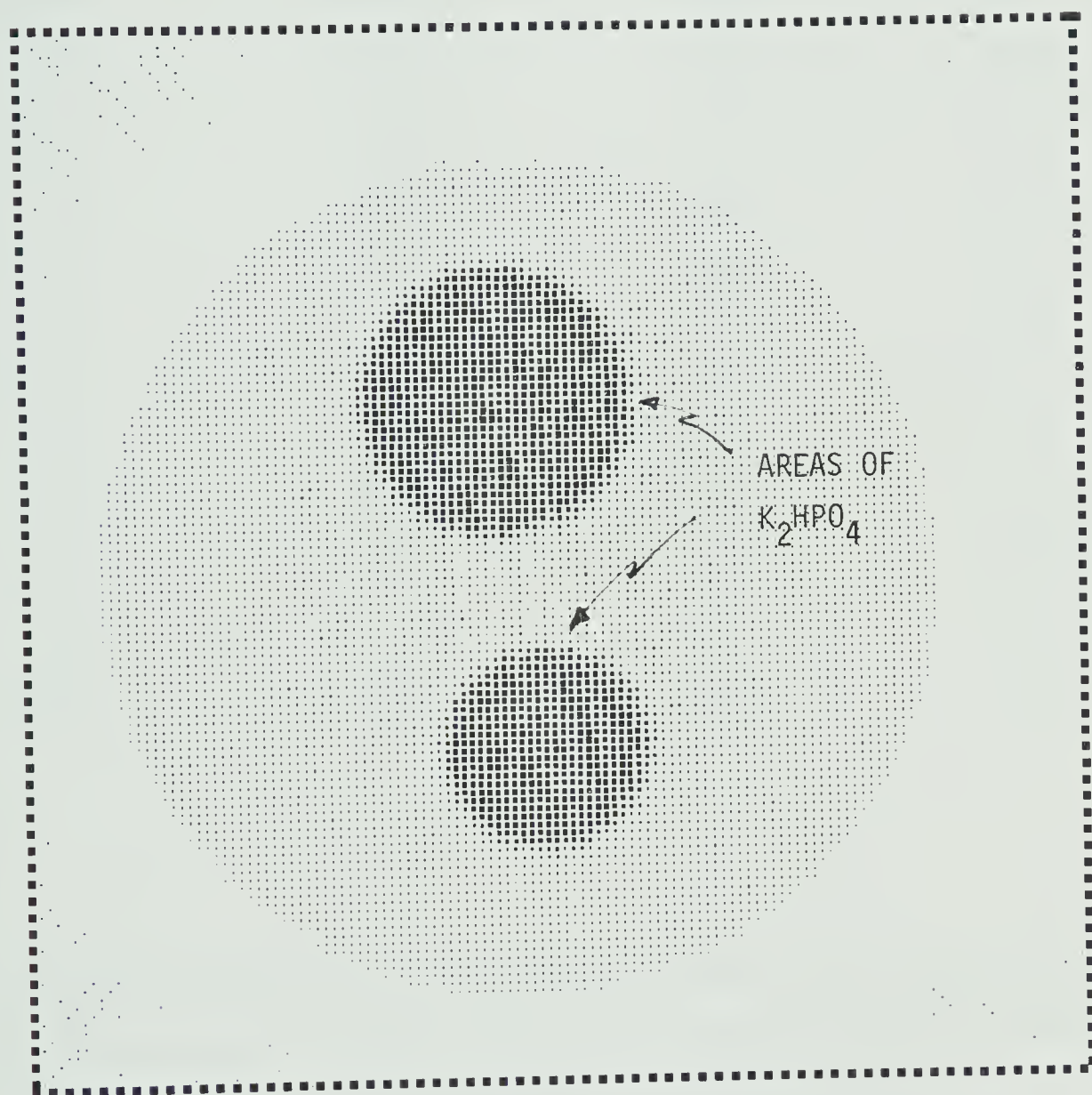


FIGURE 35. TEST CYLINDER

ACCURACY EVALUATION

Measured Linear Attenuation Coefficient (per cm.)	Percent of Maximum Measured Linear Attenuation Coefficient	Calculated Linear Atten. Coefficient (per cm.)	Percent of Maximum Calculated Linear Attenuation Coefficient
1.882	100	1.709	100
1.852	98.4	1.675	98.0
1.814	96.4	1.641	96.0
1.776	94.4	1.606	94.0
1.765	93.8	1.598	93.5
1.747	92.8	1.589	93.0
1.739	92.4	1.581	92.5
1.735	92.2	1.572	92.0
1.690	89.8	1.538	90.0
1.654	87.9	1.504	88.0
1.615	85.8	1.470	86.0

A linear regression of the percent calculated linear attenuation coefficient was run against the percent measured linear attenuation coefficient (using the SPSS package) and found to have a correlation of $r=0.9987$ and a significance of $p < 0.0001$

TABLE 3.

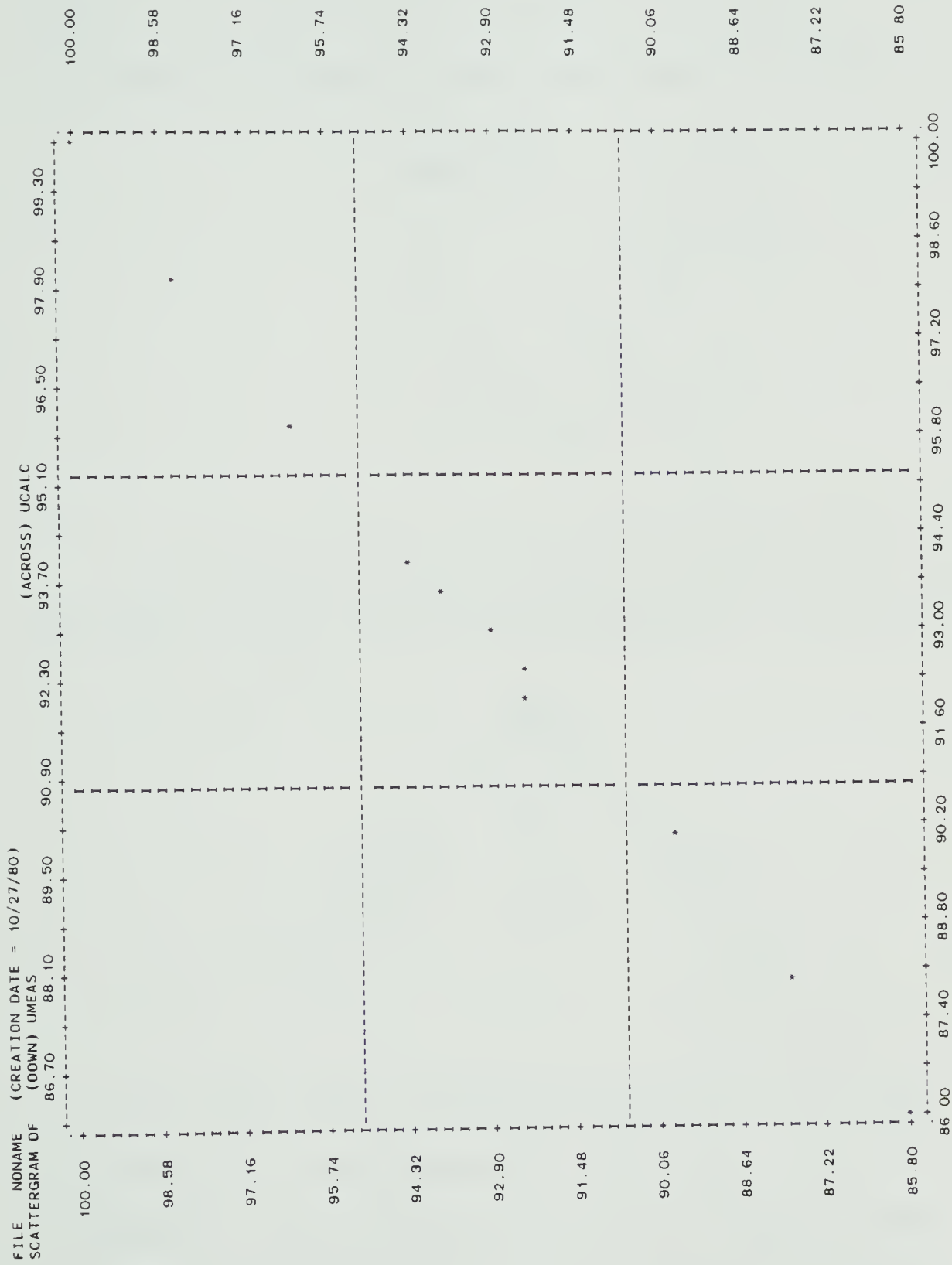
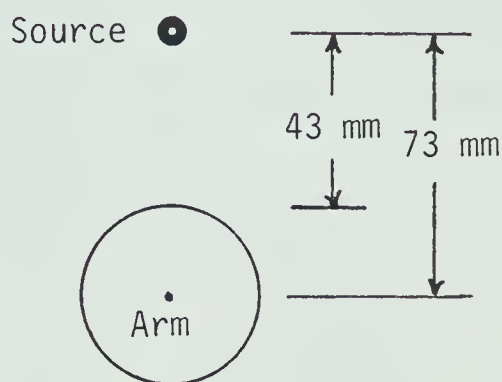


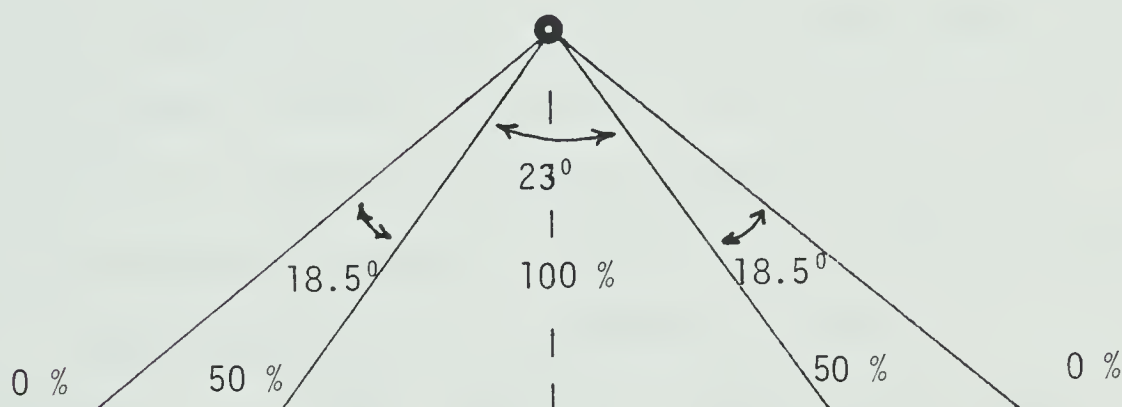
FIGURE 36. SYSTEM ACCURACY

Radiological Dose

Assume that an arm of diameter 60 mm is placed in the center of the scan area. This results in a distance of 43 mm from the source to the nearest point on the arm.



At a distance of 43 mm the source-collimator configuration was found to produce the following approximate intensity distribution.



The scanner moves a distance of 106.2 mm in 12.89 sec resulting in an average speed of 8.24 mm / sec. The area irradiated at 100 % intensity consists of a length L , where $L = 2 \tan (23^\circ/2) (43 \text{ mm}) = 17.5 \text{ mm}$. The area irradiated at an average intensity of $1/2(100\% + 50\%) = 75\%$ consists

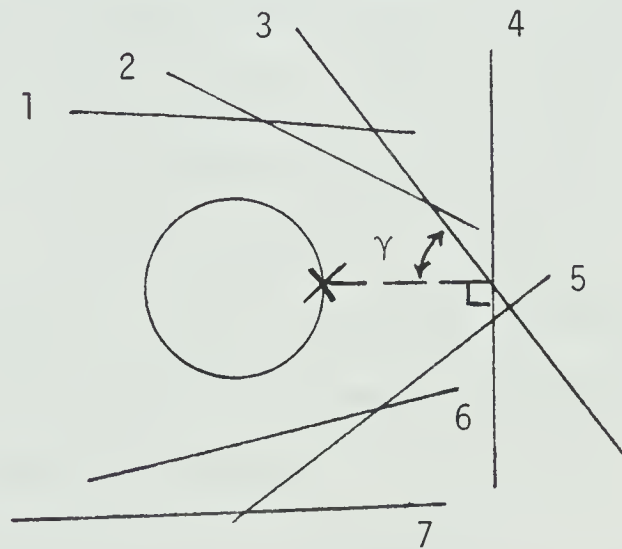
of 2 lengths, each one of length $L1$, where

$$L1 = 1/2 (2 \tan (60^\circ/2) 43 \text{ mm} - 17.5 \text{ mm}) = 16.08 \text{ mm}.$$

Thus the total length irradiated at effectively 100% is

$$17.5 (100\%) + 2(16.08)(75\%) = 41.61 \text{ mm which at a speed of } 8.24 \text{ mm / sec means an effective (100\%) irradiation time of } 41.61 \text{ mm / } 8.24 \text{ mm/sec} = 5.05 \text{ seconds}.$$

This is the irradiation time for one translation. However, each scan consists of 7 translations made at varying angles.



The rotation between angles is 25.71° and the approximate "hotspot" (area subjected to maximum radiation) is that point on the arm perpendicular to translation number 4 (denoted by point x).

Thus at $\gamma = 90^\circ$ the irradiation is 100% while at $\gamma = 0^\circ$ the irradiation is 0%. Hence irradiation is proportional to $\sin \gamma$.

Translation 1	$\gamma = 90^\circ - 3(25.71^\circ) = 12.87^\circ$	$\sin \gamma = 0.22$
Translation 2	$\gamma = 90^\circ - 2(25.71^\circ) = 38.58^\circ$	$\sin \gamma = 0.62$
Translation 3	$\gamma = 90^\circ - 1(25.71^\circ) = 64.29^\circ$	$\sin \gamma = 0.90$
Translation 4	$\gamma = 90^\circ$	$\sin \gamma = 1.00$
Translation 5	$\gamma = 64.29^\circ$	$\sin \gamma = 0.90$
Translation 6	$\gamma = 38.58^\circ$	$\sin \gamma = 0.62$
Translation 7	$\gamma = 12.87^\circ$	$\sin \gamma = 0.22$

4.48

Therefore, for one scan the total irradiation time (100% intensity) at the hotspot is $4.48 (5.05 \text{ sec}) = 22.62 \text{ seconds}$.

A new source of 1.5 Ci I^{125} was measured using an ionization chamber at a distance of 0.5 meters (so that the entire chamber was irradiated) and found to have a dose rate of 11 mr/min. Using the inverse square law the dose rate at 43 mm would be $11 \text{ mr/min} (500/43)^2 = 1487 \text{ mr/min} = 24.79 \text{ mr/sec}$. This means that the total dose per scan at the hotspot is $24.79 \text{ mr/sec} (22.62 \text{ sec}) = 560 \text{ mr}$. Since the speed of the scout scan is the same as for a normal scan the effective (100%) irradiation time is 5.05 sec leading to a dose of $5.05 \text{ sec} (24.79 \text{ mr/sec}) = 125 \text{ mr}$. Assuming adjacent measurements produce a 50 % increase in dose the total exposure dose for 1 scout scan and 3 adjacent scans is $1.5(560 + 125) = 1027.5 \text{ mr} \approx 1 \text{ r (roentgen)}$. At 30 KeV this is approximately equal to an absorbed dose of 0.9 rad.

Although these theoretical calculations do provide a rough estimate of dose there are a number of associated problems. One major problem is the assumption that absorption of radiation is only significant at the surface. Although this may be true for denser objects with high linear attenuation coefficients it is not true for skin. The linear attenuation coefficient of skin is approximately 0.45/cm (for 30 KeV) which means that some 1.5 cm of skin must be traversed before the intensity of the radiation is down by a factor of 2. Since there is a limited amount of skin at the forearm, radiation passing through skin only will have a significant effect on the dose rate whether or not it directly impinges upon the area of consideration. Although most rays do pass through some bone and thereafter do not contribute appreciably to skin dose it should be realized that there is an element of variation from person to person.

Another area of concern is the effects of scattered radiation from the bones and their effect on the dose at a particular point. It is relatively complicated to account for scatter on a theoretical basis and as such the use of Thermo-Luminescent Detectors (TLD's) has been suggested.

Thermo-Luminescent Detectors

TLD's are capsules of powder or crystals that react chemically when exposed to radiation. After exposure to radiation the powder is removed from the capsules and heated up. When heated the powder produces photon flashes the number and intensity of which are proportional to the radiation exposure.

It is presently being proposed that a number of holes be drilled in a plexiglass phantom and filled with TLD powder. Subsequent to making a number of measurements on the phantom the powder is to be removed and tested to determine the radiation exposure. The plexiglass phantom will contain aluminum tubes to simulate the radius and ulna and will be made in the approximate size and shape of a human forearm. Measurements of dose performed in this manner should produce a profile of the radiation dose throughout a human forearm.

E. Contrast Resolution

Contrast resolution could be measured by examining the limiting spatial resolution with differing contrast media in the holes. One possible contrast media is di-Potassium Hydrogen Phosphate (K_2HPO_4) mixed in a water base. If solutions of varying concentration were placed in the 1/16 th of an inch diameter holes then the system limited contrast resolution would be defined by comparing the smallest linear attenuation coefficient of the imageable solutions with that of plexiglass. The major difficulties in

these measurements will be placing the proper concentration solutions in the holes and ensuring that no air bubbles are present. Measurements of contrast resolution have not been made due to these difficulties and the limited usefulness of such measurements.

VI. System Limitations and Future Plans

Four of the major limitations at present are: (1) statistical limitations due to the use of a radioisotope photon source, (2) a lengthy scanning time due to use of a second (versus a third or fourth) generation CT scanner, (3) a lack of flexibility in regards to scanner control, and (4) an inability to view the image immediately after scanning due to limited processing facilities. This chapter will explore these limitations and will suggest ways to reduce or eliminate them.

A. X-Ray Tube

Subject to appropriate funding present plans include the purchase of a mini-X-ray tube. As a result of physical considerations photon flux is more limited in the case of a radioisotope source than for an X-ray tube. Although use of an X-ray tube may result in higher radiation dose rates it will also facilitate a reduced scan time and hence the net radiation exposure may not be radically altered. With the aid of filters the X-ray tube will also allow a greater selection of photon energies to be used. This may allow the scanner to perform elemental identifications through the use of differential energy scans and to be used for scans of areas of high radiological attenuation such as the knee. The use of filters may also reduce the problems of beam hardening caused by the multi-energy X-ray radiation. Although beam hardening will be a problem, so long as the

"raw" data is available, it is possible to correct for.

B. System Three

Present plans include the construction of a generation three system. This improvement will result in a substantial decrease in scan time hence reducing movement artifacts, improving patient comfort and reducing the dose of radiation.

C. Control System

The major constraint at present is that the control programs are "locked" into EPROMs. In order to alter any of the scan parameters, such as speed, scan length, distance between projections and/or the angle between profiles, a new program must be written into the EPROMs. To circumvent this problem it is proposed that the EPROMs be programmed with a number of basic subroutines and that all control parameters be loaded into the MPU from external sources. One of the subroutines contained in the EPROMs would be a program that reads data into the MPU via the PIA (M6820). Data to be read into the MPU would be loaded into the HP 2100 from either the console or a series of programs contained on magnetic tape. This data will be subsequently transferred from the HP 2100 into a memory module contained in the CAMAC system. The transfer of data from the HP to the memory module (4000 16 bit words) will free the HP to perform other functions subsequent to loading the CAMAC. Control parameters will be

loaded from the memory module to the 512 bytes of RAM (M6810) contained in the MPU. Direct interrupts will also be provided between the MPU and the HP 2100 computer. The read program which is the subroutine that reads data from the memory module to the microprocessor unit has been assembled and is included in the appendix.

D. Processing Facilities

A new 32 bit minicomputer has been ordered (SEL 32/57) and delivery is expected for the fall of 1980. Purchase of an array processor dedicated to the reconstruction is also being considered and appears likely at this point in time. The resultant upgrading of computing facilities will allow the image to be displayed on the Grinnell imaging system at the same time or shortly after a scan is performed. This means that the validity of the scan can be checked immediately and should another scan be required the patient will still be present.

References

1. Bocage EM: Patent No. 536,464, Paris France 1921 (Quoted in 'History of Tomography' by J Massiot, 1974 Medica Mundi, 19(3), 106-115).
2. Radon J: Ueber die Bestimmung von Funktionen durch ihre Integralwerte laengs gewisser Mannigfaltigkeiten. Ber Verh Saechs Akad Wiss 69:262-277, 1917.
3. Bracewell RN: Strip integration in radioastronomy. Australian Journal of Physics 9:198-217, 1956.
4. Cormack AM: Representation of a function by its line integrals with some radiological applicactions. Journal of Applied Physiology 34:2722-2727, 1963.
5. Hounsfield GN: Computerized transverse axial scanning (tomography): Part 1. Description of system. British Journal of Radiology 46:1016-1022, Dec. 1973.
6. Health Research Group, Washington D.C.: Computerized axial tomography (CAT) scanners is fancier technology worth a billion dollars of health consumer's money? U.S. Department of Commerce - National Technical Information Service, HRP-0019236, 1977.
7. Brooks RA, Di Chiro G: Principles of computer assisted tomography (CAT) in radiographic and radioisotopic imaging. Phys. Med. Biol. 21:681-732, 1976.
8. Rügsegger P, Elsasser U: Computerassistierte Photonenabsorptionsmessung zur Quantifizierung der Spongiosadichte. Premier Symposium CEMO, La Chaux-de-Fonds, Oct. 5-8, 1975.

9. Snyder W, et al: Report of the Task Group on Reference Man, ICRP 23. Oxford, Pergamon Press, 1975.
10. Overton TR, Silverberg DS, Rigal WM, Friedenbergl: University of Alberta bone mineral analysis system - performance and clinical application. (In) Proceedings of International Conference On Bone Mineral Measurement, ed. RB Mazess, Chicago, DHEW Publication No. (NIH) 75-683, 1973.
11. Elsasser U: Quantifizierung der Spongiosadichte an Röhrenknochen mittels Computertomographie. Diss. ETH, Zurich, 1977.
12. Guyton A: Textbook of Human Physiology. Philadelphia, Saunders, 1971.
13. Heaney RP: Bone physiology and calcium homeostasis. (In) Textbook of Medicine, ed. by PB Beeson and W McDermott, Philadelphia, Saunders, 1971.
14. Sodeman WA, Sodeman WA: Pathologic Physiology, Philadelphia, Saunders, 1967.
15. Frost HM: Treatment of osteoporoses by manipulation of coherent bone cell populations, (In) Clinical Orthopaedics and Related Research, JB Lippincott Co., 1979.
16. Brown DM: Rickets and osteomalacia. (In) Current Therapy 1977, ed. by HF Conn, Philadelphia, Saunders, 1977.
17. Henry JB: Clinical chemistry: clinico pathologic correlations in bone diseases. (In) Clinical Diagnosis, ed. by I Davidsohn and JB Henry, Philadelphia, WB

Saunders Co., 1974.

18. Saville PD: Osteoporosis. (In) Current Therapy 1977, ed. by HF Conn, Philadelphia, Saunders, 1977.
19. Cameron JR, Sorenson J: Measurement of bone mineral in vivo: An improved method. Science 142:230-232, 1963.
20. Cameron JR, Mazess RB, Sorenson J: Precision and accuracy of bone mineral determination by direct photon absorptiometry. Invest. Radiol. 3:141-150, 1968
21. Smith DM, Johnstone CC, Yu P: In vivo measurement of bone mass, its use in demineralization states such as osteoporosis. Journal of American Medical Association 291:325-329, 1972.
22. Goldsmith NF, Johnstone JO, Ury H, Vose G, Colbert C: Bone-mineral estimation in normal and osteoporotic women. Journal of Bone and Joint Surgery 53A1:83-100, Jan. 1971.
23. Lewellen TK, Nelp WB: Total body calcium analysis using the $^{40}\text{Ca}(n,\alpha)^{37}\text{Ar}$ Reaction. NASA Technical Report contract number NAS9-13029.
24. Webber CE, Kennett TJ: Bone density measured by photon scattering: A system for clinical use. Dep't of Nuclear Medicine, McMaster University Medical Centre.
25. Hinderling Th, Rüegsegger P, Anliker M: C.T. reconstruction from hollow projections: an application to in vivo evaluation of artificial hip joints. Journal of Computer Assisted Tomography 3(1):52-57, Feb/1979.
26. Brooks RA, DiChiro G : Theory of image reconstruction in

computed tomography. Radiology 117:561-572, December 1975

27. Shepp LA, Kruskal JB, Logan BF: Computerized tomography: the new medical x-ray technology. Bell Laboratory Publication 07974, Murray Hill, New Jersey, 1974.
28. Ledley RS: Introduction to computerized tomography. Computerized Biological Medicine 6:239-246, 1976.
29. McCullough EC, Payne JJ: X-ray transmission computed tomography. Medical Physics 4(2), Mar./Apr. 1977.
30. Bates RHT, Peters TM: Towards improvements in tomography. New Zealand Journal of Science 14:883-896.
31. Bracewell RN, Riddle AC: Inversion of fan-beam scans in radio astronomy. Journal of Astrophysics 150:427-434, 1967.
32. Peters TM, Lewitt RM: Computed tomography with fan beam geometry. Journal of Computer Assisted Tomography 1(4), 1977.
33. Shepp LA, Logan BF: Reconstructing interior head tissues from x-ray transmissions. Bell Laboratories Report, Murray Hill, New Jersey, 1974.
34. Ramachandran GN, Lakshminarayanan AV: Three-dimensional reconstruction from radiographs and electron micrographs: application of convolutions instead of Fourier transforms. Proc. Natl. Acad. Sci. U.S. (68), 2236-2240.
35. Stanton L: Basic Medical Radiation Physics, New York, Meredith Corporation, 1969.

36. Siegbahn K: Alpha-, Beta- And Gamma-Ray Spectroscopy, Amsterdam, North-Holland Publishing Co., 1966.
37. Larsson S, Bergstrom M, Dahlqvist I, Israelsson A, Lagergren C: A method for determining bone mineral content using Fourier image reconstruction and dual source technique. *Journal of Computer Assisted Tomography* 2:347-351, July 1978. *Journal of Computer Assisted Tomography* 2:184-188, 1978.
38. Latchaw RE, Payne JT, Gold LHA: Effective atomic number and electron density as measured with a computed tomographic scanner: computation and correlation with brain tumour histology. *Journal of Computer Assisted Tomography* 2:199-208, 1978.
39. Chesler DA, Riederer SJ, Pelc NJ: Noise due to photon counting statistics in computed x-ray tomography. *Journal of Computer Assisted Tomography* 1(1):64-67, 1977.
40. Gore JC, Tofts PS: Statistical limitations in computed tomography. *Phys. Med. Biol.* 23:1176-1182, 1978.
41. Riedler SJ, Pelc JN, Chesler DA: The noise power spectrum in computed x-ray tomography. *Phys. Med. Biology* 23(3):446-454, 1978.
42. Tretiak OJ: Noise limitations in x-ray computed tomography. *Journal of Computer Assisted Tomography* 2:477-480, 1978.
43. Brooks RA, Di Chiro G: Statistical limitations in x-ray reconstruction tomography. *Medical Physics* 3:237-240,

1976.

44. Evans RD: The Atomic Nucleus, New York, McGraw-Hill, 1955.
45. Brooks RA, Di Chiro G: Beam hardening in x-ray reconstructive tomography. Phys. Med. Biol. 21:390-398, 1976.
46. Sandrik JM, Judy PF: Effects of the polyenergetic character of the spectrum of iodine 125 on the measurement of bone mineral content. Department of Radiology, University of Wisconsin Medical Center, Madison Wisconsin.
47. Kijewski PK, Bjarngard BE: Correction for beam hardening in computed tomography. Medical Physics 5(3), May/June 1978.
48. Ruegsegger P, Hangartner Th, Keller HU: Standardization of C.T. images by means of a material selective beam hardening correction. Journal of Computer Assisted Tomography 2:253-262, July 1978.
49. General Electric: CT/T technology continuum, Milwaukee, GE Medical Systems Division, 1979.
50. Ruegsegger P, Niederer P, Anliker M : An extension of classical bone mineral measurements. Annals of Biomedical Engineering 2:194-205, 1974
51. Lancaster D: TTL Cookbook, Indianapolis, HW Sams & Co., 1974.
52. Hangartner Th, Ridley JD: Internal communication.
53. Ridley JD: Internal communication.

54. Hangartner Th: Internal communication.
55. Medical Internal Radiation Dose Committee of the Society of Nuclear Medicine: MIRD Pamphlet No. 10, Iodine-125 electron capture decay.

$^{125}_{53}\text{I}$ DECAY MECHANISM
 53

$^{125}_{53}\text{I}$ decays via electron capture to $^{125}_{52}\text{Te}$ and in doing

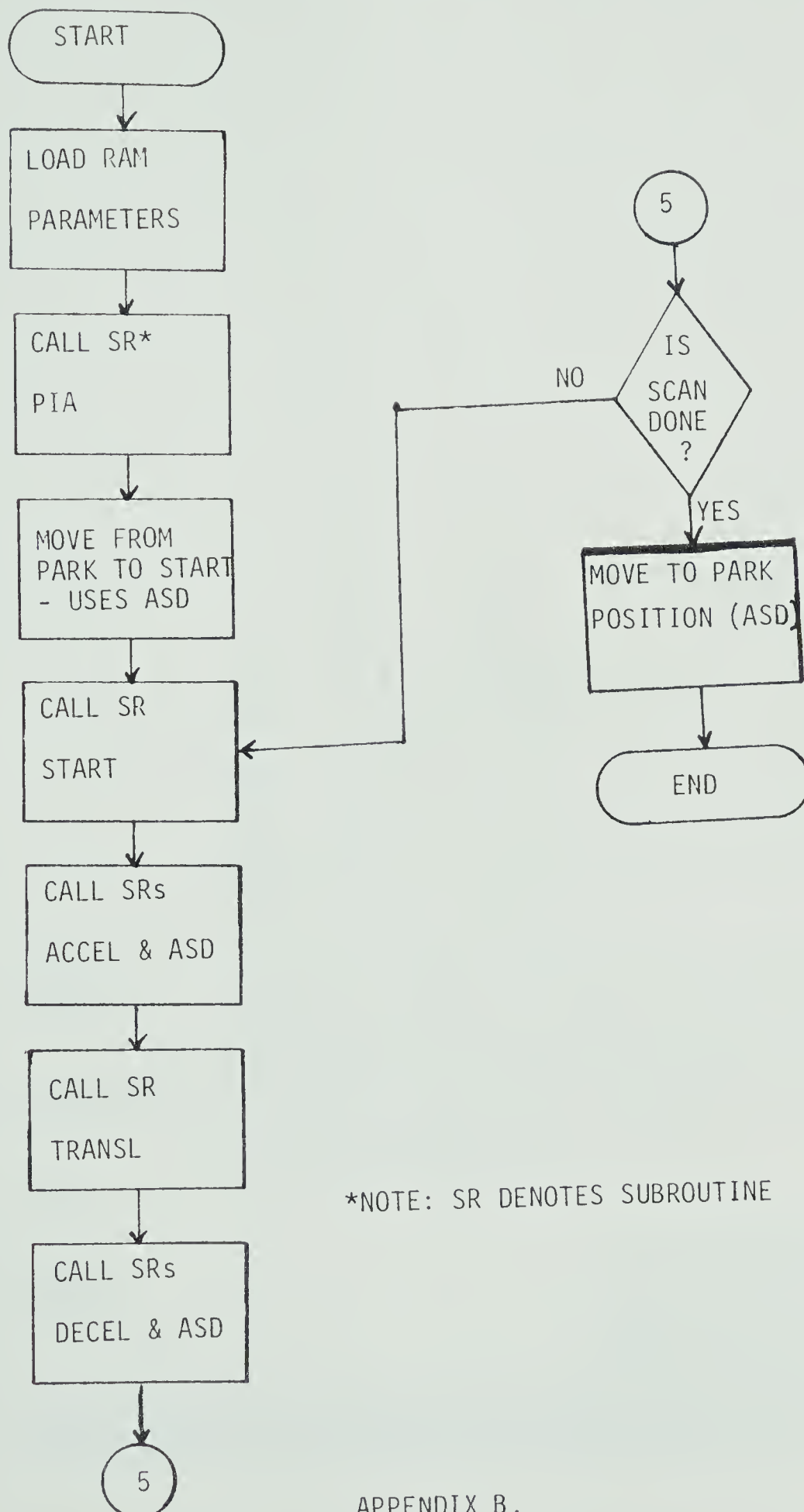
so gives off a 35.4 KeV gamma ray. This gamma ray will:

- 1) appear on the outside .0666 times per disintegration;
- 2) cause a k alpha-1 x-ray .7615 times per disintegration (27.4 KeV);
- 3) cause a k alpha-2 x-ray .3906 times per disintegration (27.2 KeV);
- 4) cause a k beta-1 x-ray .2056 times per disintegration (30.9 KeV);
- 5) cause a k beta-2 x-ray .0426 times per disintegration (31.8 KeV);
- 6) cause an L x-ray .2226 times per disintegration (3.7 KeV).

Thus in general the original gamma ray energizes an electron in the k shell causing it to move out of its orbit. This gap is filled by a loose electron which, in falling into the k shell, gives off an x-ray of approximately 27.5 KeV. The associated half-life is 60.2 days.

APPENDIX A.

NORMAL SCAN



*NOTE: SR DENOTES SUBROUTINE

CONTAINING ALL MAIN PROGRAMS AND ALL SUBROUTINES (EXCEPT READ) ***

Motorola M68SAM Cross-Assembler

00001	8004	ORA	EQU	\$8004
00002	8004	DDRA	EQU	\$8004
00003	8005	CRA	EQU	\$8005
00004	0000	M	EQU	\$0000
00005			NAM	DET8
6000			ORG	\$6000
00007		*		* REVISED APR 24, 1980
00008		*		
00009		*		
00010		*		THIS PROGRAM WILL BE USED TO PERFORM
00011		*		A MULTI-DETECTOR SCAN USING 8 DETECTORS.
00012		*		USING A 1:1 PULLEY RATIO THE TRANSLATION
00013		*		IS 16992 STEPS (106.2 MM).
00014		*		1 MM = 1600 STEPS.
00016		*		BE SCANNED WITH THIS ARRANGEMENT IS 76.8 MM DIAMETER.
00017		*		THE SCANNER WILL COLLECT 1416 DATA. FROM THE
00018		*		PARK POSITION THE SCANNER MUST MOVE BACK (-)
00019		*		1447 STEPS (+200 FOR ACCEL.) BEFORE
00020		*		STARTING THE SCAN.
00021		*		MOTOR PULSES ARE SENT EVERY 466 CYCLES
00022		*		(APPROX. 760 US) AND DATA PULSES ARE SENT TO
00023		*		THE HP EVERY 12 MOTOR PULSES. THE SCANNER IS TO
00024		*		ROTATE 25.71 DEG. AFTER EACH TRANSLATION & IS
00025		*		TO PERFORM 7 TRANSLATIONS & 6 ROTATIONS.
00026		*		EACH TRANSLATION TAKES APPROX. 13 SECONDS
6000	86 OF	LDA A	#\$OF	
6002	97 2C	STA A	M+44	;TRANSLATIONAL DIRECTION
6004	86 07	LDA A	#07	
6006	97 2D	STA A	M+45	;# OF TRANSLATIONS
6008	86 0C	LDA A	#12	
600A	97 32	STA A	M+50	;# OF MOTOR STEPS / HP SIGNAL
600C	86 08	LDA A	#08	;DETERMINES DELAY IN TRANSLATION
600E	97 33	STA A	M+51	
6010	86 04	LDA A	#04	;DETERMINES DELAY IN TRANSLATION
6012	97 34	STA A	M+52	
6014	86 05	LDA A	#05	;DETERMINES DELAY IN TRANSLATION
6016	97 35	STA A	M+53	;CALLS INIT AND F AS WELL
6018	BD C278	JSR	P1A	
00040		*		* MOVE FROM PARK TO START POSITION
00041		*		ONE GROUP OF 1647 PULSES
00042		*		MAKES USE OF THE R21 RAMP
00043		*		1647=400 + 1247*1
601B	86 17	LDA A	#\$17	; TRANSLATIONAL DIRECTION
00045				


```

00046 601D 97 00      STA A M
00047 601F CE 04DF    LDX #1247
00048 6022 DF 2A      STX M+42
00049 6024 CE 066F    LDX #1647
00050 6027 DF 25      STX M+37
00051 6029 BD C000    JSR ASD
00052 602C BD C29B    JSR START
00053 602F C6 1B      LDA B #$1B
00054 6031 F7 8004    STA B ORA
00055 6034 BD C28C    JSR DELAY
00056 6037 C6 1F      LDA B #$1F
00057 6039 F7 8004    STA B ORA
00058                * BEGIN ACCELERATION
00059 603C BD C1F5    JSR ACCEL
00060 603F BD C000    JSR ASD
00062                * SCAN - UP PROVIDES A MOTOR PULSE EVERY 466 CYCLES & A HP PULSE
00063                * EVERY 12 MOTOR PULSES
00064                * HP PULSE IS SENT EVERY M+46 MOTOR PULSES
00065 6042 CE 4260    LDX #16992
00066 6045 BD C2B0    JSR TRANSL
00067                * DELAY BETWEEN PULSES = 4*68 + 42 + 8*12 + 56 = 466 CYCLES
00069 6048 BD C208    JSR DECEL
00070 604B 7A 002D    DEC M+45
00071 604E 27 0C      BEQ JMPE
00072 6050 BD C28D    JSR R8D
00073 6053 96 2C      LDA A M+44
00074 6055 88 18      EOR A #$18
00075 6057 97 2C      STA A M+44
00076 6059 7E 602C    JMP ST
00078                * MOVE BACK TO PARK POSITION
00079                * MUST MOVE BACKWARD 15744 PULSES
00080                * SHOULD MOVE BACK 15745
00081                * HOWEVER SCAN APPEARS TO BE OUT
00082                * ONE PULSE AT SOME POINT
00083 605C 86 17      JMPE LDA A #$17
00084 605E 97 00      STA A M
00085 6060 CE 3BFO    LDX #15344
00086 6063 DF 2A      STX M+42
00087 6065 CE 3D80    LDX #15744
00088 6068 DF 25      STX M+37
00089 606A BD C000    JSR ASD
00090                * ROTATE BACK TO PARK POSITION
00091                * MUST ROTATE BACK 31080 PULSES
00092 606D CE 77D8    LDX #30680
00093 6070 DF 2A      STX M+42
00094 6072 CE 7968    LDX #31080
00095 6075 DF 25      STX M+37

```

;TELL HP RAMP IS BEGINNING
 ;IS SCAN FINISHED?
 ;CHANGE TRANSLATIONAL DIRECTION


```

00096 6077 86 1D          LDA A  #$1D
00097 6079 97 00          STA A  M
00098 607B BD C000        JSR    ASD
00099 607E 3F            SWI
00100 6090              ORG    $6090
00104          * NAM CENT
00105          * THIS IS A PROGRAM WHICH WILL BE USED TO CENTER
00106          * THE SCANNER. IT'S USE WILL BE REQUIRED WHENEVER ANY OF
00107          * THE MECHANICS OF THE SYSTEM (SUCH AS THE SOURCE)
00108          * ARE CHANGED. USING A 1:1 RATIO ON THE PULLEYS
00109          * THE TRANSLATIONAL MOTION IS 6500 STEPS
00110          * PULSES ARE SENT TO THE HP EVERY 2 MOTOR PULSES
00111          * (EVER 6.79 MS OR EVERY 4172 CYCLES).
00112          * THE TRANSLATION TAKES 22 SEC. AT WHICH POINT THE
00113          * SCANNER IS ROTATED THROUGH 180 DEG. AND THEN THE
00114          * IS PERFORMED ONE ADDITIONAL TIME AND THE SCANNER IS ROTATED
00115          * BACK. PRESET FROM THE PARK POSITION IS +3600 -32 FOR ACCEL = 3568 STEPS
00116 6090 86 OF          LDA A  #$OF
00117 6092 97 2C          STA A  M+44
00118 6094 86 02          LDA A  #02
00119 6096 97 2D          STA A  M+45
00120 6098 86 02          LDA A  #02
00121 609A 97 32          STA A  M+50
00122 609C 86 01          LDA A  #01
00123 609E 97 33          STA A  M+51
00124 60A0 86 13          LDA A  #19
00125 60A2 97 34          STA A  M+52
00126 60A4 86 08          LDA A  #08
00127 60A6 97 35          STA A  M+53
00128 60A8 BD C278        JSR    PIA
00130          * MOVE FROM PARK TO START POSITION
00131          * ONE GROUP OF 3568 PULSES
00132          * MAKES USE OF THE R21 RAMP
00133          * 3568 = 400 + 3168
00134 60AB 86 OF          LDA A  #$OF
00135 60AD 97 00          STA A  M
00136 60AF CE OC60        LDX    #3168
00137 60B2 DF 2A          STX    M+42
00138 60B4 CE ODFO        LDX    #3568
00139 60B7 DF 25          STX    M+37
00140 60B9 BD C000        JSR    ASD
00141 60BC BD C29B        JSR    START
00142 60BF C6 1B          LDA B  #$1B
00143 60C1 F7 8004        STA B  ORA
00144 60C4 BD C28C        JSR    DELAY
00145 60C7 C6 1F          LDA B  #$1F

```

; TELL HP RAMP IS BEGINNING


```

00146 60C9 F7 8004 STA B ORA
00147 *
00148 * SCAN - UP PROVIDES A MOTOR PULSE EVERY 2086 CYCLES & A HP PULSE
00149 * EVERY 412 CYCLES (EVERY 2 MOTOR PULSES)
00150 * HP PULSE IS SENT EVERY M+46 MOTOR PULSES
00151 * ACCELERATE UP TO SPEED
00152 60CC BD C1F5 JSR ACCEL
00153 60CF CE 0020 LDX #32
00154 60D2 DF 25 STX M+37
00155 60D4 BD C000 JSR ASD
00156 60D7 CE 1964 LDX #6500 ;PULSES REQUIRED FOR SCAN
00157 60DA BD C2B0 JSR TRANSL
00158 *DELAY BETWEEN PULSES =98 + 12 + 19*104 = 2086 CYCLES
00159 *OECEL.
00160 60DD B0 C242 JSR DEC32
00161 * THIS IS A PROGRAM DESIGNED TO OBTAIN A SUITABLE RAMP
00162 * FOR ROTATION OF 180 DEGREES
00163 * IT MAKES USE OF A GENERAL SUBROUTINE ASO (ACCELERATION,SPEED,DECELERATION
00164 * 35882 PULSES ARE
00165 * REQUIRED AT MAX. FREQ. WE WILL USE 35882 GROUPS OF
00166 * 1 PULSE
00167
00168 60E0 96 2D LDA A M+45
00169 60E2 81 02 CMP A #02
00170 60E4 27 04 BEQ K5
00171 60E6 86 10 LDA A #$1D
00172 60E8 97 00 STA A M
00173 60EA 7A 002D K5 DEC M+45
00174 60ED CE 8C2A LDX #35882 ;35882*M+12
00175 60EF DF 2A STX M+42
00176 60F0 DF 2A LDX #36282
00177 60F2 CE 8DBA STX M+37
00178 60F5 DF 25 JSR ASD
00179 60F7 BD C000 LDA A M+45
00180 60F9 96 2D BEQ JMPE1
00181 60FA 96 2D LDA A M+44
00182 60FC 27 09 EOR A #$18
00183 60FE 96 2C STA A M+44
00184 6100 88 18 JMP ST1
00185 6102 97 2C * MOVE BACK TO PARK POSITION
00186 6104 7E 60BC * MUST MOVE FORWARD 3568 STEPS
00187
00188
00189 JMPE1 LDA A #$17
00190 6107 86 17 STA A M
00191 6109 97 00 LDX #3568
00192 610B CE ODFO STX M+37
00193 610E DF 25 LDX #3168
00194 6110 CE OC60 STX M+42
00195 6113 DF 2A

```



```

00196 6115 BD C000      JSR   ASD
00201      * NAM SSCAN
00202 6140      ORG   $6140
00203      * (SCOUT SCAN)
00204      * THIS SCAN IS USED TO AID IN ACCURATE REPOSITIONING
00205      * OF THE ARM. THE SCANNER WILL ROTATE 90 DEGREES, PRESET
00206      * A DISTANCE OF +3125 - 200 (FOR ACCEL.) STEPS FROM THE PARK POSITION
00207      * AND THEN START MEASUREMENTS. THERE WILL BE 26 MEASUREMENTS
00208      * EACH CONSISTING OF A SINGLE SCAN OF 7848 STEPS AND 654 INTERVALS
00209      * (760 US / STEP). THERE IS A 2 SEC. DELAY BETWEEN EACH MEASUREMENT
00210      * TO ALLOW THE ARM POSITION TO BE ADJUSTED. THE SCANNER IS THEN SET
00211      * BACK TO THE PARK POSITION AND IS ROTATED BACK TO ITS ORIGINAL POSITION
00212 6140 86 OF      LDA A #0F
00213 6142 97 2C      STA A M+44
00214 6144 86 1A      LDA A #26
00215 6146 97 2D      STA A M+45
00216 6148 86 0C      LDA A #12
00217 614A 97 32      STA A M+50
00218 614C 86 08      LDA A #08
00219 614E 97 33      STA A M+51
00220 6150 86 04      LDA A #04
00221 6152 97 34      STA A M+52
00222 6154 86 05      LDA A #05
00223 6156 97 35      STA A M+53
00224 6158 BD C278    JSR   PIA
00225      * 90 DEGREES=18141 STEPS
00226 615B CE 4540    LDX #17741 ;17741*M+12 PULSES
00227 615E DF 2A      STX M+42
00228 6160 CE 46DD    LDX #18141
00229 6163 DF 25      STX M+37
00230 6165 BD C000    JSR   ASD
00232      * MOVE FROM PARK TO START POSITION
00233      * ONE GROUP OF 2925 PULSES
00234      * MAKES USE OF THE R21 RAMP
00235      * 2925 = 400 + 2525*1
00236 6168 86 OF      LDA A #0F
00237 616A 97 00      STA A M
00238 616C CE 09DD    LDX #2525
00239 616F DF 2A      STX M+42
00240 6171 CE 0B6D    LDX #2925
00241 6174 DF 25      STX M+37
00242 6176 BD C000    JSR   ASD
00243 6179 BD C29B    ST2
00244 617C C6 1B      LDA B #$1B
00245 617E F7 8004    STA B ORA

```

;TRANSLATIONAL DIRECTION
 ;# OF TRANSLATIONS
 ;# OF MOTOR STEPS / HP SIGNAL
 ;DETERMINES DELAY IN TRANSLATION
 ;DETERMINES DELAY IN TRANSLATION
 ;DETERMINES DELAY IN TRANSLATION
 ;CALLS INIT AND F AS WELL
 ;TELL HP RAMP IS BEGINNING


```

00246 6181 BD C28C      JSR      DELAY
00247 6184 C6 1F      LDA B   #$1F
00248 6186 F7 8004     STA B   ORA
00249                      * BEGIN ACCELERATION
00250 6189 B0 C1F5     JSR      ACCEL
00251 618C BD C000     JSR      ASO
00253                      * SCAN - UP PROVIDES A MOTOR PULSE EVERY 1010 CYCLES & A HP PULSE
00254                      * EVERY 12 MOTOR PULSES
00255                      * HP PULSE IS SENT EVERY M+46 MOTOR PULSES
00256 618F CE 1EA8     LDX      #7848      ;PULSES REQUIRED FOR SCAN
00257 6192 BD C2B0     JSR      TRANSL
00258                      * DELAY BETWEEN PULSES = 152 + 42 + 68*4=466 CYCLES
00259                      * DECELERATION
00260 6195 BD C208     JSR      DECEL
00261 6198 7A 002D     DEC      M+45      ;IS SCAN FINISHED?
00262 619B 27 18     BEQ      JMPE2
00263 619D 96 2C     LDA A   M+44
00264 619F 88 18     EOR A   #$18      ;CHANGE TRANSLATIONAL DIRECTION
00265 61A1 97 2C     STA A   M+44
00267                      * 2 SECOND DELAY BETWEEN MEASUREMENTS
00268 61A3 CE B89C     LDX      #47260
00269 61A6 78 0029     MC1      M+41      ;6
00270 61A9 78 0029     ASL      M+41      ;6
00271 61AC 78 0029     ASL      M+41      ;6
00272 61AF 09         DEX      ;4
00273 61B0 26 F4     BNE      MC1      ;4
00274 61B2 7E 6179     JMP      ST2
00276                      *MOVE BACK TO PARK POSITION
00277                      *MUST MOVE FORWARD 2925
00278 61B5 86 17     JMPE2     LOA A   #$17
00279 61B7 97 00     STA A   M
00280 61B9 CE 09DD     LDX      #2525
00281 61BC 0F 2A     STX      M+42
00282 61BE CE 086D     LDX      #2925
00283 61C1 DF 25     STX      M+37
00284 61C3 B0 C000     JSR      ASO
00285                      * ROTATE BACK 90 DEGREES
00286 61C6 CE 4540     LOX      #17741
00287 61C9 0F 2A     STX      M+42
00288 61CB CE 46D0     LDX      #18141
00289 61CE 0F 25     STX      M+37
00290 61D0 86 1D     LDA A   #$1D
00291 6102 97 00     STA A   M
00292 61D4 B0 C000     JSR      ASD
00293 6107 3F     SWI

```



```

00296 61EO
00297
00298
00299
00300
00301
00302
00303
00305
00306
00307
00308
00309
00310
00311
00312
00313
00314
00315
00316
00317
00318
00319
00320
00321
00323
00324
00325
00326
00327
00328
00329
00330
00331
00332
00333
00334
00335
00336
00337
00338
00339
00340
00342
00343
00344
00345

ORG 61EO
NAM 8DETM
THIS PROGRAM WILL BE USED TO PERFORM
A MULTI-DETECTOR SCAN USING 8 DETECTORS.
USING A 1:1 PULLEY RATIO THE TRANSLATION
IS 16992 STEPS (106.2 MM). IT WILL COLLECT 1416 DATA. FROM THE
PARK POSITION THE SCANNER MUST MOVE BACK
1447 STEPS +32 FOR ACCEL.) BEFORE STARTING THE SCAN.
MDTOR PULSES ARE SENT EVERY 1862 CYCLES
(APPROX. 3030.6 US) AND DATA PULSES ARE SENT TO
THE HP EVERY 12 MOTDR PULSES. THE SCANNER IS TO
RDIAE 25.71 DEG. AFTER EACH TRANSLATION & IS
TO PERFORM 7 TRANSLATIONS & 6 ROTATIONS.
LDA A #50F
STA A M+44
LDA A #07
STA A M+45
LDA A #12
STA A M+50
LDA A #07
STA A M+51
LDA A #84
STA A M+52
LDA A #01
STA A M+53
MDVE FROM PARK TO START POSITION
DNE GROUP DF 1479 PULSES
MAKES USE DF THE R21 RAMP
1479=400 + 1079+1
JSR PIA
LDA A #17
STA A M
LDX #1079
STX M+42
LDX #1479
STX M+37
JSR ASD
JSR START
LDA B #1B
STA B DRA
JSR DELAY
LDA B #1F
STA B DRA
JSR ACCEL
LDX #32
STX M+37
JSR ASD

```

; TRANSLATION DIRECTION
 ; # OF TRANSLATIONS
 ; # OF MOTDR STEPS / HP SIGNAL
 ; DETERMINES DELAY IN TRANSLATION
 ; DETERMINES DELAY IN TRANSLATION
 ; DETERMINES DELAY IN TRANSLATION
 ; TELL HP RAMP IS BEGINNING


```

00347 * SCAN - UP PROVIDES A MOTOR PULSE EVERY 1862 CYCLES & A HP PULSE
00348 * EVERY 12 MOTOR PULSES
00349 * HP PULSE IS SENT EVERY M+46 MOTOR PULSES
00350 LDX #16992 ;PULSES REQUIRED FOR SCAN
00351 JSR TRANSL
00352 * DELAY BETWEEN PULSES = 84*(1*12+8)+42+7*12+6 = 1862 CYCLES
00353 * DECELERATION
00354 JSR DEC32
00355 DEC M+45 ;IS SCAN FINISHED?
00356 BEQ JMPE3
00357 JSR R8D
00358 LDA A M+44
00359 EOR A #$18 ;CHANGE TRANSLATIONAL DIRECTION
00360 STA A M+44
00361 JMP ST3
00362 *MOVE BACK TO PARK POSITION
00363 *SHOULD MOVE BACK 15577
00364 *HOWEVER APPEARS TO BE OUT ONE PULSE
00365 JMPE3 LDA A #$17
00366 6241 86 17 STA A M
00367 6243 97 00 LDX #15176
00368 6245 CE 3B48 STX M+42
00369 6248 DF 2A LDX #15576
00370 624A CE 3C08 STX M+37
00371 624D DF 25 JSR ASD
00372 624F BD C000 * ROTATE BACK TO PARK POSITION
00373 * MUST ROTATE BACK 31080 PULSES
00374 LDX #30680 ;30680*M+12 PULSES
00375 6252 CE 77D8 STX M+42
00376 6255 DF 2A LDX #31080
00377 6257 CE 7968 STX M+37
00378 625A DF 25 LDA A #$1D
00379 625C 86 1D STA A M
00380 625E 97 00 JSR ASD
00381 6260 BD C000 SWI
00382 6263 3F ORG $6280
00386 6280
00387 * NAM 8DETS
00388 * THIS PROGRAM WILL BE USED TO PERFORM
00389 * A MULTI-DETECTOR SCAN USING 8 DETECTORS.
00390 * USING A 1:1 PULLEY RATIO THE TRANSLATION
00391 * IS 16992 STEPS (106.2 MM). IT WILL COLLECT 1416 DATA. FROM THE
00392 * PARK POSITION THE SCANNER MUST MOVE BACK
00393 * 1447 STEPS +5 FOR ACCEL.) BEFORE
00394 * STARTING THE SCAN.
00395 * MOTOR PULSES ARE SENT EVERY 7458 CYCLES

```



```

00396 * (APPROX. 12139 US) AND DATA PULSES ARE SENT TO
00397 * THE HP EVERY 12 MOTOR PULSES. THE SCANNER IS TD
00398 * ROTATE 25.71 DEG. AFTER EACH TRANSLATION & IS
00399 * TO PERFORM 7 TRANSLATIONS & 6 ROTATIONS.
00400 LDA A #50F
00401 STA A M+44 ;TRANSLATIONAL DIRECTION
00402 LDA A #07
00403 STA A M+45 ;# OF TRANSLATIONS
00404 LDA A #12
00405 STA A M+50 ;# DF MOTOR STEPS / HP SIGNAL
00406 LDA A #08
00407 STA A M+51 ;DETERMINES DELAY IN TRANSLATION
00408 LDA A #227
00409 STA A M+52 ;DETERMINES DELAY IN TRANSLATION
00410 LDA A #02
00411 STA A M+53 ;DETERMINES DELAY IN TRANSLATION
00413 * MOVE FROM PARK TO START POSITION
00414 * ONE GROUP OF 1452 PULSES
00416 * 1452=400 + 1052*1
00417 JSR PIA ; CALLS INIT AND F AS WELL
00418 LDA A #17 ; TRANSLATIONAL DIRECTION
00419 STA A M
00420 LDX #1052
00421 STX M+42
00422 LDX #1452
00423 STX M+37
00424 JSR ASD
00425 JSR START
00426 LDA B #1B
00427 STA B ORA
00428 JSR DELAY
00429 LDA B #1F
00430 STA B DRA
00431 * BEGIN ACCELERATION
00432 JSR ACCEL
00433 LDX #05
00434 STX M+37
00435 JSR ASD
00437 * SCAN - UP PROVIDES A MOTOR PULSE EVERY 7458 CYCLES & A HP PULSE
00438 * EVERY 12 MOTOR PULSES
00439 * HP PULSE IS SENT EVERY M+46 MOTOR PULSES
00440 LDX #16992 ;PULSES REQUIRED FOR SCAN
00441 JSR TRANSL
00442 * DELAY BETWEEN PULSES = 227(2*12+8)+42+56+8*12 = 7458 CYCLES
00443 * DECELERATION
00444 JSR DEC5
00445 DEC M+45 ;IS SCAN FINISHED?

```



```
00446 62D3 27 OC          BEQ      JMPE4
00447 62D5 BD C28D        JSR      R8D
00448 62D8 96 2C          LDA      A M+44
00449 62DA 88 18          EDR      A #$18
00450 62DC 97 2C          STA      A M+44
00451 62DE 7E 62AC        JMP      ST4
00453                      *MOVE BACK TO PARK PDSITIDN
00454                      *SHOULD MDVE BACK 15550
00455                      *HDWEVER APPEARS TD BE OUT DNE PULSE
00456 62E1 86 17          JMPE4    LDA      A #$17
00457 62E3 97 00          STA      A M
00458 62E5 CE 3B2D        LDX      #15149
00459 62E8 DF 2A          STY      M+42
00460 62EA CE 3CBD        LDX      #15549
00461 62ED DF 25          STX      M+37
00462 62EF BD C000        JSR      ASD
00463                      * RDTATE BACK TO PARK POSITIDN
00464                      * MUST RDTATE BACK 31080 PULSES
00465 62F2 CE 77D8        LDX      #30680 ;30680*M+12 PULSES
00466 62F5 DF 2A          STX      M+42
00467 62F7 CE 7968        LDX      #31080
00468 62FA DF 25          STX      M+37
00469 62FC 86 1D          LDA      A #$1D
00470 62FE 97 00          STA      A M
00471 6300 BD C000        JSR      ASD
00472 6303 3F            SWI
00476 6320                DRG      $6320
00477                      * NAM RAT
00478                      * THIS PRDGRAM WILL BE USED TD PERFRM
00479                      * A SINGLE DETECTDR SCAN.
00480                      * USING A 1:1 PULLEY RATIO THE TRANSLATIDN
00481                      * IS 2560 STEPS (16.0 MM). IT WILL COLLECT 128 DATA. FROM THE
00482                      * PARK PDSITIDN THE SCANNER MUST MDVE FDRWARD(+)
00483                      * 6500 STEPS -O FOR ACCEL. BEFDRE
00484                      * STARTING THE SCAN.
00485                      * MOTOR PULSES ARE SENT EVERY 15,358 CYCLES
00486                      * (APPRDX. 24,997 US) AND DATA PULSES ARE SENT TD
00487                      * THE HP EVERY 20 MDTR PULSES. THE SCANNER IS TD
00488                      * ROTATE 3.214 DEG. AFTER EACH TRANSLATIDN & IS
00489                      * TD PERFORM 56 TRANSLATIDNS & 55 ROTATIDNS.
00490 6320 86 OF            LDA      A #50F
00491 6322 97 2C          STA      A M+44 ;TRANSLATIONAL DIRECTION
00492 6324 86 38          LDA      A #56
00493 6326 97 2D          STA      A M+45 ;# DF TRANSLATIDNS
00494 6328 86 14          LDA      A #20
00495 632A 97 32          STA      A M+50 ;# DF MDTR STEPS / HP SIGNAL
```



```

00496 632C 86 08      LOA A #08
00497 632E 97 33      STA A M+51      ;OETERMINES DELAY IN TRANSLATION
00498 6330 86 0F      LOA A #223
00499 6332 97 34      STA A M+52      ;OETERMINES DELAY IN TRANSLATION
00500 6334 86 05      LDA A #05
00501 6336 97 35      STA A M+53      ;OETERMINES DELAY IN TRANSLATION
00503                      * MOVE FROM PARK TO START POSITION
00504                      * ONE GROUP OF 6500 PULSES
00505                      * MAKES USE OF THE R21 RAMP
00506                      * 6500=400 + 6100*1
00507 6338 BD C278      JSR PIA
00508 633B 86 0F      LOA A #$0F      ; CALLS INIT AND F AS WELL
00509 633D 97 00      STA A M      ; TRANSLATIONAL DIRECTION (+)
00510 633F CE 1704      LOX #6100
00511 6342 0F 2A      STX M+42
00512 6344 CE 1964      LDX #6500
00513 6347 DF 25      STX M+37
00514 6349 BD C000      JSR ASO
00515 634C BD C29B      JSR START
00516 634F C6 1B      LOA B #$1B
00517 6351 F7 8004      STA B ORA
00518 6354 BD C28C      JSR DELAY
00519 6357 C6 1F      LDA B #$1F
00520 6359 F7 8004      STA B ORA
00522                      * SCAN - UP PROVIDES A MOTOR PULSE EVERY 15,358 CYCLES & A HP PULSE
00523                      * EVERY 20 MOTOR PULSES
00524                      * HP PULSE IS SENT EVERY M+46 MOTOR PULSES
00525 635C CE 0A00      LOX #2560      ;PULSES REQUIRED FOR SCAN
00526 635F B0 C2B0      JSR TRANSL
00527                      * DELAY BETWEEN PULSES = 223(5*12+8)+42+56+8*12 = 15358 CYCLES
00528 6362 7A 0020      DEC M+45      ;IS SCAN FINISHED?
00529 6365 27 1A      BEQ JMPE5
00530                      * ROTATE 3.214 DEG. (648 PULSES)
00531 6367 86 1E      LDA A #$1E
00532 6369 97 00      STA A M
00533 636B CE 00F8      LOX #248
00534 636E 0F 2A      STX M+42
00535 6370 CE 0288      LOX #648
00536 6373 DF 25      STX M+37
00537 6375 B0 C000      JSR ASO
00538 6378 96 2C      LDA A M+44
00539 637A 88 18      EOR A #$18
00540 637C 97 2C      STA A M+44
00541 637E 7E 634C      JMP ST5
00543                      * MOVE BACK TO PARK POSITION
00544                      * SHOULO MOVE BACK 6500
00545                      * HOWEVER APPEARS TO BE OUT ONE PULSE
00546
00547
00548
00549
00550
00551
00552
00553
00554
00555
00556
00557
00558
00559
00560
00561
00562
00563
00564
00565
00566
00567
00568
00569
00570
00571
00572
00573
00574
00575
00576
00577
00578
00579
00580
00581
00582
00583
00584
00585
00586
00587
00588
00589
00590
00591
00592
00593
00594
00595
00596
00597
00598
00599
00600
00601
00602
00603
00604
00605
00606
00607
00608
00609
00610
00611
00612
00613
00614
00615
00616
00617
00618
00619
00620
00621
00622
00623
00624
00625
00626
00627
00628
00629
00630
00631
00632
00633
00634
00635
00636
00637
00638
00639
00640
00641
00642
00643
00644
00645
00646
00647
00648
00649
00650
00651
00652
00653
00654
00655
00656
00657
00658
00659
00660
00661
00662
00663
00664
00665
00666
00667
00668
00669
00670
00671
00672
00673
00674
00675
00676
00677
00678
00679
00680
00681
00682
00683
00684
00685
00686
00687
00688
00689
00690
00691
00692
00693
00694
00695
00696
00697
00698
00699
00700
00701
00702
00703
00704
00705
00706
00707
00708
00709
00710
00711
00712
00713
00714
00715
00716
00717
00718
00719
00720
00721
00722
00723
00724
00725
00726
00727
00728
00729
00730
00731
00732
00733
00734
00735
00736
00737
00738
00739
00740
00741
00742
00743
00744
00745
00746
00747
00748
00749
00750
00751
00752
00753
00754
00755
00756
00757
00758
00759
00760
00761
00762
00763
00764
00765
00766
00767
00768
00769
00770
00771
00772
00773
00774
00775
00776
00777
00778
00779
00780
00781
00782
00783
00784
00785
00786
00787
00788
00789
00790
00791
00792
00793
00794
00795
00796
00797
00798
00799
00800
00801
00802
00803
00804
00805
00806
00807
00808
00809
00810
00811
00812
00813
00814
00815
00816
00817
00818
00819
00820
00821
00822
00823
00824
00825
00826
00827
00828
00829
00830
00831
00832
00833
00834
00835
00836
00837
00838
00839
00840
00841
00842
00843
00844
00845
00846
00847
00848
00849
00850
00851
00852
00853
00854
00855
00856
00857
00858
00859
00860
00861
00862
00863
00864
00865
00866
00867
00868
00869
00870
00871
00872
00873
00874
00875
00876
00877
00878
00879
00880
00881
00882
00883
00884
00885
00886
00887
00888
00889
00890
00891
00892
00893
00894
00895
00896
00897
00898
00899
00900
00901
00902
00903
00904
00905
00906
00907
00908
00909
00910
00911
00912
00913
00914
00915
00916
00917
00918
00919
00920
00921
00922
00923
00924
00925
00926
00927
00928
00929
00930
00931
00932
00933
00934
00935
00936
00937
00938
00939
00940
00941
00942
00943
00944
00945
00946
00947
00948
00949
00950
00951
00952
00953
00954
00955
00956
00957
00958
00959
00960
00961
00962
00963
00964
00965
00966
00967
00968
00969
00970
00971
00972
00973
00974
00975
00976
00977
00978
00979
00980
00981
00982
00983
00984
00985
00986
00987
00988
00989
00990
00991
00992
00993
00994
00995
00996
00997
00998
00999

```


00546	6381	86	17	JMPE5	LOA A	#\$17	
00547	6383	97	00		STA A	M	
00548	6385	CE	1703		LOX	#6099	
00549	6388	DF	2A		STX	M+42	
00550	638A	CE	1963		LOX	#6499	
00551	6380	DF	25		STX	M+37	
00552	638F	B0	C000		JSR	ASO	
00553				*	ROTATE BACK TO PARK POSITION		
00554				*	MUST ROTATE BACK 35640 PULSES		
00555	6392	CE	89A8		LDX	#35240	;35240*M+12 PULSES
00556	6395	DF	2A		STX	M+42	
00557	6397	CE	8B38		LOX	#35640	
00558	639A	DF	25		STX	M+37	
00559	639C	86	10		LOA A	#\$1D	
00560	639E	97	00		STA A	M	
00561	63A0	B0	C000		JSR	ASO	
00562	63A3	3F			SWI		
00566	C000				ORG	\$C000	
00567				*	NAM SUBROUTINES		
00568				*	SUBROUTINE ASD (ACCELERATION, SPEED,		
00569				*	DECELERATION)		
00570				*	MUST HAVE PARAMETERS SET INTO M THROUGH M+43 BEFORE INITIATION.		
00571				*	M IS THE TYPE OF MOTION AND DIRECTION (\$10 & \$1E ARE ROTATION WHILE		
00572				*	\$OF & \$17 ARE TRANSLATION) M+1 THROUGH M+23 ARE		
00573				*	THE LENGTHS OF THE RAMPS INVOLVE		
00574				*	M+25 THROUGH M+36 ARE THE FREQUENCY OF THE PULSES ASSOCIATED WITH		
00575				*	THE SETS OF RAMPS		
00576				*	WHILE M+24 IS A SPARE LOCATION.		
00577				*	M+37 M+38 IS THE TOTAL # OF PULSES NEEDED FOR THE DESIRED MOTION		
00578				*	M+39 IS A PROGRAM LOCATION DEVICE		
00579				*	M+40 IS USED TO STORE ACC A		
00580				*	M+41 IS MERELY A DELAY MECHANISM		
00581				*	M+42 M+43 = THE # OF TIMES THE RAMP AT		
00582				*	MAX FREQ. IS TO BE PERFORMED		
00583	C000	CE	0000	ASD	LDX	#\$0000	
00584	C003	7F	0027		CLR	M+39	
00585	C006	7F	0028		CLR	M+40	
00586	C009	08		ASO0	INX		;4
00587	C00A	96	28		LOA A	M+40	;3
00588	C00C	4C			INC A		;2
00589	C00D	97	28		STA A	M+40	;4
00591				*	THE FOLLOWING BRANCH TO C1 THROUGH C9 SINCE BRANCHES TO		
00592				*	B2 THROUGH B8 WOULD BE OUT OF RANGE		
00594	C00F	91	01		CMP A	M+1	;3
00595	C011	2F	23		BLE	C1	

00596	C013	91	02	CMP	A	M+2
00597	C015	2F	22	BLE		C2
00598	C017	91	03	CMP	A	M+3
00599	C019	2F	21	BLE		C3
00600	C01B	91	04	CMP	A	M+4
00601	C01D	2F	20	BLE		C4
00602	C01F	91	05	CMP	A	M+5
00603	C021	2F	1F	BLE		C5
00604	C023	91	06	CMP	A	M+6
00605	C025	2F	1E	BLE		C6
00606	C027	91	07	CMP	A	M+7
00607	C029	2F	1D	BLE		C7
00608	C02B	91	08	CMP	A	M+8
00609	C02D	2F	1C	BLE		C8
00610	C02F	91	09	CMP	A	M+9
00611	C031	2F	1B	BLE		C9
00612	C033	7E	C051	JMP		J5
00613	C036	7E	C0E7	JMP		B1
00614	C039	7E	C0EC	JMP		B2
00615	C03C	7E	C0F1	JMP		B3
00616	C03F	7E	C0F6	JMP		B4
00617	C042	7E	C0FB	JMP		B5
00618	C045	7E	C100	JMP		B6
00619	C048	7E	C105	JMP		B7
00620	C04B	7E	C10A	JMP		B8
00621	C04E	7E	C10F	JMP		B9
00623				* THE FOLLOWING (PRE BLE B10) IS NECESSARY SINCE THE BLE INSTRUCTION		
00624				* USES TWO S COMPLEMENT ARITHMETIC WHICH RESTRICTS THE		
00626				* SIZE OF AN 8 BIT NUMBER TO +127 & THE SIZE OF A RAMP SPEC TO +126		
00628	C051	86	01	LDA	A	#01
00629	C053	97	27	STA	A	M+39
00630	C055	7F	0028	CLR		M+40
00631	C058	09		DEX		
00632	C059	96	28	LDA	A	M+40
00633	C05B	4C		INC	A	
00634	C05C	97	28	STA	A	M+40
00635	C05E	08		INX		
00636	C05F	91	0A	CMP	A	M+10
00637	C061	2F	03	BLE		C10
00638	C063	7E	C069	JMP		K1
00639	C066	7E	C114	JMP		B10
00640	C069	91	0B	CMP	A	M+11
00641	C06B	2F	03	BLE		C11
00642	C06D	7E	C073	JMP		K2
00643	C070	7E	C119	JMP		B11
00644	C073	86	02	LDA	A	#02
00645	C075	97	27	STA	A	M+39
				;B10 IS OUT OF RANGE FOR BRANCH		
				;B11 IS OUT OF RANGE FOR BRANCH		

00646	C077	7F	0028	P1	CLR	M+40
00647	C07A	09			DEX	
00648	C07B	D6	2B		LDA B	M+43
00649	C07D	27	06		BEQ P4	
00650	C07F	7A	002B		DEC M+43	
00651	C082	7E	C08F		JMP ASD2	
00652	C085	D6	2A	P4	LDA B	M+42
00653	C087	27	16		BEQ P6	
00654	C089	7A	002A		DEC M+42	
00655	C08C	7A	002B		DEC M+43	
00656	C08F	96	28	ASD2	LDA A	M+40
00657	C091	4C			INC A	
00658	C092	97	28		STA A	M+40
00659	C094	08			INX	
00660	C095	91	0C		CMP A	M+12
00661	C097	2F	03		BLE C12	
00662	C099	7E	C077		JMP P1	
00663	C09C	7E	C11E	C12	JMP B12	
00664	C09F	86	03	P6	LDA A #03	
00665	COA1	97	27		STA A M+39	
00666	COA3	7F	0028		CLR M+40	
00667	COA6	09			DEX	
00668	COA7	96	28	ASD3	LDA A	M+40
00669	COA9	4C			INC A	
00670	COAA	97	28		STA A	M+40
00671	COAC	08			INX	
00672	COAD	91	0D		CMP A	M+13
00673	COAF	2F	68		BLE B11	
00674	COB1	91	0E		CMP A	M+14
00675	COB3	2F	5F		BLE B10	
00676	COB5	91	0F		CMP A	M+15
00677	COB7	2F	56		BLE B9	
00678	COB9	86	04		LDA A #04	
00679	COBB	97	27		STA A M+39	
00680	COBD	7F	0028		CLR M+40	
00681	COCO	09			DEX	
00682	COC1	96	28	ASD4	LDA A	M+40
00683	COC3	4C			INC A	
00684	COC4	97	28		STA A	M+40
00685	COC6	08			INX	
00686	COC7	91	10		CMP A	M+16
00687	COC9	2F	3F		BLE B8	
00688	COCB	91	11		CMP A	M+17
00689	COCd	2F	36		BLE B7	
00690	COCF	91	12		CMP A	M+18
00691	COD1	2F	2D		BLE B6	
00692	COD3	91	13		CMP A	M+19
00693	COD5	2F	24		BLE B5	

; B12 IS OUT OF RANGE FOR A BRANCH

00694	COD7	91	14	CMP	A	M+20	
00695	COD9	2F	1B	BLE		B4	
00696	CODB	91	15	CMP	A	M+21	
00697	CODD	2F	12	BLE		B3	
00698	CODF	91	16	CMP	A	M+22	
00699	COE1	2F	09	BLE		B2	
00700	COE3	91	17	CMP	A	M+23	
00701	COE5	2F	00	BLE		B1	
00702	COE7	96	19	LDA	A	M+25	:3
00703	COE9	7E	C120	JMP		J	:3
00704	COEC	96	1A	LDA	A	M+26	
00705	COEE	7E	C120	JMP		J	
00706	COF1	96	1B	LDA	A	M+27	
00707	COF3	7E	C120	JMP		J	
00708	COF6	96	1C	LDA	A	M+28	
00709	COF8	7E	C120	JMP		J	
00710	COFB	96	1D	LDA	A	M+29	
00711	COFD	7E	C120	JMP		J	
00712	C100	96	1E	LDA	A	M+30	
00713	C102	7E	C120	JMP		J	
00714	C105	96	1F	LDA	A	M+31	
00715	C107	7E	C120	JMP		J	
00716	C10A	96	20	LDA	A	M+32	
00717	C10C	7E	C120	JMP		J	
00718	C10F	96	21	LDA	A	M+33	
00719	C111	7E	C120	JMP		J	
00720	C114	96	22	LDA	A	M+34	
00721	C116	7E	C120	JMP		J	
00722	C119	96	23	LDA	A	M+35	
00723	C11B	7E	C120	JMP		J	
00724	C11E	96	24	LDA	A	M+36	
00725	C120	C6	1F	LDA	B	#\$1F	
00726	C122	F7	8004	STA	B	ORA	
00727	C125	C6	09	LDA	B	#09	
00728	C127	78	0029	ASL		M+41	
00729	C12A	5A		DEC	B		
00730	C12B	26	FA	BNE		D1	
00731	C12D	8C	0000	CPX		#0000	
00732	C130	4A		DEC	A		
00733	C131	26	F2	BNE		DEL	
00734	C133	D6	00	LDA	B	M	
00735	C135	F7	8004	STA	B	ORA	
00736	C138	9C	25	CPX		M+37	
00737	C13A	27	21	BEQ		Z2	
00738	C13C	96	27	LDA	A	M+39	
00739	C13E	81	01	CMP	A	#01	:2

: 2
: 5
: 2
: 6
: 2
: 4
: 3
: 2
: 4
: 3
: 5
: IS MOTION COMPLETE ? 4
: 2

)B*12=9*12=108
)

00740	C140	27	OF	BEQ	Z3		:4
00741	C142	81	O2	CMP	A #O2		:2
00742	C144	27	OE	BEQ	Z4		:4
00743	C146	81	O3	CMP	A #O3		:2
00744	C148	27	OD	BEQ	Z5		:4
00745	C14A	81	O4	CMP	A #O4		:2
00746	C14C	27	OC	BEQ	Z6		:4
00747	C14E	7E	COO9	JMP	ASDO		:3
00748	C151	7E	CO59	JMP	ASD1		
00749	C154	7E	CO8F	JMP	ASD2		
00750	C157	7E	COA7	JMP	ASD3		
00751	C15A	7E	COC1	JMP	ASD4		
00752	C15D	C6	1F	LDA	B #S1F		
00753	C15F	F7	80O4	STA	B DRA		
00754	C162	39		RTS			
00757							
00758							
00759							
00760	C163	86	FF	LDA	A #255		:20.2HZ
00761	C165	97	19	STA	A M+25		
00762	C167	86	81	LDA	A #129		:39.9HZ
00763	C169	97	1A	STA	A M+26		
00764	C16B	86	4A	LDA	A #74		:69.3 HZ
00765	C16D	97	1B	STA	A M+27		
00766	C16F	86	2F	LDA	A #47		:108.6 HZ
00767	C171	97	1C	STA	A M+28		
00768	C173	86	22	LDA	A #34		:148.9 HZ
00769	C175	97	1D	STA	A M+29		
00770	C177	86	13	LDA	A #19		:261.4 HZ
00771	C179	97	1E	STA	A M+30		
00772	C17B	86	OC	LDA	A #12		:402.3 HZ
00773	C17D	97	1F	STA	A M+31		
00774	C17F	86	O9	LDA	A #9		:548 HZ
00775	C181	97	2O	STA	A M+32		
00776	C183	86	O7	LDA	A #7		:677 HZ
00777	C185	97	21	STA	A M+33		
00778	C187	86	O5	LDA	A #5		:917 HZ
00779	C189	97	22	STA	A M+34		
00780	C18B	86	O4	LDA	A #4		:1115 HZ
00781	C18D	97	23	STA	A M+35		
00782	C18F	86	O3	LDA	A #3		:1422 HZ
00783	C191	97	24	STA	A M+36		
00784	C193	39		RTS			
00787							
00788							
00789							

* THE FOLLDWING FREQUENCIES ARE APPRDXIMATE ONLY
* & ARE SLIGHTLY DIFFERENT FDR ACCELERATION & DECELERATION
* F IS THE REQUIRED FREQUENCIES FDR ACCELERATION/DECELERATION

* INIT. GIVES THE LENGTHS DF RAMPS
* 360 DEGREES . = 360/.9*464/128*50.044=72564 STEPS
* 25.7 DEGREES=5180.25 STEPS

* 50.044 IS APPROX. THE RATIO OF THE WORM GEAR		
00790	INIT	LDA A # \$1E
00791	C194 86 1E	STA A M
00792	C196 97 00	LDA A #O1
00793	C198 86 01	STA A M+1
00794	C19A 97 01	LDA A #O2
00795	C19C 86 02	STA A M+2
00796	C19E 97 02	LDA A #O5
00797	C1AO 86 05	STA A M+3
00798	C1A2 97 03	LDA A #12
00799	C1A4 86 0C	STA A M+4
00800	C1A6 97 04	LDA A #20
00801	C1A8 86 14	STA A M+5
00802	C1AA 97 05	LDA A #32
00803	C1AC 86 20	STA A M+6
00804	C1AE 97 06	LDA A #50
00805	C1BO 86 32	STA A M+7
00806	C1B2 97 07	LDA A #83
00807	C1B4 86 53	STA A M+8
00808	C1B6 97 08	LDA A #118
00809	C1B8 86 76	STA A M+9
00810	C1BA 97 09	LDA A #40
00811	C1BC 86 28	STA A M+10
00812	C1BE 97 0A	LDA A #82
00813	C1CO 86 52	STA A M+11
00814	C1C2 97 0B	LDA A #O1
00815	C1C4 86 01	STA A M+12
00816	C1C6 97 0C	LDA A #42
00817	C1C8 86 2A	STA A M+13
00818	C1CA 97 0D	LDA A #82
00819	C1CC 86 52	STA A M+14
00820	C1CE 97 0E	LDA A #117
00821	C1DO 86 75	STA A M+15
00822	C1D2 97 0F	LDA A #33
00823	C1D4 86 21	STA A M+16
00824	C1D6 97 10	LDA A #51
00825	C1D8 86 33	STA A M+17
00826	C1DA 97 11	LDA A #63
00827	C1DC 86 3F	STA A M+18
00828	C1DE 97 12	LDA A #71
00829	C1EO 86 47	STA A M+19
00830	C1E2 97 13	LDA A #78
00831	C1E4 86 4E	STA A M+20
00832	C1E6 97 14	LDA A #81
00833	C1E8 86 51	STA A M+21
00834	C1EA 97 15	


```

00835 C1EC 86 52          LDA A #82
00836 C1EE 97 16          STA A M+22
00837 C1FO 86 53          LDA A #83
00838 C1F2 97 17          STA A M+23
00839 C1F4 39             RTS
00842                      * ACCELERATION
00843 C1F5 BD C194 ACCEL  JSR  INIT
00844 C1F8 96 2C          LDA A M+44
00845 C1FA 97 00          STA A M
                                ;INIT MAY NOT BE REQUIRED ( I.E. THIS IS A CHECK )

00846 C1FC 7F 002A        CLR  M+42
00847 C1FF 7F 002B        CLR  M+43
00848 C202 CE 00C8        LDX  #200
00849 C205 DF 25          STX  M+37
00850 C207 39             RTS
00853                      * DECELERATION
00854 C208 96 2C          DECEL LDA A M+44
00855 C20A 97 00          STA A M
00856 C20C 7F 0001        CLR  M+1
00857 C20F 7F 0002        CLR  M+2
00858 C212 7F 0003        CLR  M+3
00859 C215 7F 0004        CLR  M+4
00860 C218 7F 0005        CLR  M+5
00861 C21B 7F 0006        CLR  M+6
00862 C21E 7F 0007        CLR  M+7
00863 C221 7F 0008        CLR  M+8
00864 C224 7F 0009        CLR  M+9
00865 C227 7F 000A        CLR  M+10
00866 C22A 7F 000B        CLR  M+11
00867 C22D 7F 000C        CLR  M+12
00868 C230 7F 002A        CLR  M+42
00869 C233 7F 002B        CLR  M+43
00870 C236 CE 00C8        LDX  #200
00871 C239 DF 25          STX  M+37
00872 C23B BD C000        JSR  ASD
00873 C23E BD C194        JSR  INIT
00874 C241 39             RTS
                                ;32+51
00877 C242 CE 0053 DEC32  LDX  #83
00878 C245 DF 25          STX  M+37
00879 C247 86 33          LDA A #51
00880 C249 97 28          STA A M+40
00881 C24B CE 0033        LDX  #51
00882 C24E 86 04          LDA A #04
00883 C250 97 27          STA A M+39
00884 C252 96 2C          LDA A M+44
00885 C254 97 00          STA A M
00886 C256 BD C0C1        JSR  ASD4

```



```

00887 C259 BD C194      JSR      INIT
00888 C25C 39      RTS
00889      * USED FOR DECELERATION FROM 100 HZ. < F. MAX. <400 HZ.
00892 C250 CE 0053      LDX      #83
00893 C260 OF 25      STX      M+37
00894 C262 86 4E      LOA      A #78
00895 C264 97 28      STA      A M+40
00896 C266 CE 004E      LDX      #78
00897 C269 86 04      LOA      A #04
00898 C26B 97 27      STA      A M+39
00899 C260 96 2C      LDA      A M+44
00900 C26F 97 00      STA      A M
00901 C271 BD C0C1      JSR      AS04
00902 C274 B0 C194      JSR      INIT
00903 C277 39      RTS
00904      * USED FOR DECELERATION FROM F. MAX. < 100 HZ.
00907 C278 7F 8005      PIA      CRA
00908 C27B C6 1F      LOA      B #$1F
00909 C270 F7 8004      STA      B DDRA
00910 C280 C6 04      LOA      B #04
00911 C282 F7 8005      STA      B CRA
00912 C285 B0 C194      JSR      INIT
00913 C288 BD C163      JSR      F
00914 C28B 39      RTS
00915      * U P HAS BEEN INITIALIZED
00916      * BITS 0+1 = ROTATION, 2= O/P TO HP, 3+4 = TRANSLATION, 5= I/P FROM HP,
00917      * 6+7 ARE NOT PRESENTLY USED.
00918      * BITS 0-4 ARE ACTIVE ON THE POSITIVE TRANSITION, BIT 2
00921 C28C 39      DELAY .RTS ;5
00924      * R80 (ROTATE FOR 8 DETECTORS)
00925      * PRODUCES 25.7 DEGREES ROTATION
00926      * ACCEL.+ OECEL. = 400 STEPS
00927      * A BIT PATTERN IS NOT REQUIRED FOR 25.7 DEG.
00928 C280 CE 143C      R80      LDX      #5180 ; 5180 STEPS = 25.7 DEGREES
00929 C290 OF 25      STX      M+37
00930 C292 CE 12AC      LDX      #4780 ; 4780*M+12
00931 C295 OF 2A      STX      M+42
00932 C297 B0 C000      JSR      AS0
00933 C29A 39      RTS
00936      * START SENDS A SIGNAL TO THE HP
00937      * AND WAITS FOR A SIGNAL IN RETURN
00938 C29B C6 1B      START      LOA      B #$1B ;TELL HP SCAN IS READY TO START & SET
00939      *      ROT. & TRANSL. BITS HIGH
00940 C29D F7 8004      STA      B ORA
00941 C2A0 B0 C28C      JSR      DELAY
00942 C2A3 C6 1F      LOA      B #$1F

```



```

00943 C2A5 F7 8004 STA B DRA
00944 C2A8 F6 8004 LDA B DRA
00945 C2AB C4 20 AND B #$20
00946 C2AD 27 F9 BEQ J3
00947 C2AF 39 RTS ; WAIT FOR HP SIGNAL
00950
00951 * TRANSLATION - A SIGNAL IS SENT TO THE HP
00952 * EVERY M+50 MOTOR STEPS. M+51,M+52 AND M+53
00953 * DETERMINE THE DELAY BETWEEN MDTOR STEPS
00954 * DELAY BETWEEN STEPS
00955 * =M+52((M+53*12)+8) + 42 +M+51*12 +56
00956 TRANSL LDA B #01
00957 STA B M+46
00958 LDDP6 INX
00959 LDA A M+52
00960 DEC M+46
00961 BNE N2
00962 C2BC C6 1B LDA B #$1B
00963 C2BE F7 8004 STA B DRA
00964 C2C1 BD C28C JSR DELAY
00965 C2C4 C6 1F LDA B #$1F
00966 C2C6 F7 8004 STA B ORA
00967 C2C9 F7 8004 STA B DRA
00968 C2CC D6 32 LDA B M+50
00969 C2CE D7 2E STA B M+46
00970 C2D0 7E C2E8 JMP J1
00971 *
00972 C2D3 78 0029 N2
00973 C2D6 78 0029 ASL M+41
00974 C2D9 78 0029 ASL M+41
00975 C2DC 78 0029 ASL M+41
00976 C2DF 78 0029 ASL M+41
00977 C2E2 78 0029 ASL M+41
00978 C2E5 78 0029 ASL M+41
00979 C2E8 09 DEX J1
00980 C2E9 27 23 BEQ J2
00981 C2EB D6 33 LDA B M+51
00982 C2ED 78 0029 J4 ASL M+41
00983 C2FO 5A DEC B
00984 C2F1 26 FA BNE J4
00985 C2F3 D6 2C LDA B M+44
00986 C2F5 F7 8004 STA B ORA
00987 C2F8 BD C28C JSR DELAY
00988 C2FB C6 1F LDA B #$1F
00989 C2FD F7 8004 STA B ORA
00990 C300 D6 35 LDDP5 M+53
00991 C302 78 0029 J6 LDA B M+41

```

; PULSES IN INX = # DF PULSES FDR TRANSLATION
 ; PRDDUCES DESIRED DELAY BETWEEN PULSES 3 CYCLES
 ; 6
 ; 4
 ; 2) SEND SIGNAL TD HP
 ; 5)
 ; 9+5)
 ; 2) 42
 ; 5)
 ; 5)
 ; 3) HP SIGNAL EVERY M+50 STEPS
 ; 4)
 ; 3)
 ; 6) TIME TO J1 IS THE SAME EITHER WAY
 ; 6)
 ; 6)
 ; 6) 42
 ; 6)
 ; 6)
 ; 6)
 ; 4
 ; 4
 ; 3
 ; 6)
 ; 2)B*12=M+51*12
 ; 4)
 ; 3
 ; 5
 ; 9+5
 ; 2
 ; 5
 ; 2
 ; 6)


```
00992 C305 5A          DEC B          :2 ) M+53*12
00993 C306 26 FA      BNE          :4 )
00994 C308 4A          DEC A          :2
00995 C309 26 F5      BNE          :4
00996 C308 7E C2B5    JMP          :4
00997 C30E 39          RTS          :3
01000                      END
```

Symbol Table

DRA	8004	DDRA	8004	CRA	8005	M	0000	ST	602C	JMPE	605C	ST 1	60BC	K5	60EA
MC1	61A6	JMPE2	61B5	ST3	620C	JMPE3	6241	ST4	62AC	JMPE4	62E1	ST5	634C	JMPE5	6381
C1	C036	C2	C039	C3	C03C	C4	C03F	C5	C042	C6	C045	C7	C048	C8	C04B
ASD1	C059	C10	C066	K1	C069	C11	C070	K2	C073	P1	C077	P4	C085	ASD2	C08F
ASD3	COA7	ASD4	COC1	B1	COE7	B2	COEC	B3	COF1	B4	COF6	B5	COFB	B6	C100
B9	C10F	B10	C114	B11	C119	B12	C11E	J	C120	DEL	C125	D1	C127	Z3	C151
Z6	C15A	Z2	C15D	F	C163	INIT	C194	ACCEL	C1F5	DECEL	C208	DEC32	C242	DEC5	C25D
R8D	C28D	START	C29B	J3	C2A8	TRANSL	C2B0	LDDP6	C2B5	N2	C2D3	J1	C2E8	J4	C2ED
J2	C30E	JMPE1	6107	ST2	6179	ASD	C000	ASDO	C009	C9	CO4E	J5	CO51	C12	C09C
P6	C09F	B7	C105	B8	C10A	Z4	C154	Z5	C157	PIA	C278	DELAY	C28C		

*** SOME PRDGRAM LINE NUMBERS MAY BE MISSING DUE TO DELETION OF SOME COMMENTS. THIS WAS DONE FOR FORMATTING PURPOSES.

*** APPENDIX Q - CONTAINS READ SUBROUTINE ***

Motorola M68SAM Cross-Assembler

00001	8004	ORA	EQU	\$8004	
00002	8004	ODRA	EQU	\$8004	
00003	8005	CRA	EQU	\$8005	
00004	8006	ORB	EQU	\$8006	
00005	8006	ODRB	EQU	\$8006	
00006	8007	CRB	EQU	\$8007	
00007	0000	M	EQU	\$0000	
00008			NAM	READ	
00009	C300		ORG	\$C300	
00010					* 4 TYPES OF INFORMATION WILL BE
00011					* SENT FROM THE CAMAC.
00012					* (1) 8 BIT DATA SENT THROUGH A SIDE
00013					* BITS B7-BO (HIGH-LOW)
00014					* (2) 9 BIT ADDRESS FOR DATA (512 BYTES RAM)
00015					* B SIDE BO (HIGH). A SIDE B7-BO (LOW)
00016					* (3) 9 BIT ADDRESS FOR STARTING PROGRAMS
00017					* IN RAM (AS IN (2)) AND
00018					* (4) 16 BIT ADDRESS FOR STARTING PROGRAMS IN ROM
00019					* PIA A SIDE B7-BO IS SENT TWICE.
00020					* THE FIRST BYTE SENT IS THE HIGH
00021					* BYTE OF THE ADDRESS.
00022					* THE TYPE OF INFORMATION
00023					* BEING SENT IS ENCODED IN B SIDE
00024					* BITS 1&2.
00025					* TYPE 1 =B1=B2=0
00026					* TYPE 2 =B1=0, B2=1
00027					* TYPE 3 =B1=B2=1
00028					* TYPE 4 =B1=1, B2=0
00029	C300 7F 8005	CLR	CRA		; SET CRA FOR ODRA
00030	C303 7F 8007	CLR	CRB		; SET CRB FOR OORB
00031	C306 7F 8004	CLR	ODRA		; A SIDE I/P'S
00032	C309 C6 F8	LOA	B	#\$F8	; B SIDE BITS 0-2 I/P.
00033	C30B F7 8006	STA	B	ODRB	; BITS 3-7 O/P
00034	C30E C6 E6	LDA	B	#\$E6	; SET CRA
00035					* CRA = 1110 0110
00036					* B5=1 CA2 = 0/P;
00037					* B4=B3=0 HANDSHAKE MOOE, CA2 GOES
00038					* LOW ON READ ORA & RETURNS HIGH
00039					* WHEN IRQA1 IS SET BY CA1;
00040					* B2=1 ORA; B1=1 +VE TRANSITIONS OF
00041					* CA1 SET IRQA1; BO=0 OISABLES IRQA1
00042					* INTERRUPT BY CA1.
00043	C310 F7 8005	STA	B	CRA	
00044	C313 C6 F0	LDA	B	#\$F0	; SET CRB


```
00045
00046
00047
00048
00049
00050
00051
00052
00053
00054
00055
00056
00057
00058
00059
00060
00061
00062
00063
00064
00065
00066
00067
00068
00069
00070
00071
00072
00073
00074
00075
00076
00077
00078
00079
00080
00081
00082
00083
00084
00085
00086
00087
00088
00089

* CRB = 1111 1101
* B5=1 CB2= 0/P; B4=1 CB2 FOLLOWS B3
* AS CHANGED BY WRITE CRB INSTRUCTION;
* B3=1 NORMALLY HIGH, ACTIVE HIGH TO LOW;
* B2=1 ORB; B1=0 -VE TRANSITION OF CB1 SET
* IRQB1; BO=1 ENABLES IRQB MPU INTERRUPT
* BY CB1.
      STA B      CRB
      LDX      READ
      STX      $A000
      LDA A     CRA
      AND A     #$80
      BEQ      READ
      LDA A     ORB
      STA A     M+502
      AND A     #04
      BNE      B2
      LDA A     ORB
      AND A     #02
      BNE      B1
      LDA A     ORA
      STA A     X
      INX
      JMP      READ
      LDA A     ORB
      AND A     #01
      STA A     M+500
      LDA A     ORA
      STA A     M+501
      LDX      M+500
      LDA B     M+502
      AND B     #02
      BNE      B91
      JMP      READ
      JMP      X
      LDA A     ORA
      STA A     M+500
      LDA A     CRA
      AND A     #$80
      BEQ      REA
      LDA A     ORA
      STA A     M+501
      LDX      M+500
      JMP      X
      END

      ; VECTORIZE JBUG SO THAT IRQ WILL
      ; CAUSE A JUMP TO READ SR
      ; CHECK IF MESSAGE
      ; HAS BEEN SENT
      ; $01F6= SCRATCH LOCATION
      ; IS B2=0 ??
      ; B2=0
      ; IS B1=0 ??
      ; B2=0, B1=0
      ; B2=1
      ; MASK BITS SIDE B 1-7
      ;$01F4= SCRATCH LOCATION
      ; $01F5= SCRATCH LOCATION
      ; IS B1=0 ??
      ; B2=1, B1=0
      ; B2=1, B1=1
      ; B2=0, B1=1
```


Symbol Table

ORA	8004	DDRA	8004	CRA	8005	ORB	8006	DDRB	8006	CRB	8007	M	0000
READ	C31E	B2	C33F	B91	C35A	B1	C35C	REA	C362				

*** SOME PROGRAM LINE NUMBERS MAY BE MISSING DUE TO DELETION OF SOME COMMENTS. THIS WAS DONE FOR FORMATTING PURPOSES.

B30305